Laboratorio
de Microscopías
Avanzadas

Annual Report 2012-2013

LMA
LABORATORIO
DE MICROSCOPÍAS
AVANZADAS

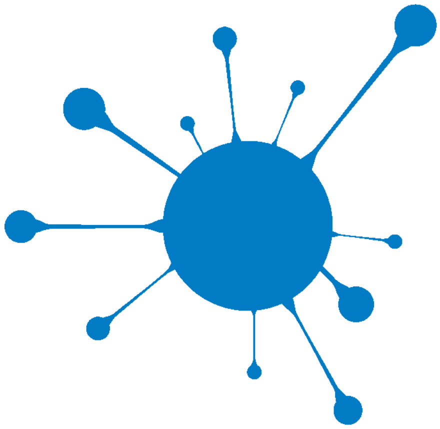

Laboratorio de Microscopías Avanzadas

Annual Report 2012-2013

LMA
LABORATORIO
DE MICROSCOPIAS
AVANZADAS

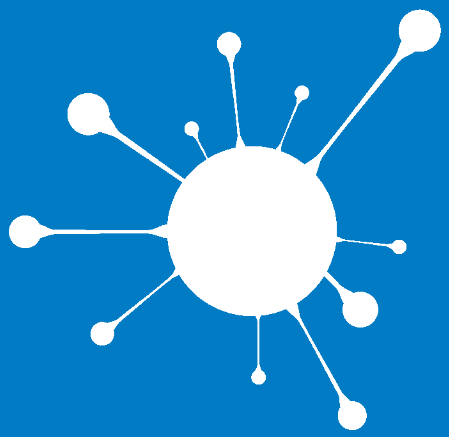

Index

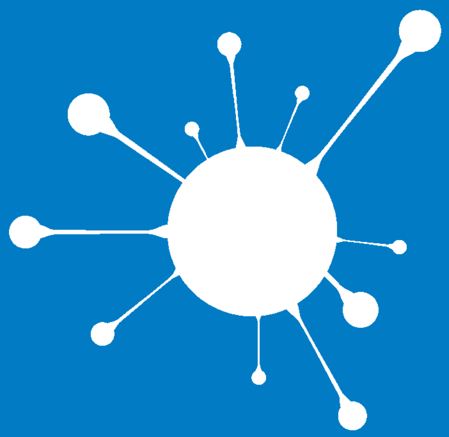

Introduction

Manuel Ricardo Ibarra García
Director

The Laboratory of Advanced Microscopies has consolidated a set of top level infrastructures in different fields of microscopies, establishing the necessary instrumentation and expertise to attend the demand of scientists and companies to face new challenges based on nanoscience and nanotechnology. Our mission is to attract world-class science, creating a high level research atmosphere and based on the selective criteria of access and internationalization of the laboratory. LMA coordinated the European INTERREG Program "Trans-Pyrenees Action on Advanced Infrastructures for Nanosciences and Nanotechnology (TRAIN2)" providing the opportunity to strengthen the collaboration in the European South West (SUDOE) region. Several international partnerships have promoted synergies which allowed raising cutting-edge scientific and technological outputs. The international collaboration with Midi-Pyrenees Region through the Associate Laboratory CNRS-UNIZAR (TALEM) and the participation in the European ESTEEM2 consortium allowed a fluent scientific exchange with top level researchers.

Our facilities have been completely settled during this period and world-class groups are frequently using our laboratories. The combination of expertise in nanofabrication and nanocharacterization at the same facility constitutes one of its most valuable characteristics, envisioning a promising future for the LMA.

Our challenge for the next period is to become an international reference Laboratory to promote and to establish new bridges among scientists and companies, through high level training based on the top level infrastructures and wide expertise in Advanced Microscopies.

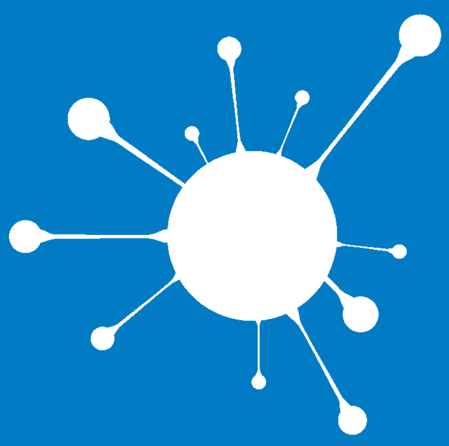

Foreword

José María De Teresa Nogueras
Coordinator

The second LMA two-year report summarizes the activities and achievements obtained in the lab along two difficult years, 2012-2013, in which Spanish Science seemed to be abducted and living in the limbo. Fortunately, the inertia has allowed the lab to consolidate a standing position in microscopy and nanofabrication at the international level. The decisions of the Spanish government in the last months of 2013, such as the additional funding for CSIC and the launch of several national projects and human resources calls, are positive and encouraging. The LMA will continue working towards meeting the highest standards in terms of producing top scientific results as well as providing service to the scientific community and industry.

I would like to single out a few points contained in the present report. A milestone in the lab has been the implementation of the access to the equipment via proposal, occurred in early 2013. This type of access is frequent in international large-scale installations, reflecting our willingness to offer service in a transparent form to high-quality scientific and technological projects. More than 30 proposals have been accepted and the corresponding experiments performed. Another milestone of the lab was the organization of the first LMA Users' Meeting, held in 2013, which hosted researchers from Spain and abroad and was a live meeting point. The LMA played also an important role in the organization of the 4th FEBIP workshop hosted by University of Zaragoza in 2012 and several international schools held in Zaragoza or Jaca. The participation of the LMA researchers in the TRAIN2 and ESTEEM2 European projects has additionally extended the international projection of the lab. The international impact being important, we cannot forget that the LMA aims to impact the local societal environment. In this sense, the role played by the LMA in the high-tech formation of Master and PhD students should be appreciated.

My next words refer to the current status of the LMA. On 15th October 2013, an application has been submitted to the Spanish Ministry of Economy (MINECO) to become an official Spanish ICTS (Infraestructura Científica y Tecnológica Singular). As suggested by the MINECO, this application has been coordinated with a second Spanish node in microscopy, located in the Universidad Complutense de Madrid. In the coming months, we expect to obtain a positive feedback from the MINECO, which would strengthen the position of the microscopy in Spain and would give potential access to additional benefits for the lab and the external users. Looking inside the lab, we can state that the LMA is currently fully operational, with the SPM area already setup and developing high-quality research like the other two areas, the TEM and Dual Beam ones. A flow of scientific and technical staff occurs in all labs and the LMA has not escaped from this. I would like to thank Rosa Córdoba for the work performed since 2007 with the Dual Beam and now searching for new scientific horizons.

Similarly to my previous address two years ago, I would like to finish giving thanks to all people contributing to the success of the LMA project: managers, scientists, technicians and users, who make the Laboratory of Advanced Microscopies a singular research center in all senses. Starting from scratch in 2007, I am proud to assert that the LMA has gained a significant position in the world of microscopy and nanofabrication. I can envision that, due to the maturity reached in this time by the lab members, the coming years will be the most fruitful ones in terms of scientific and technological output, but do not forget that *there is life beyond the lab!*

About LMA

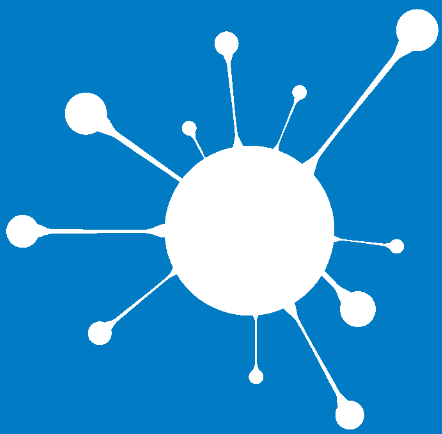

About LMA

The Advanced Microscopies Laboratory (LMA) depends administratively on the University of Zaragoza through the Instituto de Nanociencia de Aragón. The director of INA is also the director of the LMA. An international Scientific Committee evaluates periodically the activities of the LMA and provides assessment for improvement. The LMA scientific activities are managed by three area supervisors, coordinated by the LMA coordinator. Each area supervisor is responsible for the equipment and technical staff assigned to its area and in general for all the organizational issues of the area.

LMA represents a unique initiative both at national and international level. Its aim is to provide the Scientific Community with the most advanced existing infrastructures in Local Probe and Electron Microscopy for the observation, characterization, nanopatterning and handling of materials at atomic scale, as well as with a wide range of scientific tools devoted to characterization, processing and handling procedures at the nanometric scale. Its location within the University of Zaragoza's Research Institute on Nanoscience of Aragon (INA) guarantees an environment of complementary associated infrastructures and excellence-driven scientific and technical human resources which, together with the unique equipment of LMA, will boost research capacity in Nanoscience in Spain, as well as the development of new related technologies. All LMA scientific instruments and the expertise of the scientists and technical staff involved are available for public and private research centers and for the industry in general, which find in this facility a unique research capacity and technological development only available in very few research centers worldwide

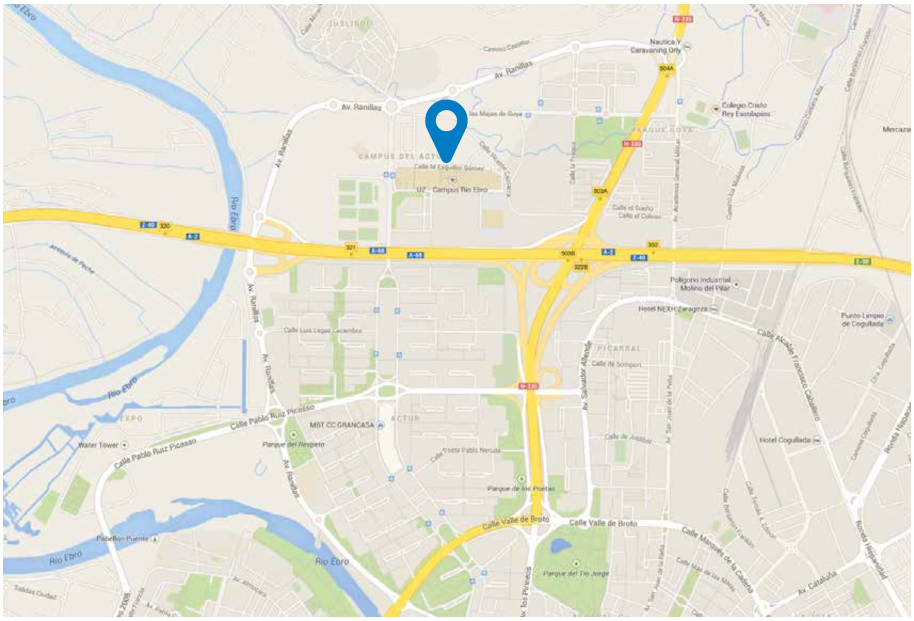

Laboratorio de Microscopías Avanzadas (LMA)
***Advanced Microscopies Laboratory* (LMA)**
Edificio I+D
Campus Río Ebro
Universidad de Zaragoza
C/ Mariano Esquillor, s/n.
50012 Zaragoza (Spain)
Tel: +34 976 762 980
Fax: +34 976 762 776
Email: lma@unizar.es
http://ina.unizar.es/lma

University Research Institutes Building – Campus Río Ebro.

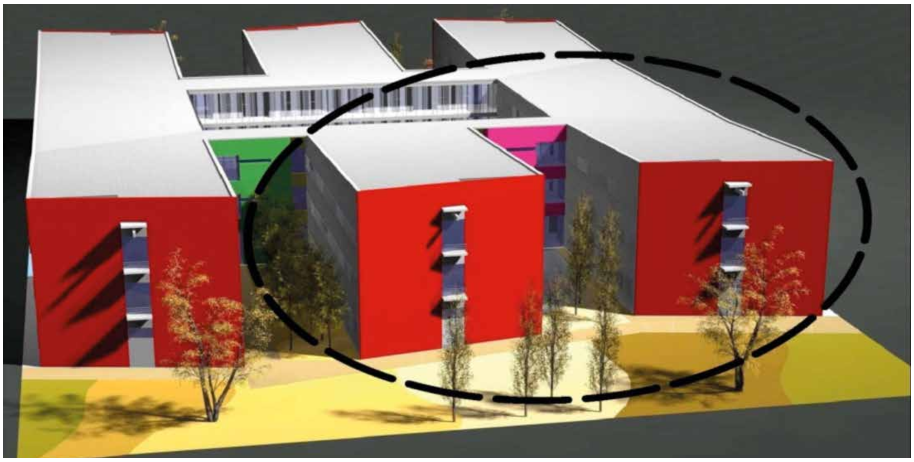

University Research Institutes Building – Campus Río Ebro.

Organization Chart

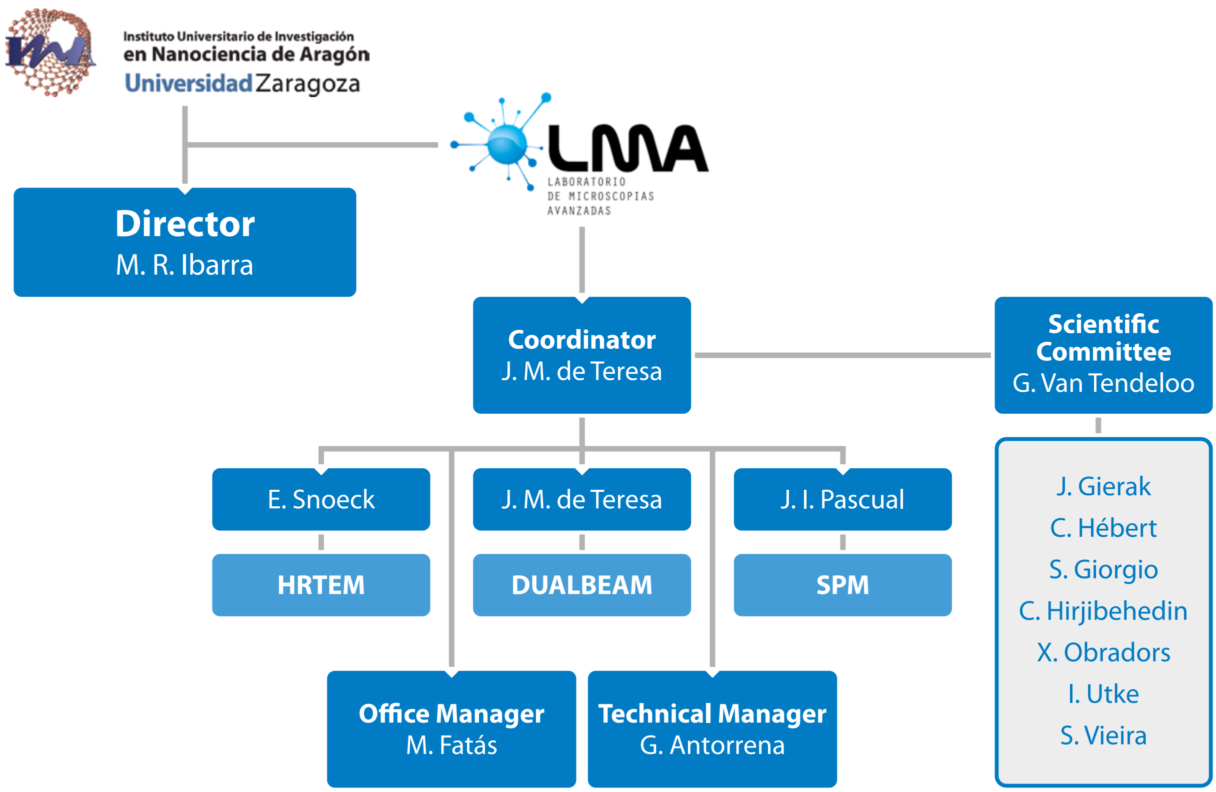

Human Resources

LMA members

Personnel	
Scientific	2
Technical staff	16
Administration	2

Associated members

Personnel	
Scientific	18
Technical staff	
Administration	

Management

M. Ricardo Ibarra	**Director**
José Mª De Teresa	**Scientific Coordinator**
Guillermo Antorrena	*Technical Manager*
Mercedes Fatás	*Office Manager*
Mª Jesús Calvera	*Administrative Support*

TEM

Arenal, Raúl	*Researcher, ARAID Foundation*
Custardoy, Laura	*Sample Prep Technician*
Fdez. Pacheco, Rodrigo	*TEM Technician*
Ibarra, Alfonso	*TEM Technician*
Magén César	*Researcher, ARAID Foundation*
Mayoral, Álvaro	*Postdoctoral Researcher*
Rodríguez, Luis Alfredo	*PhD Student*
Snoeck Etienne	*Head of TEM Area*

SPM

Arnaudas, José Ignacio	*Professor*
Cea, Pilar	*Associate Professor*
Ciria, Miguel	*Tenured Scientist, CSIC*
Coffey, David	*PhD Student*
Díez José, Luis	*SPM Technician*
Gracia, Ana Isabel	*Researcher, ARAID Foundation*
Marcuello, Carlos	*PhD Student*
Martín, Carlos	*SPM Technician*
Martín, Santiago	*Researcher, Juan de La Cierva Program*
Moro, María	*PhD Student*
Pascual, José Ignacio	*Head of SPM Area*
Piantek, Marten	*Researcher, JAE-DOC Program, CSIC*
Serrano, Luis	*PhD Student*
Serrate, David	*Researcher, Ramón y Cajal Program*

DUAL BEAM

Casado, Laura	*Dual Beam Technician*
Córdoba, Rosa	*Dual Beam Technician*
Cuestas, Carlos	*SEM Technician*
De Teresa, José Mª	*Head of DUAL BEAM Area*
Goya, Gerardo	*Associate Research Professor*
Irusta, Silvia	*Associate Research Professor*

Mtez. De la Fuente, Jesús	*Researcher, ARAID Foundation*
Pardo, José Ángel	*Associate Professor*
Rivas, Isabel	*Clean Room Technician*
Sesé, Javier	*Associate Research Professor*
Simón, Gala	*Clean Room Technician*
Tejero, Luis	*Technician*
Torres, Teobaldo	*Dual Beam Technician*
Valero, Rubén	*Clean Room Technician*

The Scientific Committee

The Scientific Committee is in charge of providing scientific and advisory support to the Management Board. It is composed of internationally prominent scientists in the field of advanced microscopies, with outstanding professional and scientific track record in line with LMA objectives.

Members

Prof. G. Van Tendeloo (Chair)	*University of Antwerp (Belgium)*
Dr. Jacques Gierak	*LPN – CNRS (France)*
Prof. Suzanne Giorgio	*CINM – CNRS (France)*
Prof. Cecile Herbert	*EPFL (Switzerland)*
Dr. Cyrus Hirjibehedin	*London Center for Nanotechnology (U.K.)*
Prof. Xavier Obradors	*ICMAB – CSIC (Spain)*
Dr. Ivo Utke	*EMPA (Switzerland)*
Prof. Sebastián Vieira	*Universidad Autónoma de Madrid (Spain)*

Functions

> Provide advice in relation with the scientific policy guidelines.

> Evaluate and inform on the Annual Report of activities and on the proposals for the Annual Action Plans.

> Provide feedback on the usefulness of programs, resources and capabilities of the different laboratories.

> Assess on the technology transfer strategy.

> Assess on the recruitment policy for scientific personnel.

> Inform on the creation of research programs.

Instituto Universitario de Investigación en Nanociencia de Aragón
Universidad Zaragoza

LMA
LABORATORIO DE MICROSCOPIAS AVANZADAS

LMA Scientific Committee meeting 03-03 May 2012

Present

INA & LMA Director
M. Ricardo Ibarra

Scientific Committee Members
Gustaaf Van Tendeloo (President), Jacques Gierak, Suzanne Giorgio, Cécile Hébert, Cyrus Hirjibedhedin Xavier Obradors, Ivo Utke, Sebastián Vieira

Heads of scientific areas
José María De Teresa, José Ignacio Pascual, Etienne Snoeck

Office Manager
Mercedes Fatás

AGENDA

1. Welcome words by R. Ibarra and G. Van Tendeloo
2. Report of activities and plans for the future
   Etienne Snoeck
   José M. De Teresa
   José Ignacio Pascual
3. Discussion
4. Closed session of the Scientific Committee members
5. Feedback to the director and the heads of the scientific areas and concluding remarks

---

MEETING REPORT

The third LMA Scientific Committee meeting was called to order on 03 May at 16:00 and continued on 04 May (09:00-12:00) in the premises of the Institute of Nanoscience of Aragon.

The meeting is introduced by the Director, Prof. M.R. Ibarra and a progress report by each of the heads of the three scientific areas, namely: Etienne Snoeck, head of the TEM area, José María de Teresa, head of the DUALBEAM area, and José Ignacio Pascual, head of the SPM area.

The progress reports lead to the following conclusions by the Scientific Committee:

Instituto Universitario de Investigación en Nanociencia de Aragón
Universidad Zaragoza

LMA LABORATORIO DE MICROSCOPIAS AVANZADAS

- The Scientific Committee is extremely impressed by the progress that has been made since the start of the laboratory and particularly since the last year.
- The major suggestion expressed by the SC in 2011, i.e. to increase the scientific output, has been taken very seriously; resulting for 2011 in over 80 ISI publications with 11 contributions published in journals with an IF >10.
- The SC is very happy to see that virtually all equipment of the three subgroups is up and running. Also the SPM facility is now ready and the SC expects some significant output in the coming year.
- A lot of projects are already made in collaboration with other research centers and with industry. 70% of all publications are actually collaborative work with non-LMA partners.
- The laboratory has made a great effort to enhance the visibility of the LMA to the scientific and technological community of Spain through workshops, colloquia and information sessions. Close contact between advanced research centers and industry is very important; particularly in a period of economical problems. This could be enhanced through an active approach of high tech. industries.
- Long term research planning should be thought off; particularly when aiming for larger contracts (such as EC contracts). He latter should be a goal for the coming years.
- The position of Snoeck (20% at the EM group) and Pascual (20% at the SPM group) should be maintained for at least another year. Both are high end scientists with an international reputation that enables them to promote LMA research. However, one should also start thinking about "what after" and prepare for an independent research and management plan.

Gustaaf Van Tendeloo
President of the Scientific committee

Instituto Universitario de Investigación en Nanociencia de Aragón
Universidad Zaragoza

LMA LABORATORIO DE MICROSCOPÍAS AVANZADAS

LMA Scientific Committee meeting 07-08 May 2013

PRESENT: *INA & LMA Director*
M. Ricardo Ibarra

Scientific Committee Members
Gustaaf Van Tendeloo (President), Jacques Gierak, Suzanne Giorgio, Cyrus Hirjibedhedin, Xavier Obradors, Sebastián Vieira

Heads of scientific areas
José María De Teresa, José Ignacio Pascual, Etienne Snoeck

Office Manager
Mercedes Fatás

AGENDA

1. Welcome words by R. Ibarra and G. Van Tendeloo
2. Report of activities and plans for the future presented by
   Etienne Snoeck
   José M. De Teresa
   José Ignacio Pascual
3. Discussion on the activities and future plans
4. Closed session of the Scientific Committee members
5. Feedback to the director and the heads of the scientific areas and concluding remarks

MEETING REPORT

The third LMA Scientific Committee meeting was called to order on 07 May at 16:00 and continued on 08 May (09:00-12:00) in the premises of the Institute of Nanoscience of Aragon.

The meeting is introduced by the Director, Prof. M.R. Ibarra and a progress report is presented by each of the heads of the three scientific areas, namely:

- Etienne Snoeck, head of the TEM area,
- José María de Teresa, head of the DUALBEAM area
- José Ignacio Pascual, head of the SPM area.

The progress reports lead to the following conclusions by the Scientific Committee:

- The Scientific Committee is extremely impressed by the efficiency of the group and the progress that has been made particularly the last year.
- The major suggestions expressed by the SC in 2012, i.e. to increase the scientific output and the visibility of the LMA has certainly been reached; resulting for 2012 in 87 ISI publications with 10 contributions published in journals with an IF >10 and over 30% of the publications in ISI journals with IF>5.

Instituto Universitario de Investigación en Nanociencia de Aragón
Universidad Zaragoza

LMA LABORATORIO DE MICROSCOPÍAS AVANZADAS

- The TEM group lead by E. Snoeck (20%) is doing exceptionally well and has, in very short time, acquired international visibility. The competition however is very strong and the group should establish its own expertise. Soft matter research might be one possibility.
- The FIB group lead by J.M. De Teresa (100%) is very well balanced and has become leading edge in the world. They also have been able to attract industrial collaborations.
- The SPM group lead by J.I. Pascual (20%) has finally most of its equipment up and running and the first high level publications have appeared. The group however faces a number of problems related to the delicate set of experiments. The SC therefore suggests to look for a strategic partnership with internationally reknown research centres. The group should also think about a balance between user facility on one side (e.g. through AFM measurements) and own research (through collaborations) on the other hand.
- The SC appreciates that a large number of projects and publications are made in collaboration with other research centres and with industry.
- The SC particularly appreciates that LMA has built up contacts with local industries as well as with large industrial concerns. Also collaboration with the ICMA should be reinforced.
- The laboratory has also made a great effort to enhance the visibility of the LMA to the scientific as well as to the technological community of Spain. This is done through workshops, colloquia and information sessions. Close contact between advanced research centres and industry is very important; particularly in a period of economical problems.
- Long term research planning should be thought off. A "strategic plan" for the future should be made to complement the LMA equipment. A suggestion of the SC is to upgrade the Titan microscope with a STEM corrector, to complement the FIB with a He ion mill and to extend the SPM lab with high B field possibilities at low T.
- A major concern of the SC is the stability of the personnel, particularly the technical staff. Continuity of the work is very important in this respect.

Gustaaf Van Tendeloo
President of the Scientific committee

Description of the access offered to the R&D community

To achieve the goals of expanding the microscopy techniques both to industry and the scientific community we offer the use of our facilities to experienced users as well as novel users and groups not directly connected with microscopy methods. Users find at LMA a flexible and competent center to carry out their characterization and research studies with the support of specialized technical staff and scientists.

In accordance with the range of experimental tools and methods, we offer access to our facilities either as a service (studies and nanofabrication carried out by our technical staff) or as project-oriented collaborations (demanding studies requiring the active participation of our scientific personnel). Our experience is that, depending on the user and the type of measurement, the support by the LMA staff varies.

LMA offers the following type of activities:

> Structural and chemical TEM studies of materials and devices

> Studies of local magnetic configuration by electron holography and magnetic force microscopy

> Plasmon mapping

> Cryo-TEM studies of soft materials

> Nanostructuration by Focused Ion Beam

> Surface analysis by scanning probe microscopy, including atomic manipulation, follow-up of catalytic reactions and thin-film growth modes.

> Studies of single molecule configuration and spectroscopy by UHV Tunneling microscopy

> Magnetic microscopy under high magnetic fields in combination with electric transport measurements.

There are three types of access depending on the experience of the applicant, on the instrument, and on the challenge of the proposed measurements:

> **Service:** measurements are carried out by our technical staff. In general the attendance of the applicant is desired. This modality is applied to industrial partners, as well as to scientific users not directly working with similar instruments, who in general seek for a measurement complementary to their own techniques.

> **Scientific Use:** Some of our equipments are used by external experience users, who do not have at hand at their institutes of the specific tools like the ones available at LMA. In this case, users are advised by our technical staff about the use of the system and allowed to work independently.

> **Collaborative Use:** when challenging measurements are required, we offer the possibility to realize collaborative works together with scientific personnel of the LMA. In this case, our scientists get deeply involved in the measurements and analysis of the results.

Administrative and scientific and technical support to users

The LMA offers to potential users all types of local supports in terms of additional equipment for sample preparation and characterization, and technical, scientific and administrative staff.

> **Before the arrival:** For each accepted project, a "local contact" is designated, who will organize with the external user(s) his/her visit (together with the administration staff) and experiment (together with the technical staff) at the infrastructure. The local contact is chosen among the respective local experts of the corresponding infrastructure, depending on their own expertise and on the equipment that has been requested. This local contact is also in charge of checking that the equipment and samples are ready for the experiment, the viability of the measurements, and of reserving enough time in advance for preparing the experiment.

> **During the measurement:** All equipment offered are continuously maintained by highly specialized technical operators, who support and train the user in their initial use, as well as in the preparation of samples for measurement. They consider each specific requirement to ensure the success of the measurement. For some specific measurements in which special sophisticated methods are needed, the local contact will be also available to assist the user(s) in performing measurements, as well as in the data analysis.

> **After the measurement:** When leaving the infrastructure, the user(s) will take away all the raw images and spectra obtained with the LMA equipment and when carried out, the data that have been analyzed with the LMA researchers. In some special cases, LMA researches could offer subsequent support in terms of interpretation, and discussion of obtained results, especially in those cases when the local contacts were particularly involved in the scientific project.

Access protocol

To gain access to the LMA facilities, eligible users need to submit a research proposal describing their requirements. A standardized proposal form is available in the LMA website and can be filled on-line (http://ina.unizar.es/lma)

The research proposal to gain access contains the administrative location of the requesting person or group leader and describes:

> The scientific aim of the project, including

- The state of the art
- The expected output
- The potential industrial applications
- Possible special requests (for example: use of particular stages, precautions, low temperature, gas atmosphere, low voltages…)

> The requested instrument(s) including measuring conditions and sample preparation facilities, if needed.

> The requested access time to the instrument and sample preparation time (if any)

- The preferred dates for the measurements.
- The requested time for computing / data treatment and analysis time (if any).

Currently there is a permanently open call for submission of proposals, which are evaluated by at least one member of the Access Committee. Successful proposals enjoy experimental time as soon as possible. The feedback time to the user is very fast, in the range of 1-2 weeks, warranting the timeliness of the experiment.

For every successful proposal, the area leader of the LMA selects **a scientific in-house correspondent (local contact).** The applicant is then notified of the acceptance of the proposal and invited to communicate details and dates of the experiment with the local contact at the LMA.

Access Committee

The evaluation of the proposals is performed by specialized committees in each of the three scientific divisions of the LMA. The committees are chaired by the corresponding responsible scientist of the TEM, SPM and Dual Beam areas and are formed by the following experienced external scientists.

TEM Experts

- Dr. B. Warot (CEMES- CNRS, Toulouse) – Expertise: EELS, in-situ TEM
- Dr. J. Verbeek (EMAT, Antwerpen) – Expertise: EELS, STEM-HAADF, Tomography
- Pr. J. Arbiol (ICMAB, Barcelona) – Expertise: HREM, HRSTEM, EELS
- Dr. Luca Ortolani (University of Bologna) – Expertise : Holography, HREM
- Dr. E. Snoeck (Coordinator TEM division of LMA) – Expertise: Lorentz, Holography, HREM

SPM Experts

- Dra. Agustina Asenjo (ICMM, Madrid). Expertise: Magnetic Force Microscopy.
- Dr. Carlos Untiedt (Univ. Alicante). Expertise: low temperature transport through nanostructures.
- Prof. José Ignacio Pascual (Coordinator SPM division of LMA). Expertise: Surface Science and low temperature UHV-SPM

Dual Beam Experts

- F. Pérez-Murano (UAB, Barcelona). Expertise: Electron Beam Lithography
- J. Gierak (LPN-CNRS – Marcoussis, France). Expertise: Ion Beam Lithography
- José Luis García Fierro (ICP-CSIC, Madrid). Expertise: XPS.
- Bruno Humbel (Univ. Lausanne, Switzerland). Expertise: Cryo Dual Beam.
- Prof. José María de Teresa (Coordinator Dual Beam division of LMA). Expertise: Nanolithography

The proposal protocol was implemented along February 2013 and is currently developed very fluently.

Description of the evaluation procedure

Depending on the requested instrument, each research proposal is sent via the WEB site to the heads of the area i.e. Prof. E. Snoeck for TEM, Prof. J.I. Pascual for SPM and Prof. J.M. de Teresa for Dual Beam, who transfers it to a member of the Access Committee.

Each proposal is assessed by the Access Committee against the following selection criteria:

> **Technological or Scientific Merit of the proposal** (rank: weak: 0 – outstanding: 10)

> **Capabilities of the user team** (rank: weak: 0 – outstanding: 10)

> **Feasibility of the experiment:** the experiment must be feasible, this is discussed with the technicians and the scientists of the LMA.

Proposals are accepted provided that the threshold mark of 5 is reached in the first two criteria and the experiment is found to be feasible. Proposals with a total ranking less than 10 are rejected and the users are normally invited to resubmit their proposal following the advice of the reviewer report to improve their application. Accepted proposals designate a local person who is the contact for the user(s) to organize and perform the experiment.

The Laboratories

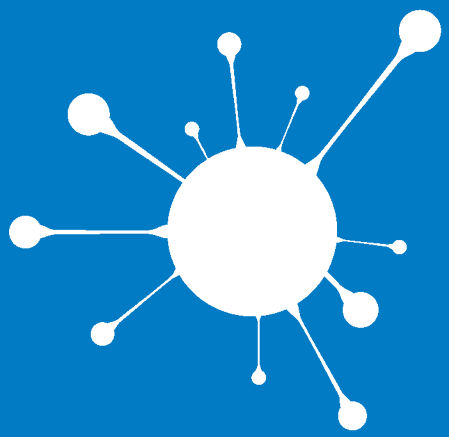

The Laboratories

Transmission Electron Microscopy Laboratories

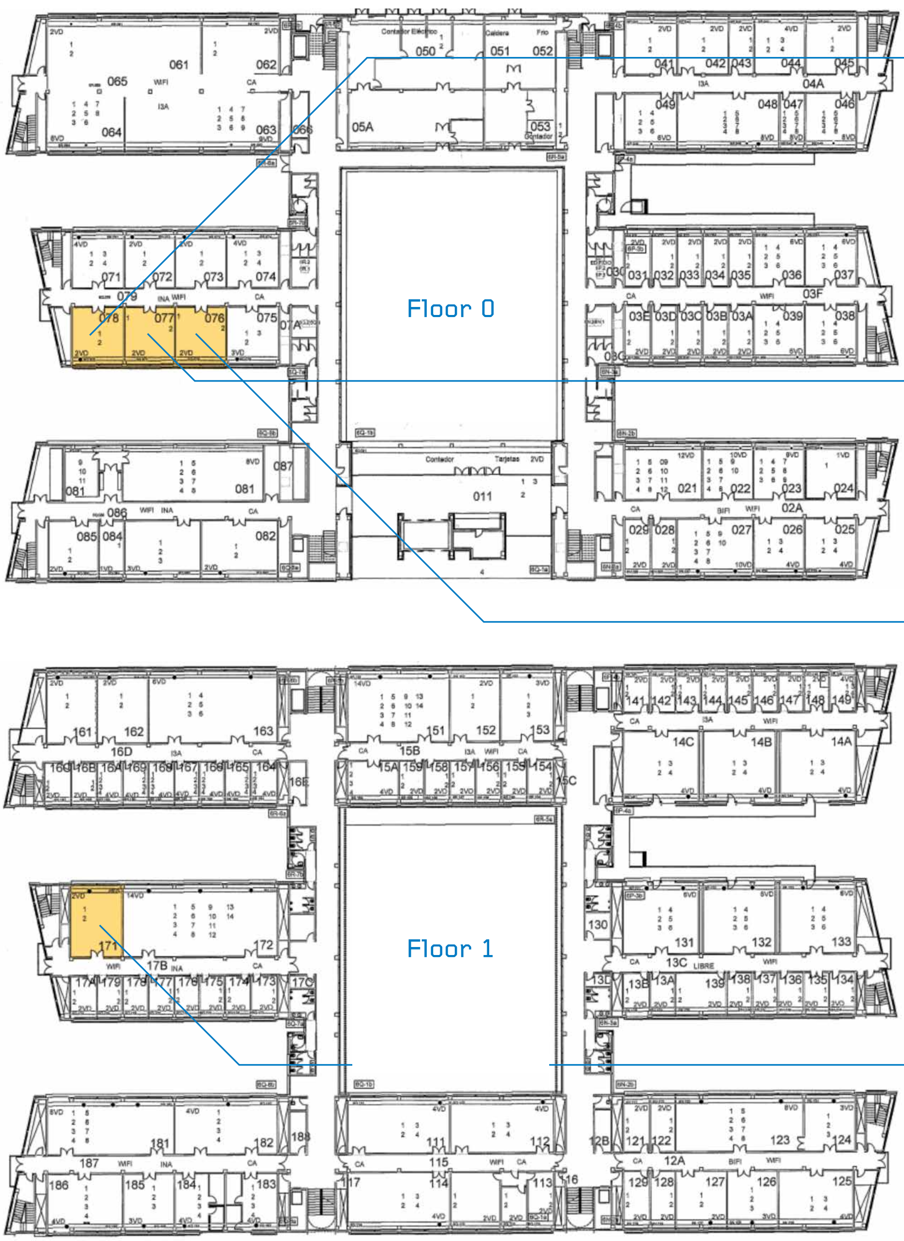

TITAN³

TITAN STEM

F30

Sample Preparation

a) Transmission Electron Microscopy Laboratories (UHRTEM snd HRTEM) & Sample Preparation

There are three HRTEM instruments working up to 300 kV available: a F30 TEM and two TITAN Cs corrected microscopes of the very last generation.

a.1) High resolution transmission electron microscope (F30) .

This 300 kV Field Emission Gun (FEG) TEM is fitted with a SuperTwin® lens allowing a point resolution of 1.9 Å. This TEM can work in TEM and STEM mode. For Z-contrast imaging in STEM mode, it is fitted with a High-Angle Annular Dark Field (HAADF) detector. This TEM is equipped for spectroscopy experiments performed either in EDS (X-Ray Microanalysis) or in Electron Energy Loss spectroscopy (EELS). For the latter, it is fitted with the "Tridiem" Gatan Energy Filter (GIF). This EELS set-up allows Energy Filtered TEM (EFTEM) images to be recorded as well as line spectra or spectrum imaging experiments to be performed. A 2K x 2K Ultrascan CCD camera (Gatan) is located before the GIF for TEM imaging. In addition to these capabilities the F30 TEM is also fitted with a Lorentz lens which permit the study of magnetic materials in an environment free of magnetic field (for magnetic domain imaging). Furthermore, the F30 allows tomography experiments to be performed both in TEM and STEM mode using a dedicated single tilt holder (+/- 70°) from Fischione.

a.2) Cs probe corrected STEM microscope (TITAN Low base) dedicated to EELS and STEM HAADF studies.

This Scanning Transmission Electron Microscope works either in TEM or in STEM mode at voltages between 60 kV and 300 kV. It can be used at low voltage to analyse electron irradiation sensitive materials. It is fitted with the last generation of a high brightness Schotky emitter developed by FEI (the so called "X-FEG" gun) a monochromator and a Gatan 2k x 2k CCD camera.

STEM: As this microscope is devoted for STEM and EELS experiments, it is equipped with a CETCOR Cs-probe corrector from CEOS Company allowing for the formation of an electron probe of 0.08 nm mean size. The TEM is equipped with all the STEM facilities (BF, DF, ADF and HAADF detectors) and 0.08 nm spatial resolution has indeed been achieved in STEM-HAADF mode.

EELS and EDS: For EELS experiments, the microscope is fitted with a Gatan Energy Filter Tridiem 866 ERS and a monochromator. An energy resolution of 0.14 eV has been recently achieved with this setup. In addition, an EDS (EDAX) detector allows performing EDX experiments in scanning mode with a spatial resolution of about ~0.2 nm.

Lorentz and holography: Beside these analytical capabilities, the Titan STEM corrected microscope is fitted with a Lorentz lens and an electrostatic biprism allowing Lorentz and medium resolution electron holography experiments to be carried out in a field-free environment (as needed for magnetic materials studies). Tomography: In addition, a tomography set-up with a +/- 70° single tilt stage permits to perform 3D analyses either in TEM or STEM modes.

a.3) Cs objective lens corrected microscope (TITAN3) dedicated to Ultra High Resolution TEM imaging

This TEM also works at voltages between 60 and 300 kV. It is located in a "box" (cube) to avoid mechanical and thermal perturbation (see figure). It contains a normal FEG (Shottky emitter) and a Gatan 2k x 2k CCD camera for (HR)TEM images acquisition.

HREM: As this microscope is devoted for High Resolution Transmission Electron Microscopy (HRTEM) studies, it is equipped with a SuperTwin® objective lens and a CETCOR Cs-objective corrector from CEOS Company allowing a point to point resolution of 0.08 nm.

STEM: In addition this Titan3 is equipped with the basic STEM facilities (BF, DF detectors) for STEM imaging at medium resolution

EELS: a Gatan Energy Filter Tridiem 863 allows Titan3 to perform EELS experiments in a standard and routine way (energy resolution of ~0.7 eV).

Lorentz and holography: As for the dedicated Titan STEM, beside these spectroscopy capabilities, the Titan3 corrected microscope is fitted with a Lorentz lens and an electrostatic biprism allowing Lorentz and medium resolution electron holography experiments to be carried on.

a.4) Sample Preparation Laboratory

TEM is based in the use of transmitted electrons to form images of the materials. However, the electron is a strongly interacting charged particle and TEM samples are required to be extremely thin (tens of nm) to be electron transparent. Some materials are inherently electron transparent (nanoparticles, nanotubes…), but most of them (bulk materials, thin films, devices…) have much larger dimensions and it is frequently required to carry out a TEM sample preparation procedure to make them thin. The LMA has set the most advanced Sample Preparation Laboratory equipped with the necessary instruments to perform this task. Among the many procedures to produce electron transparent specimens, the most important and frequently used is based on mechanical thinning of the materials in a highly controlled way. This produces a flat specimen of a few microns thickness with defect-less surfaces that afterwards follows a low-angle, low-energy ion milling of the surfaces to achieve extremely thin areas ready for TEM observation. Nowadays, this task can be also performed in many cases by means of Focused Ion Beam (FIB) techniques in the DualBeam equipment available at the LMA providing large flat electron transparent areas selected with high accuracy, which is ideal, for instance, in the TEM sample preparation of nanodevices.

Sample Preparation Laboratory

Ion mill equipment to obtain electron transparent areas in the samples for the TEM observation.

DUAL BEAM Laboratories

Dual Beam in Clean Room

µ-structural chacterization & Spectroscopy

Life Sciences

b) Dual Beam Laboratories & Microcharacterization

b.1) Dual Beams Laboratory in Clean Room

In the Clean Room facilities of the institute, several lithography facilities permit to pattern structures at the micro- and nanometer scale and to create devices. In particular, the two dual beam equipment assigned to nanolithography and lamellae preparation are placed on two concrete platforms inside the 125 m2 10000-class Clean Room.

Helios 600 dual beam equipment installed inside the Clean Room of the INA building.

Dual Beam #1

The first dual beam equipment is the Helios 600 model and has been working since December 2009 at the same place. It consists of a 30 kV field-emission scanning electron column and a 30 kV Ga focused ion beam placed at 52º one from each other. The ion column is able to work properly at low voltage (5 kV and lower), allowing the preparation of lamellae with low ion damage. Thus, in this equipment 54 lamellae have been prepared in 2011 by the technical staff, with high enough quality for atomic-resolution TEM imaging. In this equipment, there are five gas injectors as well, allowing the growth of nanodeposits with high resolution. In this equipment it has been possible to grow W-based superconducting nanodeposits with lateral size of 40 nm and Co-based ferromagnetic nanodeposits with lateral size 30 nm, these ultranarrow dimensions being at the forefront of the research in these topics.

Dual Beam #2

The second dual beam inside the Clean Room was installed in December 2010 and the model is Helios 650. Such a model is an improved version of the Helios 600 one. Thus, the SEM column has resolution of 0.9 nm and it bears a monochromator and beam deceleration. The FIB column is differentially vacuum-pumped at the lowest part, allowing a well-defined beam profile impacting on the sample surface. Preliminary results with such a column indicate that ultranarrow nanodeposits can be grown. This FIB column is nicely suited for lamellae preparation too, in combination with the Omniprobe nanomanipulator. The equipment has got 5 gas injectors and electrical microprobes. This equipment is expected to work properly for the requested main tasks: lamellae preparation and nanolithography based on ion patterning, electron beam lithography and nanodeposition.

Helios 650 equipment installed inside the Clean Room of the INA building.

Nova 200 dual beam equipment and the cryo-transfer setup, installed at INA building .

b.2) Cryogenic Dual Beam

The third dual beam equipment is used for electron sensitive materials and life sciences and has been installed in the same room as the environmental SEM and the field-emission SEM. This instrument is based on the Nova 200 model (existing in our laboratory since November 2006) but upgraded with a cryo-transfer chamber. This equipment has worked properly since 2007 and in combination with the cryo-transfer set-up is being used to produce series of ion-cuts of cells embedded in resin or frozen with the help of liquid nitrogen. These images will be used to produce 3-dimensional reconstructions. Appropriate software for 3-dimensional compositional reconstructions based on energy-dispersive x-ray micro-analysis is also included in this equipment. If needed, the equipment also holds an Omniprobe nanomanipulator for lamellae preparation as well as 5 gas injectors.

b.3) Other facilities for micro and surface characterization

Environmental SEM-FEG

An environmental SEM, model Quanta 250, is installed in the same room as the Nova 200 dual beam. The SEM column allows beam deceleration, which permits to keep resolution of 1.4 nm even at 1 kV electron landing voltage. The Quanta equipment can work under three different pressure ranges, the maximum pressure being 4000 Pa, thus close to ambient pressure. This allows observation of life-sciences samples without previous metallic coating. The equipment allows the use of a Wet-STEM, which permits to inspect samples with controlled humidity, this being crucial in life-science samples in order to maintain the same conditions as hold when functional. The equipment can also use a heater to perform observation on samples heated up to 1000 Celsius degrees.

Environmental SEM, Quanta FEG 250 equipment, installed at the INA building.

Field-emission SEM, INSPECT equipment, installed at the INA building.

SEM-FEG

The last SEM equipment, the Inspect model, is a general-purpose field-emission SEM for high-resolution imaging and composition analysis by energy-dispersive x-ray microanalysis.

Laboratory of Microstructural Characterization and Spectroscopy

> The XRD and the XPS-AES equipments are installed in the room devoted to microstructural and spectroscopy sample analysis. Those equipments have been working since 2006 and providing a great variety of useful results for most of the research groups at INA and other centres and companies mentioned later. In the following, the main characteristics of these equipments are mentioned:

> XRD (Bruker D8 Advance, four-circle diffractometer).

- Copper anode.
- Eulerian cradle.
- Parallel-beam optics.
- Incident- and diffracted-beam monochromators.
- Scintillation counter and 2D detector (GADDS).
- Analysis software and database.

> XPS-AES (Kratos):

- Analysis chamber with base pressure < 10-9 Torr
- Multi-detector energy analyser and 2D image in parallel
- Monochromator
- Ar ion milling
- Electron gun for AES
- Charge neutralizer
- Sample holder for 4-axis high-precision displacements

XRD (left image) and the XPS-AES (right image) equipment, installed at LMA

Laboratories for Local Probe Microscopy

High Magnetic Field

UHV-LT (II)

Environmental

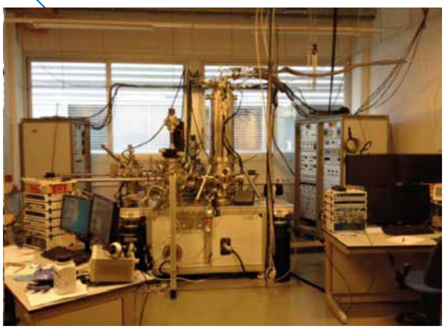

UHV-LT (I)

c) Laboratories for Local Probe Microscopy

The available facilities in the SPM section of the LMA are composed by seven SPM equipments combined in three different laboratories:

Low-temperature, ultra high vacuum (UHV-LT) probe microscopy Laboratory

The laboratory of UHV-LT is specifically designed for surface science microscopy and spectroscopy methods. The aim is to cover a wide variety of problems in surface science, from molecular chemistry to atomic magnetism. Three systems are equipped with different preparation techniques under UHV conditions, as well as equipped with large variety of epitaxial growth facilities. Force- and Tunnel-based methodologies can be combined, allowing investigating substrates with different electronic properties. The accessible temperature range for experiments is from 0.5 K to 1300 K.

The laboratory is composed by three UHV equipments hosting 4 different STM set ups, each with complementary characteristics:

c.1) Ultra low Temperature STM with axial magnetic field and variable temperature SPM.

This equipment is specifically oriented to investigate atomic scale magnetism and to high resolution spectroscopy of molecules and atoms, as well as to study the dynamics of atoms and molecules as a function of temperature. It includes two UHV STMs, one of them running at a base temperature of 1K (possibly extended down to 0.5K by using He3 as refrigerating liquid) and a variable temperature STM (from 100 K to 1300 K), with a fast and flexible measurement approach. Two chambers connected to the STMs but with independent vacuum allow the preparation of samples in situ and the epitaxial growth of organic and inorganic ultra-thin films on surfaces. The details of the equipments are the following:

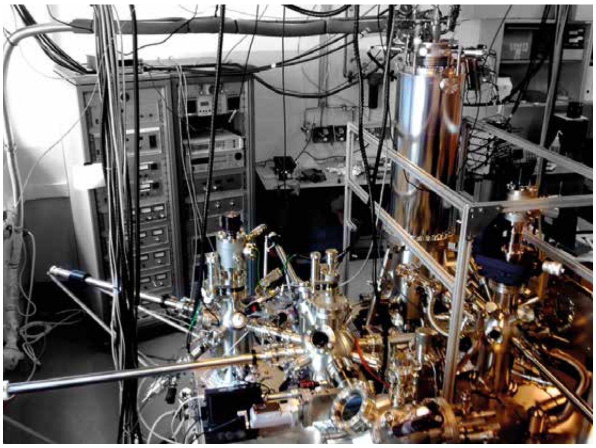

Low T STM #1:

Joule Thomson cryostat (1K-10K) UHV-STM; 3 T axial B field. Metal and organic epitaxy in situ.

Preparation:

Aarhus variable temperature (100K-1300K) STM, Non-contact-AFM

LEED/Auger characterization facilities; 9 Molecular Beam Epitaxy pockets (5 of them with fast reload option), 1 effusion cell.

c.2) Low Temperature STM in UHV.

This equipment is oriented to investigate metal-on-metal epitaxy of rare earths. It is specially oriented to the growth of magnetic thin films and nanostructures. The equipment runs at a base pressure of 4 K and has been optimized to deposition of rare-earth metals on tungsten substrates.

Low T STM #2:

Low temperature (5K) UHV STM.

Preparation:

Metal epitaxy, and LEED/Auger characterization facilities.

c.3) Low temperature STM/AFM in UHV.

Low T STM/AFM:

Low temperature (5K) UHV STM equipped with a qPlus sensor allows to correlate resonance frequency shifts of a quartz tuning fork with the gradient of forces between tip and sample.

Preparation:

Metal epitaxy, and K-cell of sublimation of organic materials.

This set up includes the last development in UHV non-contact AFM. Working at a base temperature of 5K, the use of a qPlus sensor allows to simultaneously acquire local tunneling spectroscopy and forces spectroscopy. Measurement of both forces and conductance is especially interesting in the field of molecular physics on surfaces. Force microscopy is also especially suitable to work on isolating surfaces. This experimental set up has been equipped with various methods to deposit organic materials on inorganic surfaces. The research lines are oriented to molecular interactions, self-assembly and magnetic, electronic and structural properties of hybrid metal-organic films.

c.4) Laboratory of high magnetic fields

The laboratory of high magnetic fields offers the possibility of combining probe measurements (AFM, MFM, STM) with ultra-low temperatures and a high vector magnetic field. It is composed: a variable temperature (2K-300K) STM/AFM/MFM, inserted into a large bore superconducting magnet reaching 8T/2T vector magnetic field. The equipment has a quick load facility, allowing an easy sample replacement and measurements. Additionally, a Variable Temperature module allows one to continuously change the temperature from 2 K, its lowest temperature, up to 300 K. The laboratory is especially suitable for combination of local probe and magneto-transport measurements as, for example, scanning gate microscopy. Therefore, it runs research lines oriented towards low temperature magnetism, transport through nanodevices,spintronics and superconductivity.

Several characteristics of this equipment are the following:

- AFM/MFM head with interferometric sensor.
- STM/Tuning Fork head
- Variable temperature insert (1.5K-300K) cryostat.
- 8 T (vertical) and 2 T (in-plane) superconducting magnet, combined to a rotating platform allows to apply vector fields in three dimensions.
- Compatible chip carrier with dual-beam and pulsed field facilities.

c.5) Laboratory of probe microscopies in environmental conditions

The biology, chemistry and physics community, all of them potential users of the SPM facilities, demands a set of microscopy tools with large versatility and able of working under different environmental (more real) conditions. The laboratory of probe microscopy in environmental conditions collect force and tunnel microscopies that allows a quick investigation of samples in liquid, electrolytes, or in atmosphere with controlled humidity and/or composition.

Atomic Force Microscopy

AFM is a key technique in Nanosciences, supporting multidisciplinary activities. Hence it is a central facility in the LMA. A special room with outstanding vibration isolation stages is dedicated to hold the equipments. In addition, a highly specialized technical scientist is in charge of the support to external users, training of frequent and experienced users and maintenance of the equipments. The equipments stand for their completeness. Measurements can be performed under different conditions like liquids, electrolytes, or atmosphere with controlled level of humidity. They can perform high sensitive Force spectroscopy and working under magnetic field in the Magnetic Force Microscopy mode.

Multimode 8 from Veeco-Bruker

Equipment:

1. Cervantes Fullmode SPM from Nanotec Electrónica S.L. AFM/MFM/STM equipped with variable magnetic field and liquid cell.

2. Multimode 8 from Veeco-Bruker. SPM equipped with KPM, conductive AFM, liquid and electrochemistry cells, PicoForce module for force spectroscopy measures, and variable temperature.

Cervantes Fullmode SPM from Nanotec Electrónica

Scientific Activity

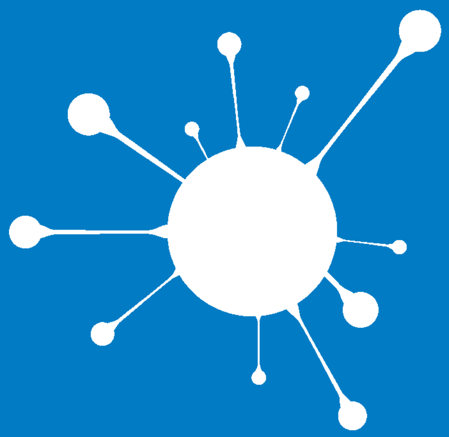

Highlights

Atomic resolution analysis of microporous titanosilicate ETS-10 through aberration corrected STEM imaging

ETS-10 is a material corresponding to the family of titanosilicates (Engelhard Corporation titanosilicate) formed by orthogonal TiO_6 octahedra and SiO_4 tetrahedra linked by corner-sharing oxygen atoms forming a three-dimensional pore system that can be used as ion exchanger, adsorption, photochemistry, membrane separation and catalysis. Due to the benefits of Z contrast it was possible to determine the Ti and Si positions on this beam sensitive material, achieving for the first time a complete atomic resolution data of the atoms conforming the framework. Moreover, novel and valuable information of the stacking faults and defects was extracted from the Cs-corrected STEM. The present results corroborate the capability of this technique to understand any zeolitic structure and provide invaluable information even about crystal growth mechanism.

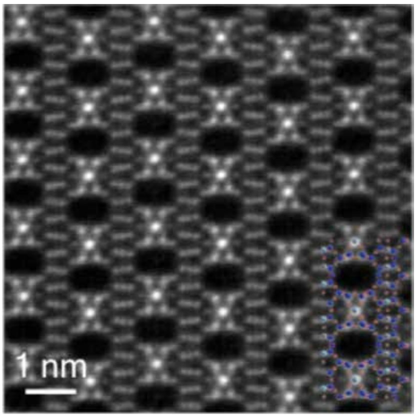

Figure caption: Cs-corrected STEM-HAADF image of ETS-10 with model, right bottom corner, superimposed, where all atoms can be identified.

Reference:

A. Mayoral, J. Coronas, C. Casado, C. Tellez, I. Díaz, Chem. Cat. Chem. 2013, 5, 2595–2598.

Highlights

Electron Tomography Studies of Platinum Nanoparticles

We have deeply studied by HAADF-STEM imaging, EDS spectroscopy and mainly electron tomography, a new class of platinum nanoparticles (NPs). These monocrystalline nanoparticles possess mono-dispersed, well-defined and complex shapes forming five-fold stars and cubic dendritic structure. The main characteristic of these NPs is their high specific surface area. These TEM works allowed better knowing the singular morphology and structure of these complex nano–objects.

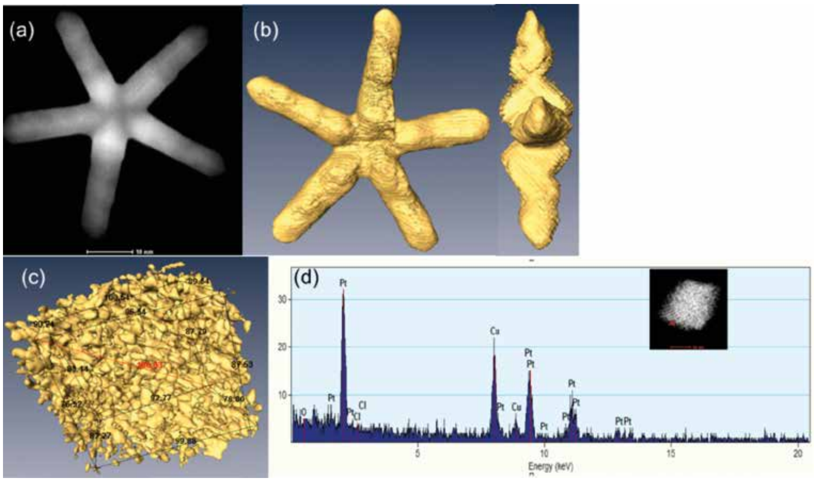

Figure caption: (a) HAADF-STEM image of a 5-fold star Pt nanoparticle (b) two different orientations of the 3D reconstruction of the same nanoparticle showing its complex morphology. (c) 3D reconstruction of a dendritic agglomerate of Pt nanoparticles. (d) EDS spectrum recorded on this agglomerate showing their Pt composition.

Reference:

L.-M. Lacroix, C. Gatel, R. Arenal, C. Garcia, S. Lachaize, T. Blon, B. Warot-Fonrose, E. Snoeck, B. Chaudret, G. Viau, "Tuning complex shapes in Pt(0) nanoparticles: from cubic dendrites to five-fold stars", Angewandte Chemie International Edition 51, 4690-4694 (2012).

Highlights

Direct Imaging of Chemical Polarity in Semiconductor Nanostructures

The polarity of the dumbbell structure semiconductors nanostructures determines decisively its growth mode and the macroscopic optoelectronic properties they present and its determination is a key issue to understand they synthesis and functionality. The TEM group of the LMA has implemented the Annular Bright Field (ABF) technique in STEM in the probe corrected Titan Low Base to directly image with 1 Å spatial resolution the chemical polarity of dumbbells composed by atoms with very different atomic number, where the conventional HAADF imaging does not resolve the light atoms and HRTEM imaging requires complex experiments and image simulations. Such is the case of the ZnO nanowires, and the GaN-AlN nanostructures shown in the figure.

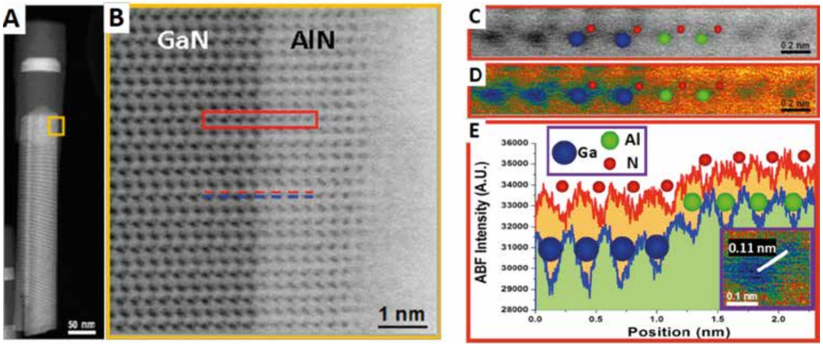

Figure caption: Polarity assignment across the interface of a heterostructured GaN-AlN wurtzite heterostructure. A) HAADF-STEM general view. B) Aberration corrected ABF-STEM in a selected region of the GaN-AlN interface (yellow rectangle). C-D) Grey scale and temperature colored detail of B (red rectangle). E) ABF intensity profile obtained across the Ga-N and Al-N dumbbell pairs from the red and blue dashed lines in B.

Reference:

M. de la Mata, C. Magén, J. Gazquez, M. Iqbal Bakti Utama, M. Heiss, S. Lopatin, F. Furtmayr, C. J. Fernández-Rojas, B. Peng, J. R. Morante, R. Rurali, M. Eickhoff, A. Fontcuberta i Morral, Q. Xiong, J. Arbiol, Nanoletters 12, 2579-86 (2012).

Highlights

Morphological modulation in Non-Planar Nanostructures grown via Van der Waals epitaxy

The role of twinning, polytypism, and polarity in the morphology of ZnTe nanostructures grown via Van der Waals epitaxy on mica substrates has been analysed by advanced imaging techniques. Van der Waals epitaxy relaxes the lattice matching requirements enabling the interfacing with the substrate of multiple crystal planes with the early stages of growth, multiplying the possibilities for smart design of growth conditions to tune the morphology of nanostructures. The morphology of these nanostructures grown is shown to be strongly influenced by the twinning density and the presence of polytypism within the nanostructures, while the growth direction is driven by the compound polarity. Flat seeds with Zn terminations give rise to nanorods, whereas octaedral seeds with Te-terminated facets produces tripods or tetrapods, the growth direction is dominated by the polarity. This work opens the possibility of growing complex architectures by a smart control of the growth conditions.

In this work, High Angle Annular Dark Field (HAADF) imaging carried out in the Titan Low Base of the LMA has enabled the determination of the crystal structure, defects and dumbbell polarity of the three different types of structures analysed: ZnTe nanorods, tripods and tetrapods, contributing decisively to determine the model of growth for each one of these nanostructures.

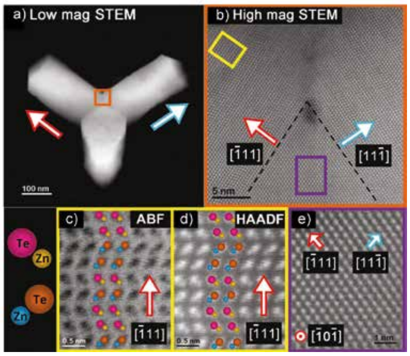

Figure caption: ZnTe tripod. a) Low magnification STEM image. b) Detail of the tripod junction, in the region as indicated with a brown square in a). c) ABF and d) HAADF image of the yellow square in b). e) The zoomed-in STEM image of region indicated by purple rectangle in (d). In all panels, the arrows mark the growth direction of the tripod branches.

Reference:

M. I. B. Utama, M. de la Mata, C. Magén, J. Arbiol, and Q. Xiong, Advanced Functional Materials 23, 1636–1646 (2013).

Highlights

Spatially Resolved EELS Analysis of Antibody Distribution on Biofunctionalized Magnetic Nanoparticles

We have used cryo-spatial-resolved electron energy loss spectroscopy (SR-EELS) for obtaining very rich information at the sub-nanometer scale on complex hybrid organic/inorganic nanomaterials: magnetic nanoparticles functionalized with a G-protein/antibody system. We showed that the functional moieties (i.e., the antibodies) are only anchored in specific areas of the surface of the nanoparticles. This result showing that the biological entities are discontinuously distributed over the nanoparticle shell is very relevant because validates our selective functionalization protocol. This will have a significant impact on biotechnological applications, as for instance biosensors, where an adequate nanoparticle functionalization approach for antibody immobilization is critical to improve the test sensitivity.

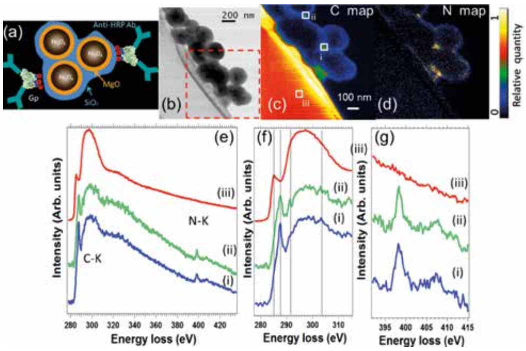

Figure caption: (a) Cartoon showing these complex hybrid organic/inorganic nanomaterials. (b) BF image of an agglomerate of biofunctionalized nanoparticles where a 300 x 300 EELS spectrum-image (SPIM) was recorded at 150 K in the marked area. (c & d) C and N chemical maps extracted, after background subtraction, from the EELS-SPIM. (e) Individual EELS spectra, after the background removal, corresponding to the sum of the spectra collected in the positions marked in panel c. (f & g) Zoom of the EELS spectra at C- and N-K edges, respectively.

References:

[1] R. Arenal, L. De Matteis, L. Custardoy, A. Mayoral, M. Tence, V. Grazu, J.M. de la Fuente, C. Marquina, M.R. Ibarra, (2013), ACS Nano 7, 4006–4013.

[2] R. Arenal, L. De Matteis, L. Custardoy, A. Mayoral, M. Tence, V. Grazu, J.M. de la Fuente, C. Marquina, M.R. Ibarra, (2013), Microscopy and Microanalysis, 19, 1628.

Highlights

Spin to charge conversion using Rashba coupling at the interface between non-magnetic materials

The Rashba effect is an interaction between the spin and the momentum of electrons induced by the spin-orbit coupling (SOC) in surface or interface states. Its potential for conversion between charge and spin currents has been theoretically predicted but never clearly demonstrated for surfaces or interfaces of metals. We have performed experiments evidencing a large spin-charge conversion by the Bi/Ag Rashba interface. We use spin pumping to inject a spin current from a NiFe layer into a Bi/Ag bilayer and we detect the resulting charge current. As the charge signal is much smaller (negligible) with only Bi (only Ag), the spin-to-charge conversion can be unambiguously ascribed to the Rashba coupling at the Bi/Ag interface. This result demonstrates that the Rashba effect at interfaces can be used for efficient charge-spin conversion in spintronics. The growth and characterization of the Bi/Ag layers have been performed at the LMA.

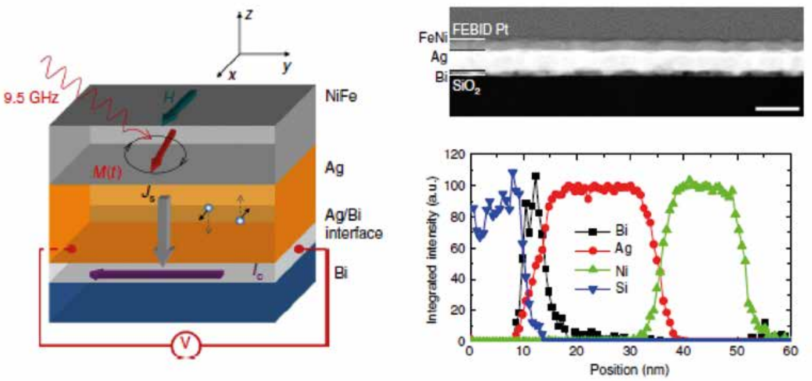

Figure caption: The left image shows a sketch of the process: First, a spin current is produced towards the Ag/Bi interface by spin pumping due to the micro-wave irradiation of a NiFe layer. Second, the Bi/Ag interface transforms such spin current in a charge current via the inverse Rashba effect. The right images show the STEM-HAADF and EDX experiments carried out on the samples at probe-corrected Titan microscope.

Reference:

J.C. Rojas Sánchez, L. Vila, G. Desfonds, S. Gambarelli, J.P. Attané, J. M. De Teresa, C. Magén, A. Fert, Nature Communications 3, 3944 (2013)

Highlights

Three dimensional magnetic nanowires grown by focused electron-beam induced deposition

We have fabricated high aspect-ratio three-dimensional (3D) Co nanowires using focused electron-beam-induced-deposition (FEBID), using $Co_2(CO)_8$. In previous studies, we proved that highly-pure cobalt 2D nanostructures can be grown by FEBID. In this work we show for the first time that 3D cobalt nanowires with ~ 85% Co can be grown by FEBID. The wires have the functional magnetic properties required for controlled motion of domain walls, opening a new route to extend the concepts of domain wall devices into the third dimension.

Moreover, this study shows two novel ways to characterize 3D nanostructures. Firstly, by growing the nanowires at an angle with respect to the substrate, direct magnetometry measurements of the wires have been performed, using magneto-optical Kerr effect. Secondly, we show a micromanipulation method to "fell" nanowires, which has allowed us to determine the mechanisms for the magnetization reversal of the wires.

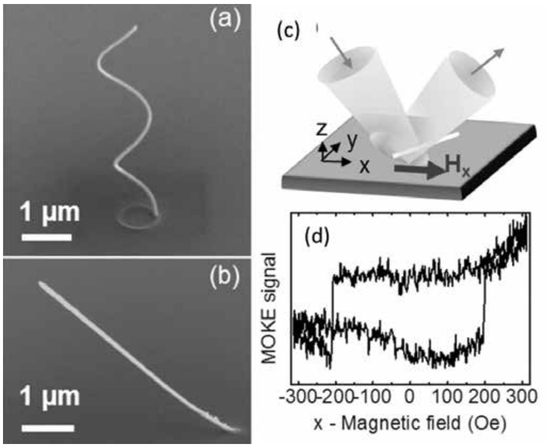

Figure caption: Two-loop (a) and (b) straight 3D Co nanowires grown by FEBID (c) MOKE experimental configuration on nanowires grown at 45 degrees. (d) MOKE loop on a single nanowire.

Reference:

Amalio Fernández-Pacheco, Luis Serrano-Ramón, Jan M. Michalik, M. Ricardo Ibarra, José M. De Teresa, Liam O'Brien, Dorothée Petit, Jihyun Lee & Russell P. Cowburn, Nature's Scientific Reports 3, 1492 (2013)

Highlights

Dissipation-free state induced by magnetic field in superconducting nanostructures

The vortex motion in superconductors usually dissipate energy leading to the degradation of them to carry electrical current with zero resistance; that is why different strategies to pin vortices have been investigated and reported in the literature so far. Here, the improvement of the vortex pinning in superconducting nanostructures at elevated temperatures and magnetic fields has been successfully studied by magnetotransport measurements (see Fig. 1). W-based superconductor ultranarrow nanowires grown by Focused Ion Beam Induced Deposition and nanopatterned TiN thin films present the re-entrance of the superconductivity under increasing magnetic fields at temperatures close to the critical one. In the case of the W-based nanowires, grown and experimentally studied at LMA, this effect is explained by the formation of a potential barrier which immobilizes one single row of vortex at the centre of the nanowire in a certain window of magnetic fields and temperatures.

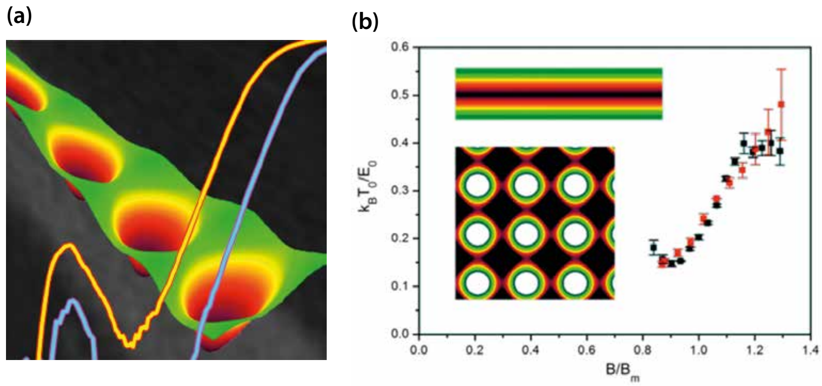

Figure 1 caption: (a) Magnetic field dependence of the resistance in a nanowire, (b) Phase slip activation barrier. The experimentally measured activation energy for the descending branch of the R(B) for the superconducting wire (black symbols) and for the perforated thin film (red symbols) as a function of the magnetic field normalized to the centre of the magnetic field region where the resistance decreases. The upper panel of the inset shows the superconducting tri-layered state in a wire. The inner (black) stripe is a nearly metallic state and the green layers show the edge-enhanced superconductivity. The lower inset panel presents corresponding superconducting state in a perforated film. The superconducting annuli surrounding the holes induce superconductivity in the interhole constrictions.

Reference:

Córdoba, R., Baturina, T.I., Sesé, J., Mironov, A.Y., De Teresa, J.M., Ibarra, M.R., Nasimov, D.A., Gutakovskii, A.K., Latyshev, A.V., Guillamón, I., Suderow, H., Vieira, S., Baklanov, M.R., Palacios, J.J., Vinokur, V.M.: Magnetic field-induced dissipation-free state in superconducting nanostructures.

Nature Communications 4, 1437 (2013) doi:10.1038/ncomms2437

Highlights

High Flux Thin Film Nanocomposite Membranes Based on Metal–Organic Frameworks for Organic Solvent Nanofiltration

Thin-film nanocomposite membranes containing a range of 50–150 nm metal-organic framework (MOF) nanoparticles [ZIF-8, MIL-53(Al), NH2-MIL-53(Al) and MIL-101(Cr)] in a polyamide (PA) thin film layer were synthesized via in situ interfacial polymerization on top of cross-linked polyimide porous supports. MOF nanoparticles were homogeneously dispersed in the organic phase containing trimesoyl chloride prior to the interfacial reaction, and their subsequent presence in the PA layer formed was inferred by a combination of contact angle measurements, FT-IR spectroscopy, SEM, EDX, XPS, and TEM. Membrane performance in organic solvent nanofiltration was evaluated on the basis of methanol (MeOH) and tetrahydrofuran (THF) permeances and rejection of styrene oligomers (PS). The effect of different posttreatments and MOF loadings on the membrane performance was also investigated..

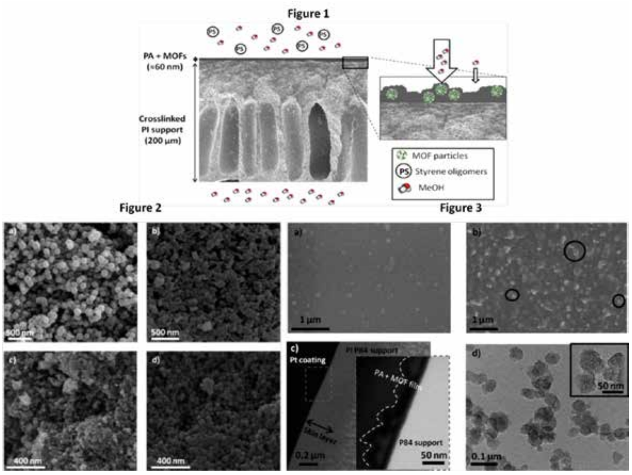

Figures caption: Figure 1: Schematic representation of the membrane. Figure 2: SEM images of (a) ZIF-8, (b) NH2-MIL-53(Al), (c) MIL- 53(Al), and (d) MIL-101(Cr) and Figure 3: (a) SEM image of thin film composite membrane surface after DMF dipping, (b) SEM image of thin film nanocomposite-MIL-101(Cr) [0.2% (w/v)] membrane surface after DMF dipping, (c) TEM image of thin film nanocomposite-MIL-101(Cr) [0.2% (w/v)] cross-section membrane lamella prepared using the FIB technique. (d) TEM image of detached PA–MIL- 101(Cr) thin film surface, where the inset is at a higher magnification.

Reference:

Sara Sorribas, Patricia Gorgojo, Carlos Téllez, Joaquín Coronas, and Andrew G. Livingston; J. Am. Chem. Soc. 2013, 135, 15201–15208.

Highlights

Yield and Shape Selection of Graphene Nanoislands Grown on Ni(111

The catalytic decomposition of hydrocarbons on transition-metal surfaces has attracted increasing interest as a method to prepare high quality graphene layers. We have studied the optimal reaction path for the preparation of graphene nanoislands of selected shape using controlled decomposition of propene on Ni(111). Scanning tunneling microscopy performed at different stages of the reaction provides insight into the temperature and dose-dependent growth of graphene islands, which precedes the formation of monolayer graphene. The effect of postreaction annealing on the morphology of the islands is studied. By adjusting the initial propene dose, reaction temperature, and postannealing procedure, islands with a triangular or hexagonal shape can be selectively obtained.

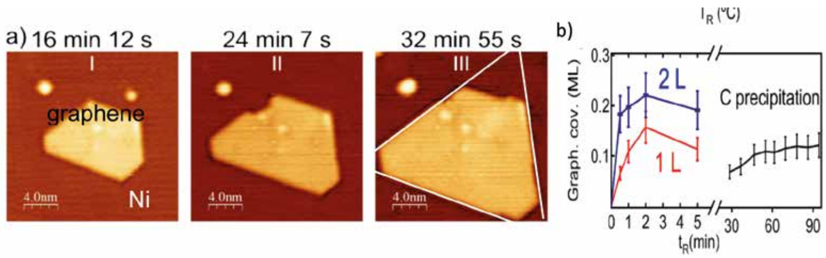

Figure caption: Growth of triangular graphene nanoislands by carbon precipitation from the bulk Ni. The sample is kept at 500 ºC during the STM experiment.

Reference:

M. Olle, G. Ceballos, D. Serrate, and P. Gambardella. Yield and Shape Selection of Graphene Nanoislands Grown on Ni(111). Nano Lett. 12, 4431-4436 (2012).

Highlights

Control of single-spin magnetic anisotropy by exchange coupling

: The properties of quantum systems interacting with their environment, commonly called open quantum systems, can be affected strongly by this interaction. We have shown that the excitation energy of a single spin, which is determined by magnetocrystalline anisotropy and controls its stability and suitability for use in magnetic data-storage devices, can be modified by varying the exchange coupling of the spin to a nearby conductive electrode. Using scanning tunneling microscopy and spectroscopy, we observed variations up to a factor of two of the spin excitation energies of individual atoms as the strength of the spin's coupling to the surrounding electronic bath changes. These observations show that exchange coupling can strongly modify the magnetic anisotropy. These effects may play a significant role in the development of spintronic devices, in which an individual magnetic atom or molecule is coupled to conducting leads.

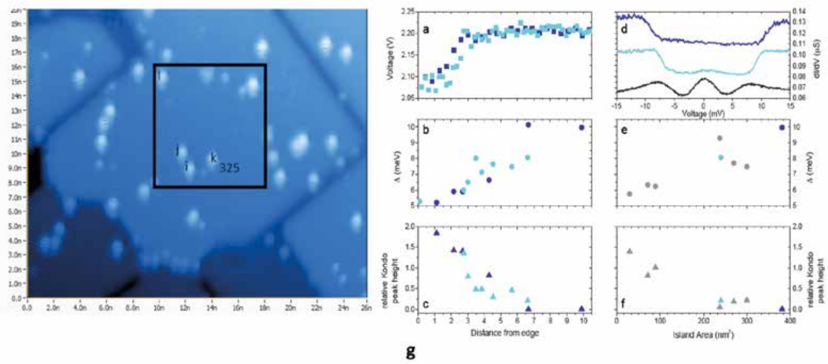

Figure caption: Island size dependence of change in exchange coupling between Co atoms and Cu(001) free electrons across a Cu2N spacing layer. (a) Energy of the centre of the gap onset extracted from high voltage dI=dV spectra on bare Cu2N vs. distance from the island edge. (b) IET step energy and (c) relative Kondo peak height (with respect to IET step height) for Co atoms on Cu2N island with areas of 18x20 nm2 (blue) and 15x16nm2 (cyan) as a function of distance from the island edge. (d) dI/dV spectra of Co atoms on Cu2N islands with areas of 18x20 nm2 (blue) and 15x16nm2 (cyan) and 5x5nm2 (black). (e) IET step energy and (f) relative Kondo peak height at the centre of Cu2N islands with different areas. Dark blue and cyan points refer to data obtained from panels b and c and were obtained at 2.5K; grey points were taken on other Cu2N islands at 5K. (g) Characteristic STM topography of Co atoms over Cu2N surface.

Reference:

Jenny C. Oberg, M. Reyes Calvo, Fernando Delgado, María Moro-Lagares, David Serrate, David Jacob, Joaquín Fernández-Rossier and Cyrus F. Hirjibehedin Nature Nanotechnology 9, 64-68 (2014).

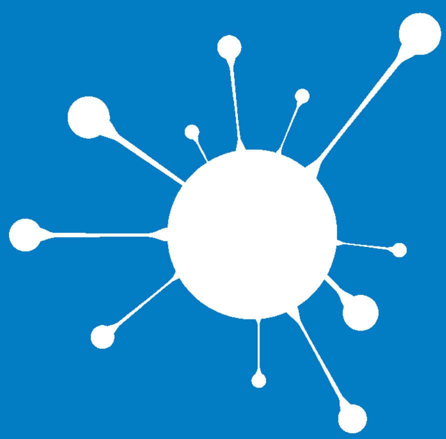

Other relevant results

Aberration-Corrected STEM Analysis of a Cubic Cd Array Encapsulated in Zeolite

Zeolites are microporous aluminosilicates formed by interconnected SiO4 and AlO4 tetrahedra, with a pore size below 2nm. Their particular structural properties have led to these materials being numbered among the most important industrial heterogeneous catalysts. Through a variety of chemical treatments, metal clusters can be located within the zeolite cages, giving potential uses in fields such as optics, electronics, photocatalysis, gas sensors or radioactive metals caption. The activity of these metallic species is directly related to their size, geometry, composition and chemical/physical environment, therefore an in-depth characterization of the clusters and of the zeolite framework is indispensable for understanding the behaviour of the materials and to underpin better and more rational design. Herein, we have exploited the ability of zeolites to capture heavy metals—cadmium—with the purpose of studying the cluster arrangement within the pores of zeolite A (LTA structure type) by means of Cs-corrected STEM. We have obtained information from the three main crystallographic orientations in order to determine the 3-dimensional conformation of the clusters.

The extremely low stability of zeolites and zeotypes under the electron beam has made extraordinary difficult to acquire atomic resolution data; which by a careful control of the electron beam current has been overcome situating the LMA as the best worldwide laboratory for characterizing this type of solids by using Cs corrected STEM microscopy.

> A. Mayoral, J. E. Readman, P. A. Anderson, J. Phys. Chem. C, 2013, 117, 24485–24489

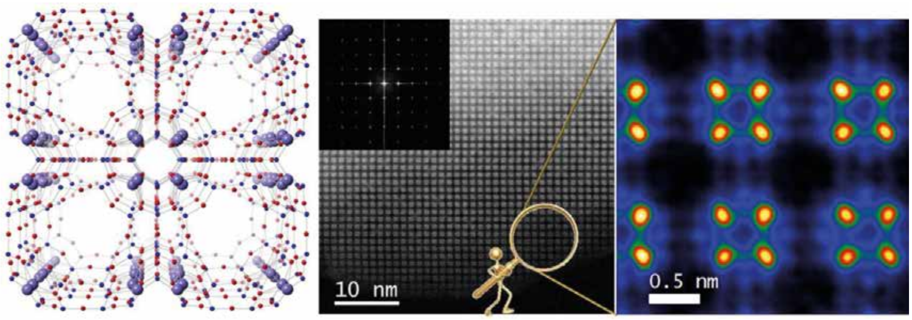

Figure caption: Model of Cd (violet) loaded zeolite A. Aberration corrected STEM image recorded along the [001] orientation and the magnified thermal colored atomic resolution image.

Location of enzyme in Lipase-SBA-12 hybrid biocatalyst

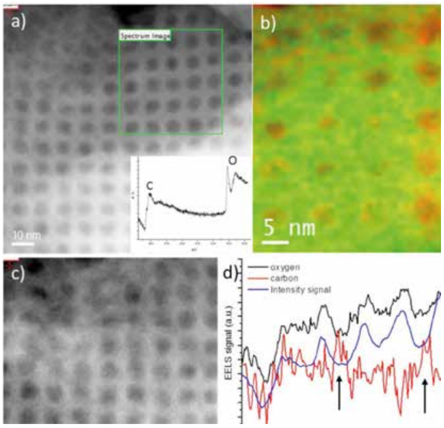

Figure caption: Spectrum image and spectrum-line analysis performed on the [100] SBA-12. a) Cs corrected STEM-HAADF, where the EELS spectrum-image has been recorded marked by a green square. Inset, the total spectrum, after background subtraction, where the different signals (C-K and O-K edges) are observed. b) Extracted spectrum image C-K edge (in red) and O-K edge (green), respectively. c) Cs corrected STEM-HAADF image with the spectrum-line marked as a green line. d) Extracted signals from the line profile in blue the intensity signal, in red the carbon and the oxygen is marked in black.

SBA-12 is an ordered mesoporous silica with cubic structure and Fm3m space group symmetry in which the enzyme lipase has been incorporated. This enzyme is particularly interesting due to their applications in stereoselective processes in the pharmaceutical industry or regioselective nutraceuticals synthesis enhancing the relevance of the process of immobilization within mesoporous matrixes. However, knowing the position of the enzyme within the mesoporous structures is complicated and the only direct method requires advanced electron microscopy methods. For this particular case, as the nature of the silica material is cubic, perfectly orientated images must be recorded in certain crystallographic orientations ([001] was used) in order to perfectly observe the pore arrangement and perform EELS analyses inside them; at 80 kV in order to minimize the beam damage that these materials suffer. All of this together, allows the observation that the enzyme was filling certain pore cages.

> A. Mayoral, R. M. Blanco, I. Diaz, J. Mol. Catal. B-Enzym., 2013, 90, 23–25.

Plamonics Studies on Nitrogen-doped Multi-Walled Carbon Nanotubes

We have studied the local dielectric/optoelectronic properties of nitrogen-doped carbon multi-walled nanotubes (CNx-MWNT) by electron energy loss spectroscopy (EELS). In order to deeply investigate these properties, we will combine these studies with very detailed analysis of the atomic configuration, spatial distribution and concentration of dopants via spatial-resolved EELS. We have analyzed the different modes and their energy shifts due to anisotropic effects, thickness, structural defects... The present study improves our knowledge of the properties of these CNx-NT and provides further insight into the potential applications of these nanomaterials.

> R. Arenal, Microscopy and Microanalysis, 19, 1230 (2013).

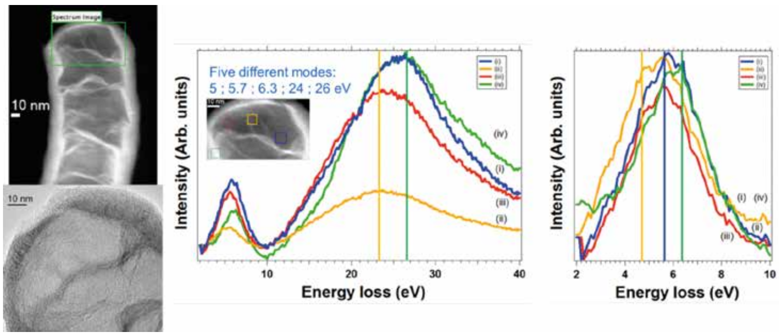

Figure caption: HAADF-STEM and HRTEM images (top and bottom respectively) of an area (the tip) of one multi-walled nitrogen doped carbon nanotube. A Low-Loss EELS spectrum-image (SPIM) has been recorded in the green area marked at the HAADF image. On the right, the spectra extracted from this SPIM are depicted; first the whole spectra after background subtraction and on the right a zoom in the spectral range of 2-10 eV. The different 5 observed modes are specified.

Designing functionalized mesoporous materials for enzyme immobilization: location of enzymes using advanced TEM techniques

Ordered mesoporous materials (OMM) belong the family of ordered solids with a pore size between 2 to 50 nm. One of the widely accepted uses of OMM is as supports of enzymes for biotechnological applications through a variety of immobilization processes. In this work it is presented two different mesoporous structures, which are able to trap enzyme molecules within their structures via two different chemical interactions. However, a great difficulty disialways arises when it comes to know whether the enzymes were inside the pores or not, and a combination of different methods have been necessary. Herein, it is presented that by combining Cs-corrected STEM-HAADF operating the microscope at 80 kV, together with electron energy loss spectroscopy the organic molecules can be located.

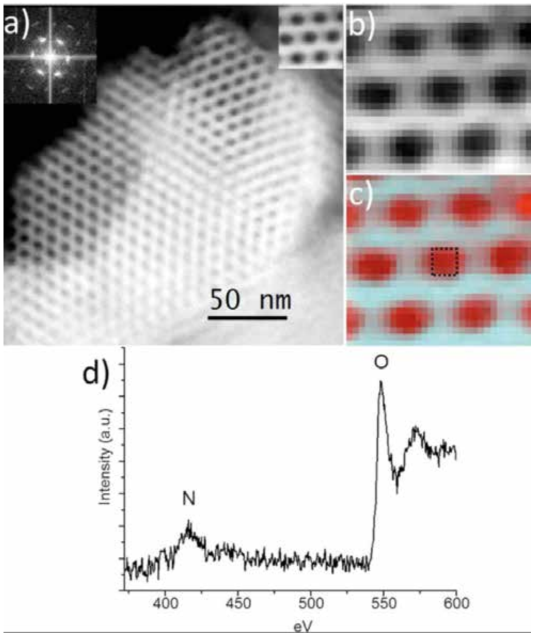

Figure caption: a) Aberration corrected STEM-HAADF image of a PMO crystal along the [001] orientation showing the hexagonal array. The FFT, left upper corner inset, confirms the 6-fold axis. On the right upper corner a magnified image of the pores is presented.

b) STEM-HAADF signal of the area analysed.

c) Map obtained from the EELS signal of the relative C/O composition (in red).

d) Sum of EEL spectra, after background subtraction, recorded in the dashed square marked in c).

One of the materials, a periodic mesoporous organosilica, was analysed by high resolution STEM together with spectrum imaging confirming that the pores were at least partially occupied with the organic material. These results corroborate the feasibility of this technique for analysing this type of beam sensitive materials when the microscope is operated at low voltages.

> A. Mayoral, R. Arenal, V. Gascón, C. Márquez-Álvarez, R. M. Blanco, I. Díaz, Chem. Cat. Chem, 2013, 5, 903–909.

Electron Tomography-EELS: development of powerful analytical tools

We have introduced the combination of electron tomography and electron energy loss spectroscopy (EELS) at low acceleration voltages to recover 3D chemical maps. We were able to reconstruct in 3D the shape (preserving their structure) and the distribution of the different components of FexCo(3-x)O4@Co3O4 mesoporous nanoparticles. Thus, EELS-tomography has been proven to be a useful tool for the characterization of nanostructures. Multivariate analysis has been the key to enable the use of the technique in beam sensitive materials with high spatial resolution.

Figure caption: a) HAADF image acquired at half through the acquisition series. b) and c) two different views of the 3D reconstruction of the HAADF images. The porous structure is clearly visible in the reconstruction. Voltex visualizations of the reconstructed volume from the extracted intensities of the background (d), O-K edge (e), Fe-L2,3 edge (f) and Co-L2,3 edge (g).

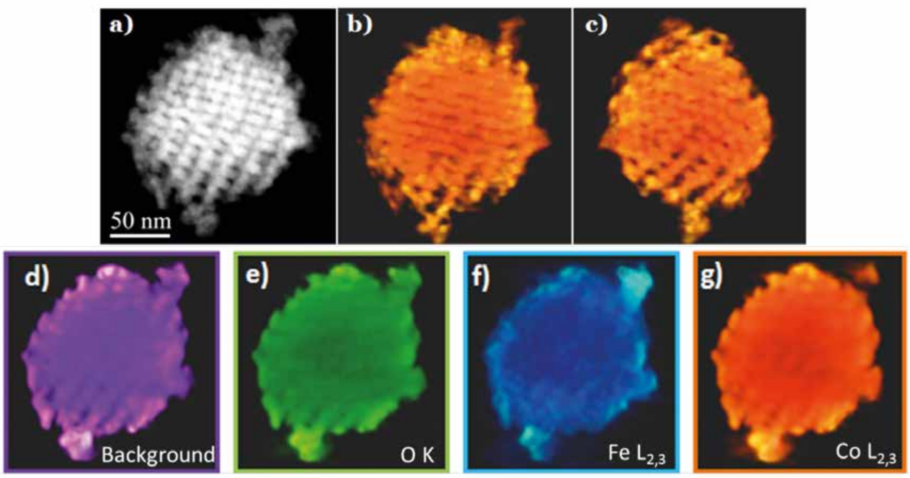

This work has been developed in collaboration with Dr. Ll. Yedra, Dr. S. Estrade and Prof. F. Peiro (U. Barcelona).

> [1] LL. Yedra, A. Eljarrat, R. Arenal, E. Pellicer, M. Cabo, A. López-Ortega, M. Estrader, J. Sort, M.D. Baró, S. Estradé, F. Peiró, "EEL spectroscopic tomography: towards a new dimension in nanomaterials analysis", Ultramicroscopy 122, 12-18 (2012).

> [2] Ll. Yedra, A. Eljarrat, R. Arenal, E. Pellicer, M. Cabo, A. López-Ortega, M. Estrader, J. Sort, M.D. Baró, S. Estradé, F. Peiró, "Recent advances in EEL spectroscopic tomography", "3D Reconstruction: Methods, Applications and Challenges", Editors: Jim Ashworth, Kenneth Brasher, Nova Publishers (2013).

On the influence of diphosphine ligands on the chemical order in small RuPt nanoparticles: combined structural and surface reactivity studies

Figure caption: Experimental aberration corrected STEM-HAADF image and the model of a bimetallic nanoparticle "protected" by diphenylphosphinobutane ligands.

Metal nanoparticles are one of the most active fields in physical, chemical, material science and nanotechnology as consequence of their particular properties they exhibit related to their size and composition. For large nanoparticles (>5 nm), the control of the chemical order within one particle is well documented but this is more complicated for small particles. Since this control is crucial for bimetallic nanoparticles, especially in catalysis, it is necessary to find efficient ways of synthesis but also to have as complete as possible characterization tools to define precisely their chemical

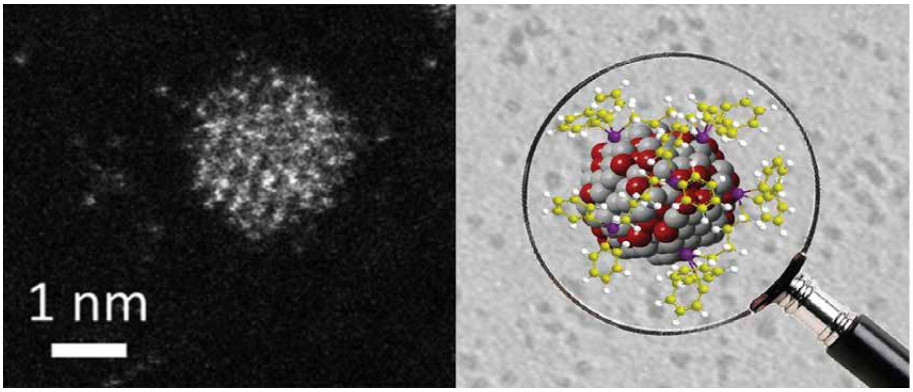

composition. In here we describe the synthesis of diphenylphosphinobutane- stabilized bimetallic RuPt nanoparticles (RuPt/dppb). The determination of the nanoparticles chemical and structural composition was achieved thanks to a combination of several characterization techniques, paying special attention to electron microscopy, associated with surface reactivity studies based on simple catalytic reactions. The complexity observed in the present structure of these nanoparticles arises from the high chemical affinity of the diphosphine ligand used as a stabilizer for both metals.

> P. Lara, T. Ayval, M. J. Casanove, P. Lecante, A. Mayoral, P. F. Fazzini, K. Philippot, B. Chaudret, Dalton Trans., 42, 372–382, (2013).

Optimization of Magnetic Domain Wall Conduit in FEBID Co Nanowires.

A close collaboration between the TEM & Dual Beam laboratories of the LMA has resulted in the succesful optimization of the growth dimensions for the best DW conduit in FEBID Co nanowires. This has been achieved by analysing quantitatively the DW nucleation and propagation by Lorentz microscopy upon in situ application of magnetic field, revealing that the optimal dimensions favoring the unambiguous DW nucleation/propagation required for applications were found in 500-nm-wide and 13-nm-thick Co nanowires. Transport-of-Intensity Equation (TIE) reconstructions from Lorentz microscopy focal series have showed that these optimal dimensions correspond to the crossover between the nucleation of transverse and vortex walls.

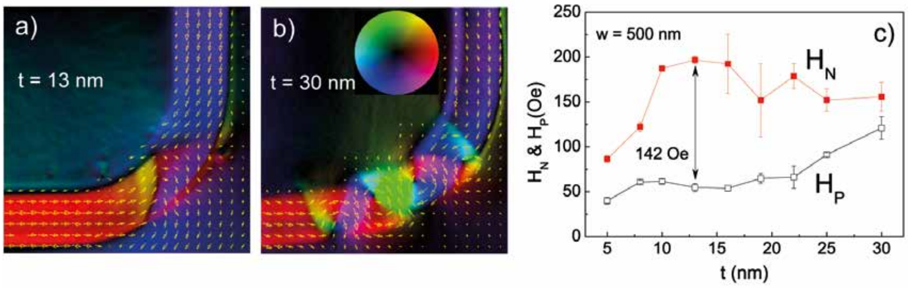

Figure caption: In situ Lorentz microscopy analysis of FEBID Co nanowires. a) TIE reconstruction of the transverse wall present in the 13-nm-thick nanowire; b) TIE reconstruction of the multiple vortex state in the 30-nm-thick nanowire. c) Thickness dependence of the nucleation and propagation fields in the series of nanowires with a width of 500 nm.

> L. A. Rodríguez, C. Magén, E. Snoeck, L. Serrano-Ramón, C. Gatel, R. Córdoba, E. Martínez-Vecino, L. Torres, J. M. De Teresa and M. R. Ibarra, Applied Physics Letters 102, 022418 (2013).

Quantitative in situ magnetization reversal studies in Lorentz microscopy and electron holography.

In situ electron microscopy is the new frontier for Electron Microscopy aiming to combine the latest technical advances of the technique with the possibility of modifying externally parameters of the sample such as the temperature, the atmosphere, the electric field or the magnetic field. The latter has been explored for at least two decades by the assistance of the microscope objective lens or by using dedicated TEM holders. In this work, a generalized procedure for the in situ application of magnetic fields by means of the excitation of the objective lens for magnetic imaging experiments in Lorentz microscopy and electron holography is quantitatively described in the Titan Cube of the LMA. A protocol for applying magnetic fields with arbitrary in-plane magnitude and orientation is presented, with several

Figure caption: Quantitative magnetization switching in a Fe-MgO-FeV magnetic tunnel junction by in situ Electron Holography. a) TEM image of the heterostructure. b) Reconstructed magnetization orientation of the junction as a function of the magnetic field. c) Magnetization hysteresis loop obtained independently from each electrode, including the correction for the magnetization component out of the sample's plane. d) Complete hysteresis loop of the magnetic tunnel junction

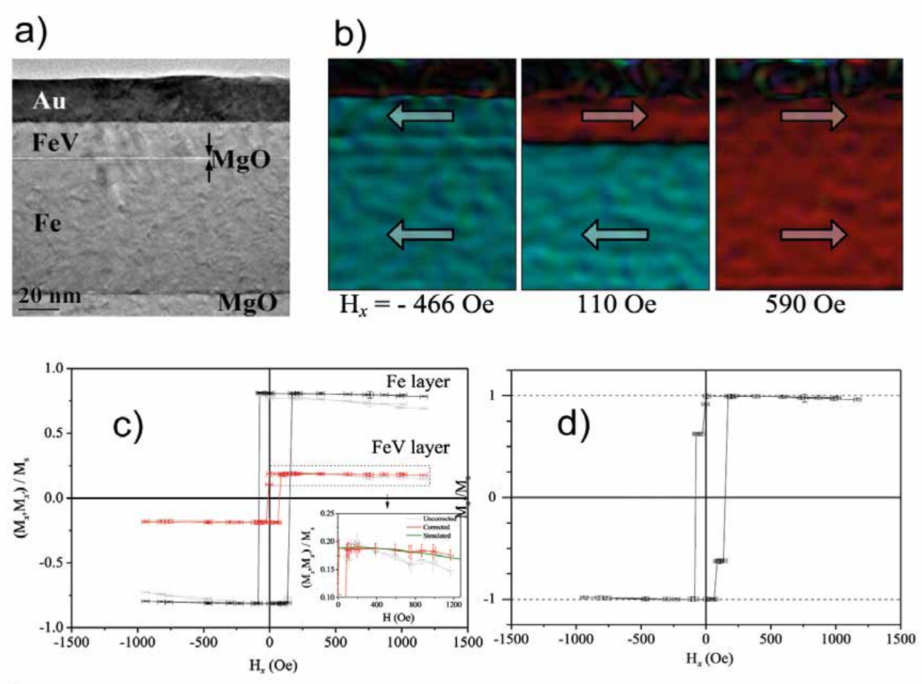

examples to demonstrate the accuracy and functionality of the methods, and a freeware script for Digital MicrographTM is provided to assist the operation of the microscope. Furthermore, a method to accurately reconstruct hysteresis loops is detailed, an example of its application is shown in the figure. We demonstrate that the out-of-plane component of the magnetic field cannot be always neglected when performing quantitative measurements of the local magnetization.

> L. A. Rodríguez, C. Magén, E. Snoeck, C. Gatel, L. Marín, L. Serrano-Ramón, J. L. Prieto, M. Muñoz, P. A. Algarabel, L. Morellon, J. M. De Teresa, and M. R. Ibarra, Ultramicroscopy 134, 144-154, (2013).

Improvement of domain wall conduit properties in cobalt nanowires by global gallium irradiation

In this work, we have systematically studied the domain wall conduit behavior, which is the difference in the nucleation and propagation fields in cobalt NWs grown by Focused Electron Beam Induced Deposition (FEBID) as a function of global gallium irradiation, for irradiation doses up to 1.24 × 1017 ions/cm2. We observe an independent evolution for both fields with the ion dose. Low doses of irradiation below 6.42·1015 ions/cm2, show a remarkable increase in the nucleation field, while the propagation field remains approximately constant. This characteristic is highly desirable for the implementation of these structures in domain wall conduit devices, stems for two different effects. Firstly, gallium irradiation produces the formation of a 20 nm-outer shell with Co crystals about twice the size of those forming the NW core, causing a net increase of the local magnetocrystalline anisotropy. Secondly the removal of the parasitic deposit coined halo and the loss of magnetic volume in the outer shell of the nanowire lead to the elimination of weak nucleation centers. This has the positive side effect of improving the shape of the wire reducing the intrinsic stochasticity of the nucleation and propagation processes. On the other hand high doses of irradiation produce physical damage in the wire, reducing the domain wall conduit and eventually leading to its loss. This apparently negative effect, have proved to be useful to create reproducible and localized domain wall pinning sites for doses above 10^{16} ions/cm2, using a Focused Ion Beam (FIB).

> L. Serrano-Ramón, A. Fernández-Pache6co, R. Córdoba, C. Magén, L. A. Rodríguez, D. Petit, R. P. Cowburn, M. R. Ibarra, J. M. De Teresa, Nanotechnology 24, 345703 (2013).

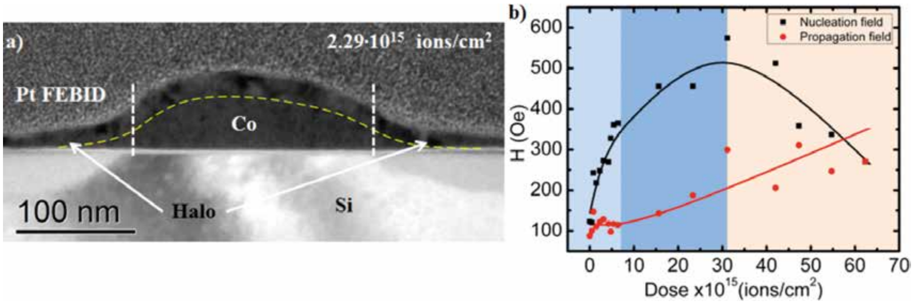

Figure caption: a) Bright field TEM of the cross sectional specimen fabricated from NWs irradiated with a dose of 2,29·10^{15} ions/cm$_2$. The yellow dashed line delimits the penetration of the Ga+ ions. The white dashed lines mark the beginning of the parasitic deposit called "halo". b) Variation of nucleation (black) and propagation field (red) as a function of the irradiation dose. The lines are guides to the eye. The three different regimes of irradiation are illustrated by changing the color of the chart: light blue for low irradiation doses, dark blue for medium irradiation doses and pale pink for high irradiation doses

Modification of domain-wall propagation in Co nanowires via Ga^+ irradiation probed by STXM experiments

The propagation of domain walls in polycrystalline Co nanowires grown by focused-electron beam-induced deposition has been explored. We have found that Ga+ irradiation via focused ion beam is a suitable method to modify the propagation field of domain walls in magnetic

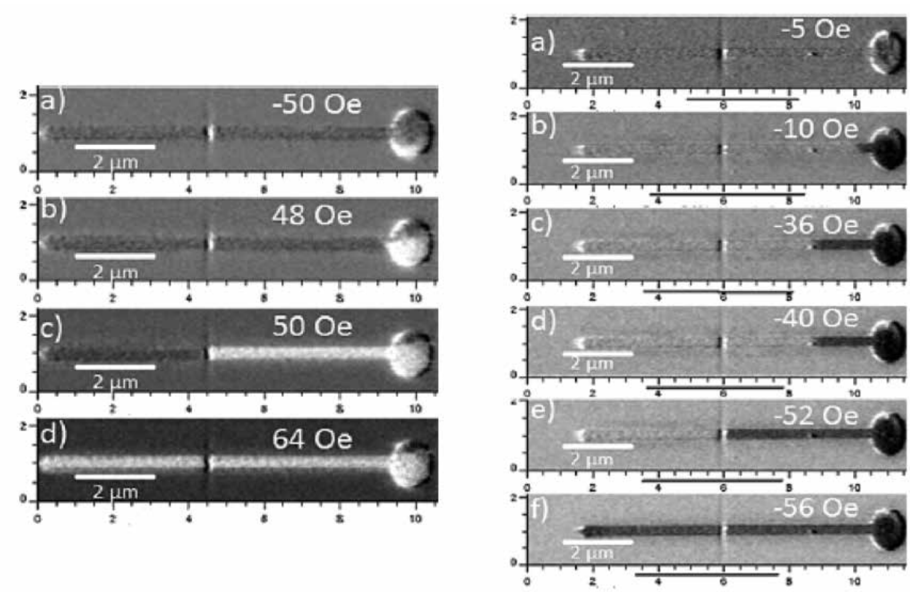

Figure caption: STXM sequences of images of the magnetization reversal in two of the devices studied with local Ga+ FIB irradiation. The left image corresponds to an irradiation dose of 4.48 × 10^{16} ions/cm2 whereas the right image corresponds to an irradiation dose of 5.97 × 10^{16} ions/cm2. In this last case, a random defect is able to pin the domain wall before reaching the central area of the nanowire.

conduits. Magneto-optical Kerr effect measurements show that global Ga^+ irradiation of the nanowires increases the domain-wall propagation field. Additionally, we have observed by means of scanning transmission X-ray microscopy (STXM) that it is possible to produce substantial domain-wall pinning via local Ga+ irradiation of a narrow region of the nanowire. In both cases, Ga^+ doses of the order of 1016 ions/cm2 are required to produce such effects. These results pave the way for the controlled manipulation of domain walls in Co nanowires via Ga^+ irradiation. The STXM experiments have been performed at Advanced Light Source (Berkeley, USA). This technique needs samples with substantial transparency to X-rays. As a consequence, a sophisticated lithography process has been carried out at LMA using silicon nitride membranes and focused beam techniques.

> L. Serrano-Ramón, A. Fernández-Pacheco, M. R. Ibarra, D. Petit, R. P. Cowburn, T. Tyliszczak, J. M. De Teresa, Eur. Phys. J. B. 86, 97 (2013).

Correlation between the magnetic imaging of cobalt nanoconstrictions and their magnetoresistance response

We present a methodology to estimate the magnetoresistance (MR) from magnetic images with nanoscale resolution. The MR of a device with a constriction can be determined from images obtained by Scanning Transmission X-ray microscopy. The MR is calculated from the y-component of the magnetization and based on the theory of anisotropic magnetoresistance (AMR) in the diffusive electrical transport regime. An excellent correlation between the MR estimated that way and the measured MR signals is obtained. Thus, we can understand the MR signals in terms of the magnetic structure of the electrodes, and correlate it with the sample thickness and constriction size.

> A Fernández-Pacheco, L E Serrano-Ramón, T Tyliszczak, K W Chou, R Córdoba, A Szkudlarek, L O'Brien, Cz Kapusta, M R Ibarra and J M De Teresa, Nanotechnology 23, 105703 (2012).

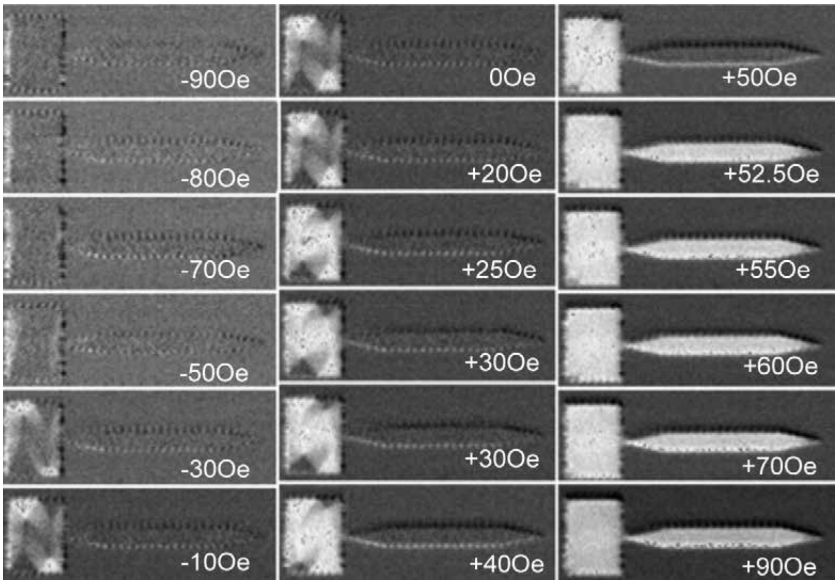

Figure caption: Room temperature STXM images of a structure as a function of the external magnetic field. The value of the x-component of the field is shown. The MR of this device is determined from the images and compared with the real MR electrically measured.

Conductance steps in electromigrated Bi nanoconstrictions

We have successfully electromigrated Bi nanoconstrictions of 150 nm in initial lateral size while imaging the nanogap formation by scanning electron microscopy. The proposed electromigration method can be useful to generate Bi nanoconstrictions with few nanometers in lateral size. Sub-quantum conductance steps have been detected before the final rupture of the constriction. These conductance steps have been confirmed by an alternative method based on focused-Ga-ion etching of the Bi nanostructures. The etching process is controlled by continuously monitoring the conductance of the nanostructure.

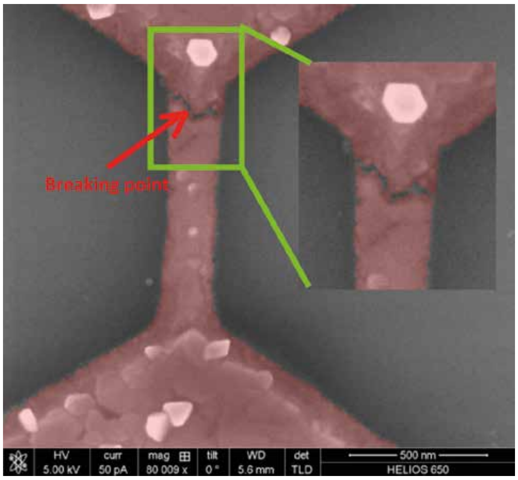

Figure caption: Scanning electron microscopy image after a typical process of electromigration performed on a Bi nanoconstriction. The arrow indicates the breaking point of the constriction.

> S. Sangiao, J. M. Michalik, L. Casado, M. C. Martínez-Velarte, L. Morellón, M.R. Ibarra and J. M. De Teresa, Phys. Chem. Chem. Phys. 15, 5132 (2013).

Thinning of organic magnetic tunnel junctions at low temperature: Cryo-dualbeam FIB preparation

We have worked on the fabrication of organic materials, which are in general highly susceptible of beam-induced damage. Optimization of working conditions regarding ion current and voltage was achieved working on low temperature conditions. This strategy opened the possibility to get the experimental conditions to avoid sample damage. Figure 1: the sample holder designed and made at LMA to produce thin lamellas of organic magnetic material for tunnel junctions, in cryo-conditions. Although few crucial steps required cryo-FIB conditions, most part of the process was carried out at room temperature.

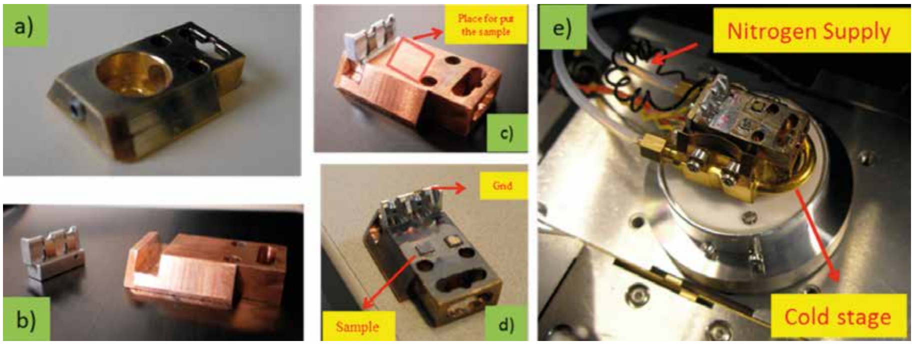

Figure 1 a) Original sample holder from Quorum Technologies b) sample holder designed and home-made in INA&LMA c) Sample holder together with grids holder d) whole sample holder, samples and grid e) whole inside to the DB chamber together with the cold stage.

In the figure 2 some TEM and EFTEM results are showed in the multilayer organic tunnel junctions.

Figure 2. TEM and EFTEM images of the following stack Si/NiFe/Al_2O_3/CCO---4 (organic) 100 nm/Al_2O_3/Co. Electrical measurements on this sample showed no short-cuts but no magnetoresistance. TEM study by B.Warot-Fonrose (CEMES, Toulouse), sample from J.F.Bobo, M.Palosse and I.Séguy (LAAS, Toulouse)

Cell toxicity induced by magnetic hyperthermia treatment

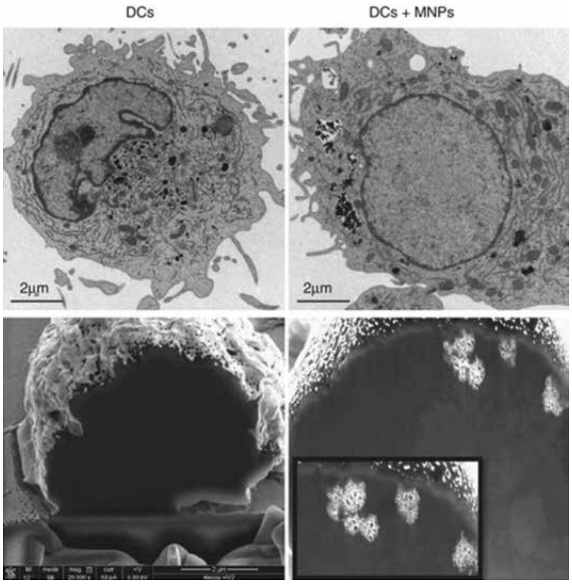

Figure 1. TEM (upper images) and dual beam etched micrographs (lower images) of DCs without MNPs as the reference sample and DCs incubated with MNPs at 50 µg Fe3O4/ml. MNPs can be observed, as black particles in TEM images and as bright particles in dual beam images, within endocytic vesicles in the cytoplasmatic region.

Magnetic hyperthermia (MH) has been used in an attempt to elucidate the mechanisms for the death of MNP-loaded cells submitted to AMF. In vitro studies have demonstrated the feasibility of inducing dramatic cell death without increasing the macroscopic temperature during AMF exposure. Here, we show that the cell death observed following AMF exposure, specifically that of MNP-loaded dendritic cells (DCs) in culture, was caused by the release of toxic agents into the cell culture supernatants and not due to a macroscopic temperature increase. We performed MH in vitro experiments to demonstrate that the supernatant of the cell culture following AMF exposure was highly toxic when added to control unloaded DCs, as this treatment led to nearly 100% cell death. It is demonstrated that heat is not the only agent responsible for triggering cell death following MH treatment. This finding offers new perspectives for the use of DCs as the proverbial Trojan horse to vectorise MNPs to the target tumour area and these results further support the use of DCs as therapeutic agents against cancer when submitted to AMF.

> Asin, L; Goya, G F; Tres, A; Ibarra, M R. Cell Death & Disease 4, E596 (2013).

Generation of Magnetized Olfactory Ensheathing Cells for Regenerative Studies in the Central and Peripheral Nervous Tissue

As olfactory receptor axons grow from the peripheral to the central nervous system (CNS) aided by olfactory ensheathing cells (OECs), the transplantation of OECs has been suggested as a plausible therapy for spinal cord lesions. The problem with this hypothesis is that OECs do not represent a single homogeneous entity, but, instead, a functionally heterogeneous population that exhibits a variety of responses, including adhesion and repulsion during cell-matrix interactions. Some studies report that the migratory properties of OECs are compromised by inhibitory molecules and potentiated by chemical gradients. We reported a system based on modified OECs carrying magnetic nanoparticles as a proof of concept experiment enabling specific studies aimed at exploring the potential of OECs in the treatment of spinal cord injuries. Our studies have confirmed that magnetized OECs (i) survive well without exhibiting stress-associated cellular responses; (ii) in vitro, their migration

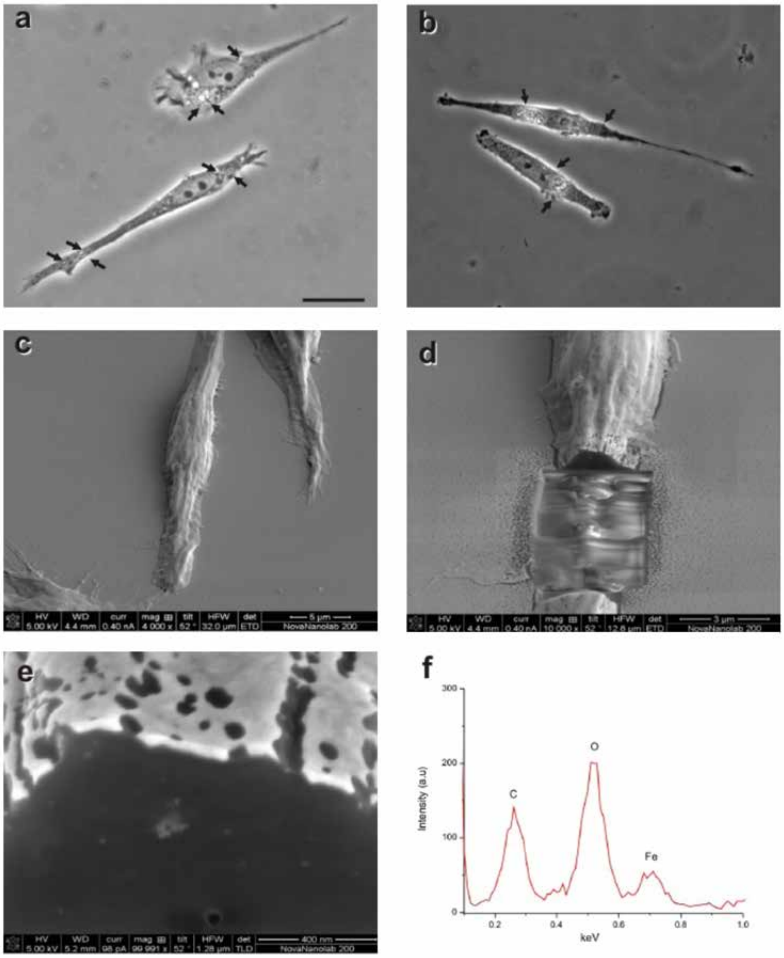

Figure 1. (a,b) Light microscopy photomicrographs of olfactory ensheathing cells (OECs)treated with 10 µg/mL (a) or 25 µg/mL (b) of MNPs (M-OECs) (arrows in a and b);(c,d) dual beam SEM/FIB images of M-OEC cells treated with 10 µg/mL of MNPs. The internalization of the MNPs can be seen in the cross section of single OEC cells (light greyspots in e) and confirmed by the Fe-content from EDS analysis of these areas (spectralanalysis in f).

can be modulated by magnetic fields; and (iii) their transplantation in organotypic slices of spinal cord and peripheral nerve showed positive integration in the model. Altogether, these findings indicate the therapeutic potential of magnetized OECs for CNS injuries.

> C. Riggio et al. Int. J. Mol. Sci., 14, 10852-10868 (2013).

Long-Lasting Antifouling Coating from Multi-Armed Polymer

We describe a new antifouling surface coating, based on aggregation of a short amphiphilic four-armed PEG-dopamine polymer into particles and on surface binding by catechol chemistry. An unbroken and smooth polymeric coating layer with an average thickness of approximately 4 ìm was formed on top of titanium oxide surfaces by a single step reaction. Coatings conferred excellent resistance to protein adhesion. Cell attachment was completely prevented for at least eight weeks, although the membranes themselves did not appear to be intrinsically cytotoxic. When linear PEG or four-armed PEG of higher molecular weight were used, the resulting coatings were inferior in thickness and in preventing protein adhesion. This

Figure caption: XPS Ti2p spectra of titanium surfaces before (black) and after (red) coating with 2 mg/ mL PEG4-dopamine solution.

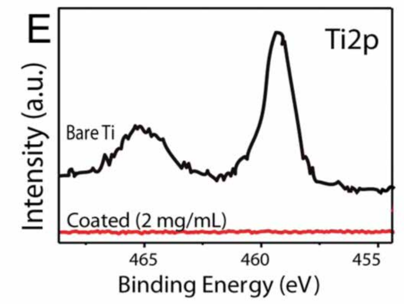

High resolution C1s spectra of bare titanium (left) and PEG4-dopamine modified surfaces at 0.5 mg/mL (middle) and 2 mg/ mL (right).

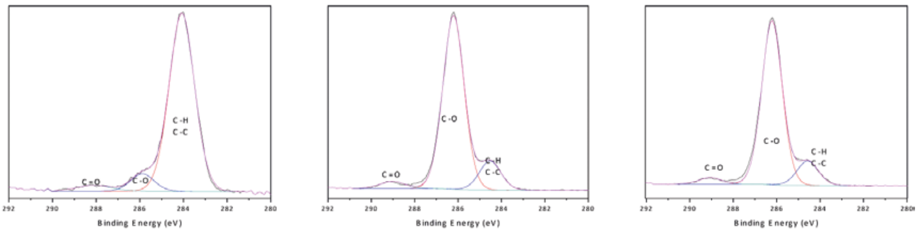

coating method has potential applicability for biomedical devices susceptible to fouling after implantation

> Boaz Mizrahi, Xiaojuan Khoo, Homer Chiang, Katalina Sher, Rose Feldman, Silvia Irusta, Robert Langer and Daniel S. Kohane. Langmuir 29, 10087-10094 (2013).

Figure caption: SEM images of (a) mesoporous silica spheres (MSSs), (b) seeded mesoporous silica spheres (MSSs) and (c) and (d) mesoporous silica–(ZIF-8) spheres (MSS–Z8)

Ordered mesoporous silica–(ZIF-8) core–shell spheres

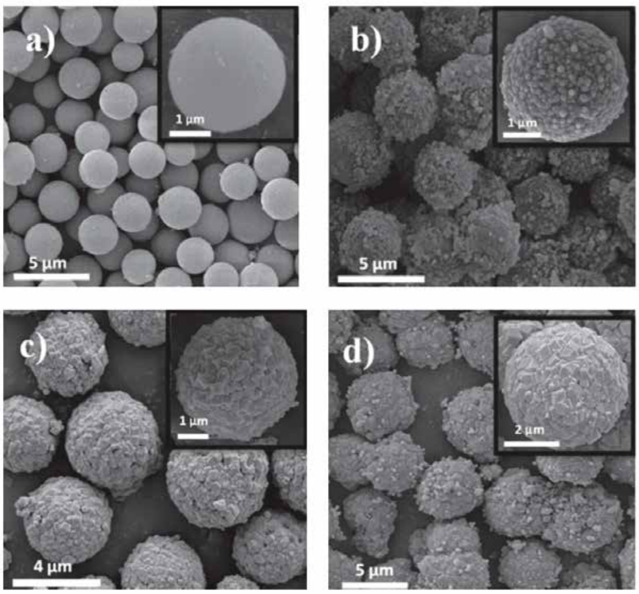

We have studied the synthesis of Silica-(ZIF-8) core-shell spheres with tuneable ordered meso-microporosity. Have been synthesized mesoporous silica–(ZIF-8) spheres (labelled MSS–Z8) at room temperature using 3 µm mesoporous silica spheres (MSSs) as the core and the template. This template, previously used to prepare hollow zeolite spheres,has high specific surface area and regular pore sizes, which make it suitable for many applications, such as separation, or magnetic materials for drug delivery. The MSS–Z8 presents two clearly differentiated phases where the hydrophobic micropore size of the Zeolite imidazolate frameworks (ZIF-8) crystallites forming the shell controls the entrance of guest molecules into the hydrophilic mesopores.

> Sara Sorribas, Beatriz Zornoza, Carlos Téllez and Joaquín Coronas. Chem. Commun., , 48, 9388–9390 (2012).

Nanostructural Characterization of Biomagnetic Cobalt Ferrite-Alginate Nanospheres

Alginate nanobeads encapsulating magnetic cobalt ferrite nanoparticles have been synthesized by an aerosol-ionotropic gelation method.
The nanobeads have been characterized in environmental-like conditions by means of advanced electron microscopy techniques (ESEM, HAADF-STEM and cryoTEM). The combination of the different electron microscopy techniques played a fundamental role for the characterization of this nanosized soft-material.

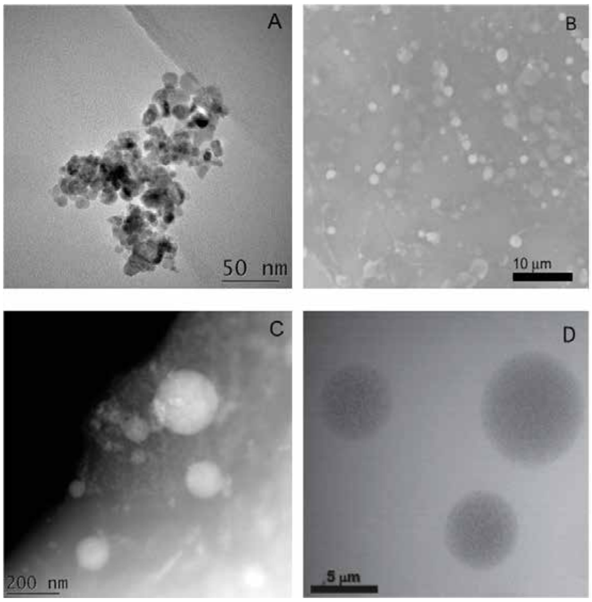

Figure caption: Electron microscopy analysis. A) BF TEM image of cobalt ferrite nanoparticles B) ESEM (under conditions: 80% relative humidity), C)STEM–HAADF images of the nanospheres; and D) ESEM analysis, Wet-STEM mode images of the nanobeads encapsulating cobalt ferrite nanoparticles (under conditions: 100% relative humidity).

> Laura De Matteis; Rodrigo Fernandez-Pacheco; Clara Marquina; M. Ricardo Ibarra; Jesus M. de la Fuente. Particle & Particle System Characterization. John Wiley & Sons, Inc., 2013.

Antimicrobial activity of Lauroyl Arginate Ethyl (LAE), against selected food-borne bacteria

The antibacterial activity of the novel antimicrobial substance, Lauroyl Arginate Ethyl (LAE) was examined against five food-borne bacteria (Staphylococcus aureus, Listeria innocua, Escherichia coli, Pseudomonas aeruginosa and Salmonella enterica). Minimum inhibitory concentration (MIC) and Minimum bactericidal concentration (MBC) determined by a broth microdilution method showed that LAE exhibit

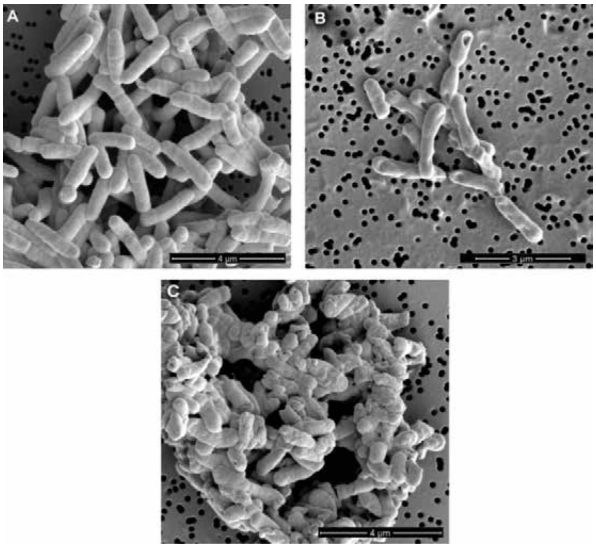

Figure caption: Scanning electron micrographs of E.coli cells. Untreated cells (A), and cells after treatment with LAE for 3 min (B) and 5 min (C).

a strong antimicrobial activity against all strains tested. This antimicrobial activity was independent of the inoculum size and remained after two heating treatments. The results obtained in the survival study demonstrated that LAE showed a fast bactericidal effect. Images of scanning electron microscope suggested that cells membranes are the principal target of LAE..

> Raquel. Becerril, Sofia. Manso, Cristina. Nerin, Rafael Gómez-Lus. Food Control. Volume 32, Issue 2, August 2013, Pages 404-408

Combined analytical and microbiological tools to study the effect on Aspergillus flavus of cinnamon essential oil contained in food packaging

Figure caption: SEM images of control samples. A, B: General view, showing normal growth of non exposed A.flavus. Many hyphae are seen covering the whole surface. C, D, E. The hyphae feature a tubular shape and have spherical, fully-formed conidiophores at the tip. F:

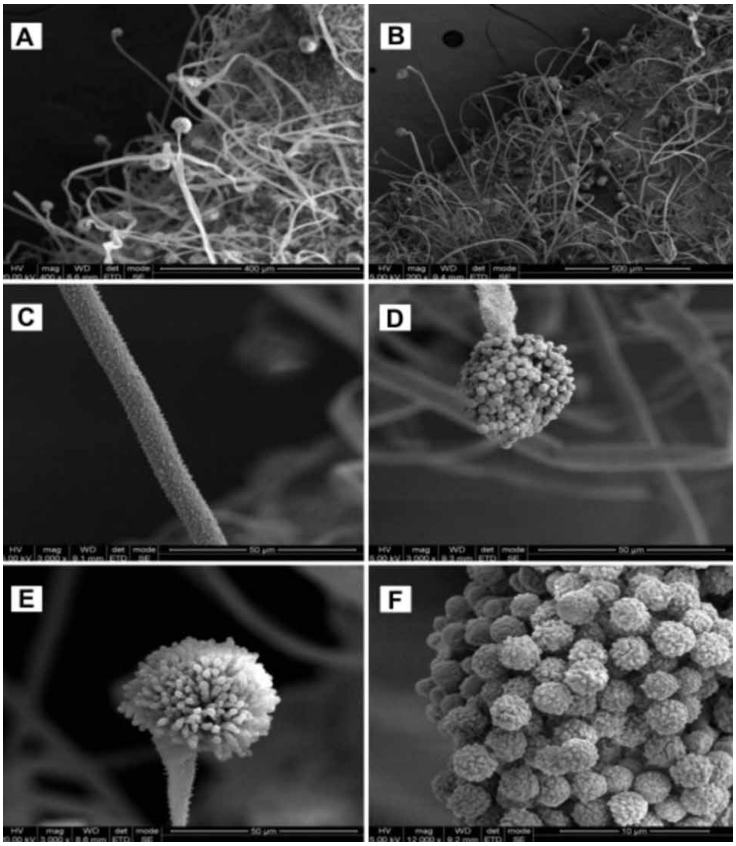

Cinnamon essential oil has been used for centuries to protect food from microbiological infection, and in the last ten years cinnamon essential oil is also incorporated into food packaging materials as antimicrobial agent. However, very little is known about the real effect that it has on the microorganism cells. This study combines analytical and microbiological tools to elucidate cell damage produced on Aspergillus flavus. SEM and FTIR were used to study the cell damage on the mold exposed to the cinnamon essential oil. Evident damage and a strong decrease in sporulation were found by SEM, while biochemical changes in conidia could be suggested from the FTIR spectra analysis. Two deposition techniques were used to prepare the samples for FTIR

> Sofia. Manso, Fernando Cacho-Nerin, Raquel. Becerril, Cristina. Nerin. Food Control.Volume 30, Issue 2, August 2013, Pages 370-378.

Halogen-Bonding Complexes Based on Bis(iodoethynyl) benzene Units: A New Versatile Route to Supramolecular Materials

Iodoalkynes [1,4-bis(iodoethynyl)benzene (p - BIB) and 1,3-bis(iodoethynyl)benzene (m -BIB)] have been used successfully to prepare halogen bonding complexes with a range of 4-pyridine derivatives showing liquid crystalline organizations. The trimeric halogen-bonded complexes obtained from p -BIB have a rod-like structure and exhibited high order calamitic phases (SmB and G). In contrast, m -BIB gives rise to bent-shaped structures that display SmAP-like mesophases. Furthermore it was found that the presence of three and five aromatic rings in these halogen-bonding complexes promotes calamitic mesophases while seven rings are required to stabilize bent-core mesophases. The formation of halogen

Scheme 1. Chemical Structures of Halogen-Bonding Donors and Acceptors Used in This Work and General Structure of the Halogen Bonded Complexes Synthesized

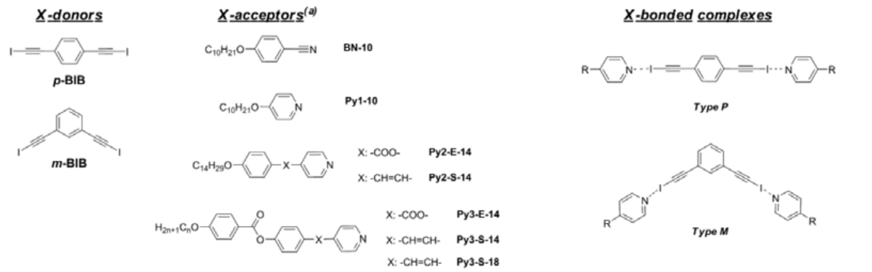

[a] **BN-10** benzonitirle derivative; **Py1-10** pyridine derivative; **Py2-E-14** two aromatic rings, ester derivative, *n*-tetradecyloxy chain; **Py2-S-14** two aromatic rings, stilbene derivative, *n*-tetradecyloxy chain; **Py3-E-14** three aromatic rings, ester derivative, *n*-tetradecyloxy chain; **Py3-S-14** three aromatic rings, stilbene derivative, *n*-tetradecyloxy chain; **Py3-S-18** two aromatic rings, stilbene derivative, *n*-octadecyloxy chain.

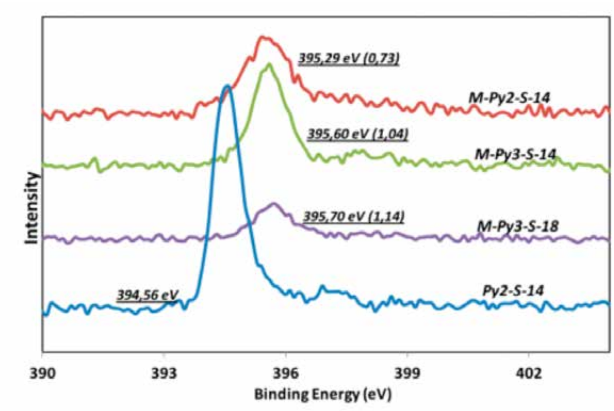

Figure caption: N1s core-level X-ray photoelectron spectra of pristine Py2-S-14 (blue) and M-type X-bonded complexes with Py2-S-14 (red), Py3-S-14 (green), and Py3-S-18 (purple). A shift to higher energy for N1s (from 0.73 to 1.16 eV) with respect to the value of the pure compound is indicative of halogen bonding formation between the constituents.

bonding in the complexes was confirmed by several techniques, including FT-IR, XPS, and single crystal X-ray diffraction and the strength of the bonds was evaluated by DFT calculations.

> Lucía González, Nélida Gimeno, Rosa María Tejedor, Victor Polo, M. Blanca Ros, Santiago Uriel, and JoséLuis Serrano. Chem. Mater., 2013, 25 (22), pp 4503–4510

Controlling the Structural and Electrical Properties of Diacid Oligo(Phenylene Ethylene) Langmuir–Blodgett Films

The preparation, characterization and electrical properties of Langmuir–Blodgett (LB) films composed of a symmetrically substituted oligomeric phenylene ethynylene derivative namely, 4,4′-[1,4-phenylene-bis(ethyne-2,1-diyl)]dibenzoic acid (OPE2A), are described. Monolayer Langmuir (L) films were transferred onto solid substrates with a transfer ratio of unity to obtain LB films. UV/Vis spectrum results together with X-ray photoelectron spectroscopic and quartz crystal microbalance experiments, conclusively demonstrate formation of onelayer LB films in which OPE2A molecules are chemisorbed onto gold substrates and consequently –COO-Au junctions are formed. In LB films prepared on a basic subphase the other terminal acid group is also deprotonated and associates with an Na+ counterion. In contrast, LB films prepared from a pure water subphase preserve the protonated acid group, and lateral H-bonds with neighboring molecules give rise to a supramolecular structure. STM-based conductance studies revealed that films prepared from a basic subphase are more conductive than the analogous films prepared from pure water, and the electrical conductance of the deprotonated films also coincides more closely with single-molecule conductance measurements.

> Luz Marina Ballesteros, Santiago Martín, Javier Cortés, Santiago Marqués-González, Simon J. Higgins, Richard J. Nichols, Paul J. Low and Pilar Cea. Chem. Eur. J. 2013, 19, 5352 – 5363

Figure caption: Figure 1 shows XPS spectra in the C 1s region of OPE2A powder and OPE2A LB films transferred onto gold substrates from the two different subphases. The powder spectrum shows carboxyl moiety. Films prepared from a basic subphase show a carboxylate carbon which clearly indicates that OPE2A is entirely deprotonated. Films prepared from a water subphase contains both carboxylate and carboxyl groups which in combination with data provided by QCM experiments and angle-resolved XPS suggests that the group attached to the gold substrate is deprotonated and chemisorbed as carboxylate, independent of the subphase used. In contrast, the other terminal carboxyl group remains protonated when the Langmuir film is prepared on a pure water subphase and is deprotonated when a basic subphase is used. Fig. 2 shows Representative C 1s XPS spectra measured at take-off angles of 90º and 60º for an OPE2A LB film prepared from pure water.

Fig. 1

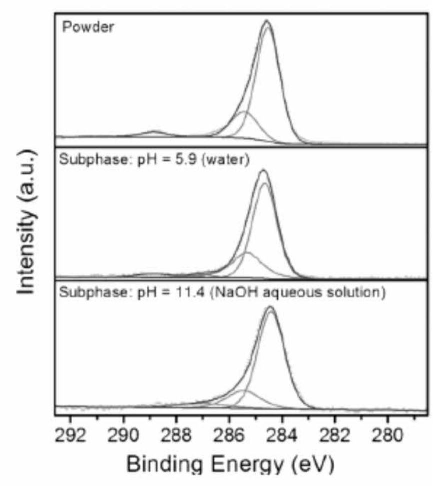

Fig. 1

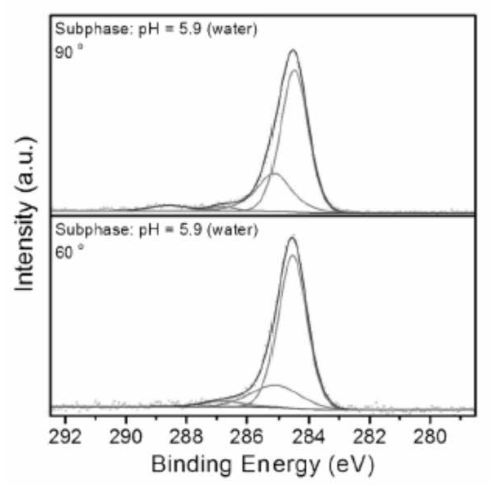

CAF@ZIF-8: one-step encapsulation of caffeine in MOF.

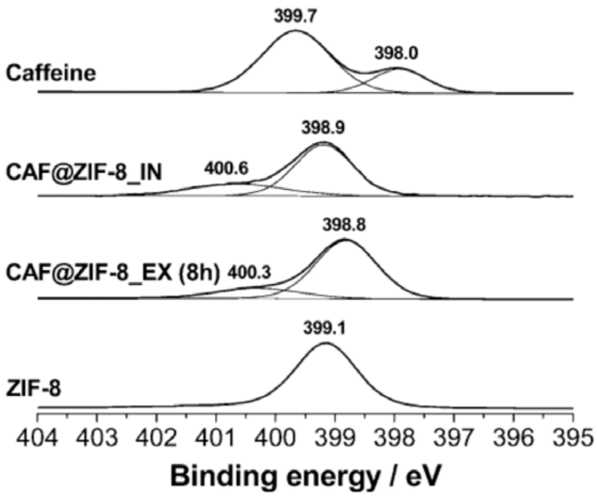

Figure caption: Two different nitrogen atoms are found in caffeine: three N–CH3 (399.7 eV) and one N=C (398.0 eV), in agreement with the peak area ratio of three found in the pure caffeine spectrum. ZIF-8 exhibits a symmetric peak (399.1 eV) indicating that there is only one form of nitrogen. In both CAF@ZIF-8 samples, a new small band appears which means that there is a displacement of the main band (N–CH3) in caffeine to 400.3 eV (ex situ) and 400.6 eV (in situ). This higher binding energy of N 1s orbital is because its charge is delocalized through the van der Waals interaction with methyl groups in ZIF-8 and the core attracts the electrons more strongly.

Two strategies for encapsulating caffeine in ZIF-8 were carried out in this work: (1) one-step, in situ encapsulation where caffeine is added to a ZIF-8 synthesis solution and the MOF structure is formed around the entrapped molecule; and (2) ex situ encapsulation whereby caffeine is put into contact with previously synthesized or purchased ZIF-8. The products obtained were analyzed with XRD, TGA, Vis-UV, GCMS, FTIR, 13C NMR, and N 1s XPS to compare both encapsulation methods. Chemical and structural evidence indicated that the preferential adsorption site of caffeine molecules inside the ZIF-8 structure is near the methyl and CH groups of 2- methylimidazole ligand. These two groups interact with caffeine by van der Waals forces with methyl groups and via CH···O hydrogen bonds with C=O groups, respectively. In addition, the one-step encapsulation of caffeine in ZIF-8 produced high guest loading (ca. 28 wt % in only 2 h at 25 °C) and controlled release (during 27 days).

> Nuria Liédana, Alejandro Galve, César Rubio, Carlos Téllez, and Joaquín Coronas ACS Appl. Mater. Interfaces, 4, 5016–5021 (2012).

Demonstration of Spin Polarized STM and first results

We have set up the spin polarized STM technique based on magnetically coated W tips. For that purpose we developed adapted heaters and full Mo tip shuttles which allow for in-situ tip exchange and choice of the magnetic sensitivity direction. We have applied this technique to the investigation of individual atomic spins over Mn/W(110) and Fe/W(110). The possibility to resolve the magnetic structure of surfaces with sub-atomic resolution grants access to the exchange coupling mechanism and strength between adatoms and magnetic surfaces, as well as in magnetic nanostructures constructed by atomic manipulation. Examples are given below.

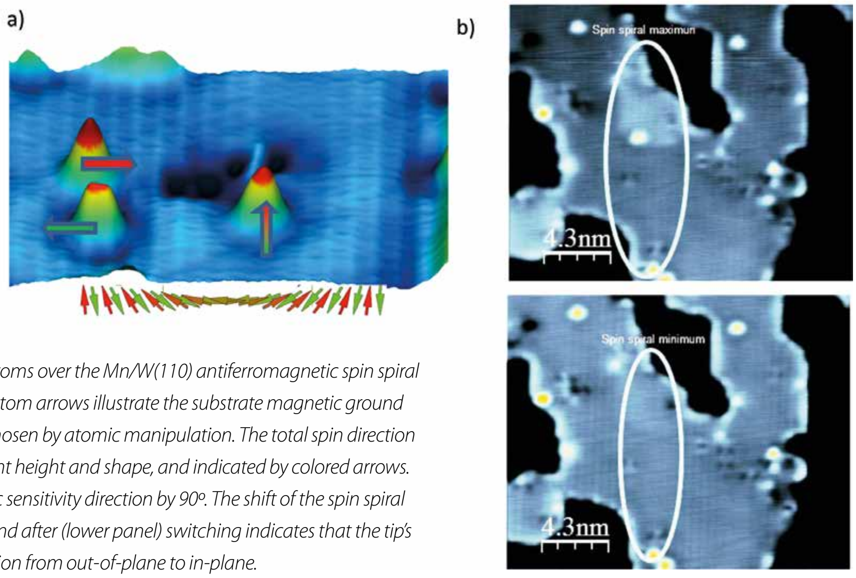

Figure caption: (a) 3D rendering of Co atoms over the Mn/W(110) antiferromagnetic spin spiral (oscillating stripped contrast in blue, bottom arrows illustrate the substrate magnetic ground state) with designated spin directions chosen by atomic manipulation. The total spin direction of the atoms is derived from the apparent height and shape, and indicated by colored arrows. (b) Controlled switch of the tip magnetic sensitivity direction by 90º. The shift of the spin spiral stripped contrast before (upper panel) and after (lower panel) switching indicates that the tip's magnetization easy axis changes direction from out-of-plane to in-plane.

Manipulation of the electronic structure in a Ruthenium complex by an STM/AFM tip

Metal- organic complexes are of high interest in a wide range of material science due to their magnetic properties. The electronic configuration of the metallic center that usually defines the magnetic state of the molecule strongly depends on the electric field induced by the coordinating ligands. Instead of axial molecular ligands we used the tip of an STM/

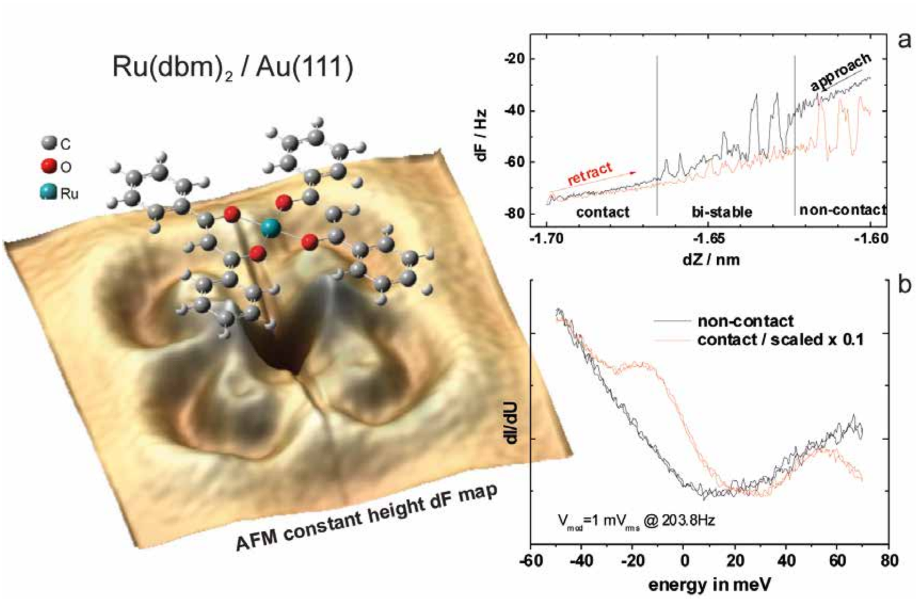

Figure caption: Left: Ru(dbm)2 molecules adsorbed on an Au(111) single crystal surface show a characteristic interaction pattern with the AFM tip mapped as frequency shift in dynamic AFM mode. In the center of the molecule a region of strong interaction is found under which the tip forms contact to the Ru ion as shown in a). After contact formation the electronic density of states changes significantly as can be seen from the corresponding dI/dU spectra in b).

AFM sensor in order to manipulate the electronic structure of the metallic center of a squared-planar Ru(dibenzoylmethanate)2 complex. With force-distance measurements we traced the interaction pathway between the Ru ion and the tip, and found a discrete jump into contact. Scanning tunneling spectroscopy revealed a change of the density of states around the Fermi level and hence a reconfiguration of the electronic states of the Ru ion after contact formation.

Ferromagnetic coupling mechanism in Fe-Phthalocyanine multi-layer assemblies on Au(111)

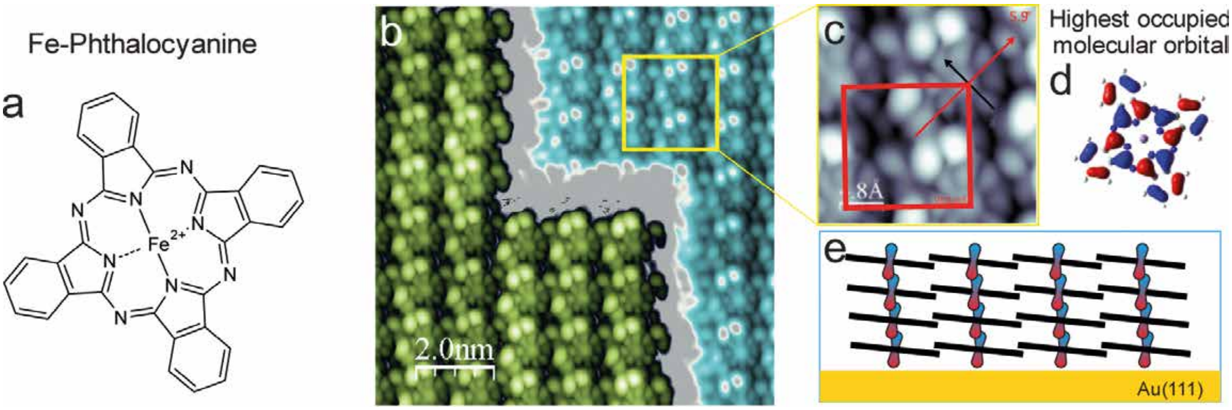

Figure caption: a) Chemical structure of a Fe-Phthalocyanine molecule, b) STM topography of two subsequent monolayers of Fe-PC on Au(111). Data are used to determine the inter-layer alignment. c) Zoom into individual Fe-PC molecules. The topography is used to determine the relative orientation of the single molecules with respect to the layer plane as well as the single layers unit cell. d) Highest occupied molecular orbital of gas-phase PC, e) relative orientation of the Fe-PC as deduced from the experimental data reveals a direct overlap of the Fe dz2 orbitals.

Molecule-based magnets form a novel class of magnetic materials. Uniquely, they combine their magnetism with electrical and optical properties that are unusual for conventional magnetic compounds. The magnetic coupling in molecule-based magnets might be mediated by a variety of different mechanisms that have to be distinguished in order to tune the material properties at wish. In multi-layer assemblies of Fe-Phthalocyanine (Fe-PC) molecules a strong inter-layer ferromagnetic coupling was found for the iron centers. By means of STM we mapped the exact alignment of the metallic centers and identified the involved magnetic interactions.

Detection of the dimer of trimers quaternary organization of C. ammoniagenes FAD synthetase at the single-molecule level and at the in cell level

Biochemical characterization of Corynebacterium ammoniagenes FADS (CaFADS) pointed to certain confusion about the stoichiometry of this bifunctional enzyme involved in the production of FMN and FAD in prokaryotes. Resolution of its crystal structure suggested that it might produce a hexameric ensemble formed by a dimer of trimers. We used atomic force microscopy (AFM) to direct imaging single CaFADS molecules bound to mica surfaces. AFM allowed solving individual CaFADS monomers, for which it was even possible to distinguish

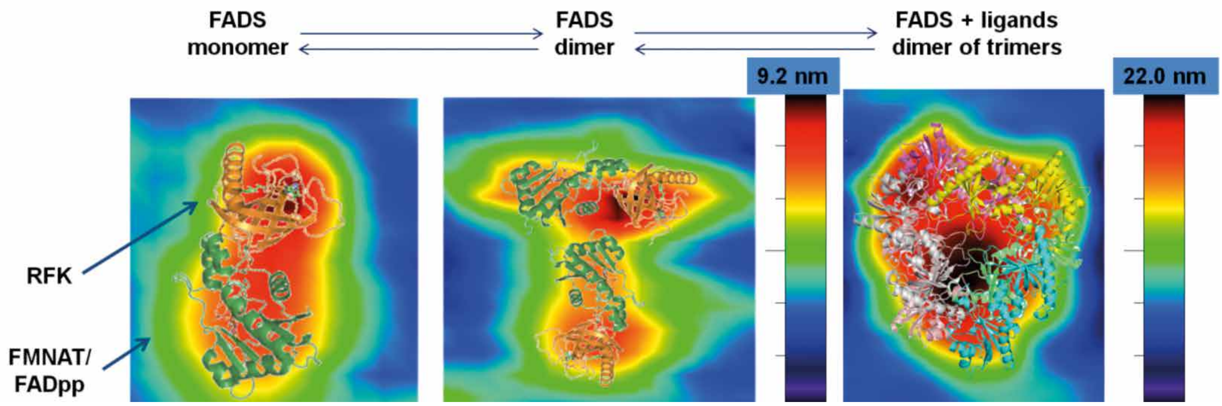

Figure Caption: Detection of the dimer of trimers quaternary organization of Corynebacterium ammoniagenes FAD synthetase at the single-molecule level and at the in cell level.

their sub-molecular individual N- and C-terminal modules in the elongated enzyme. Differences between monomers and higher stoichiometries were easily imaged, enabling us to detect formation of oligomeric species induced by ligand binding. The presence of ATP:Mg2+ particularly induced the appearance of the hexameric assembly whose mean molecular volume resembles the crystallographic dimer of trimers. Finally, the AFM results are confirmed in cross-linking solution, and the presence of such oligomeric CaFADS species detected in cell extracts. All these results are consistent with the formation of a dimer of trimers during the enzyme catalytic cycle that might bear biological relevance.

> C. Marcuello, S. Arilla, M. Medina, A. Lostao. BBA, 1834, 665-676 (2013).

An Efficient Method for Enzyme Immobilization evidenced by Atomic Force Microscopy

A new method is presented for the controlled and oriented immobilization of ordered monolayers of enzymes whose interaction site had been protected using the protein ligand. The utility of this method was demonstrated by analyzing the interactions between the enzyme Ferredoxin-NADP+ Reductase (FNR) and its redox partner Ferredoxin (Fd). The quality of the procedure was deeply evaluated through enzymatic assays and Atomic Force Microscopy. Single-Molecule Force Spectroscopy revealed that site-specifically targeted FNR samples increased the ratio of recognition events 4-fold with regard to the standard randomly-modified FNR samples. The present methodology is expected to find wide applications in surface-based protein-protein interactions biosensors, single molecule analysis, bioelectronics or drug screening.

> C. Marcuello, R. de Miguel, C. Gómez-Moreno, M. Martínez-Júlvez and A. Lostao. Protein Engineering, Design and Selection, 25(11), 715-723 (2012).

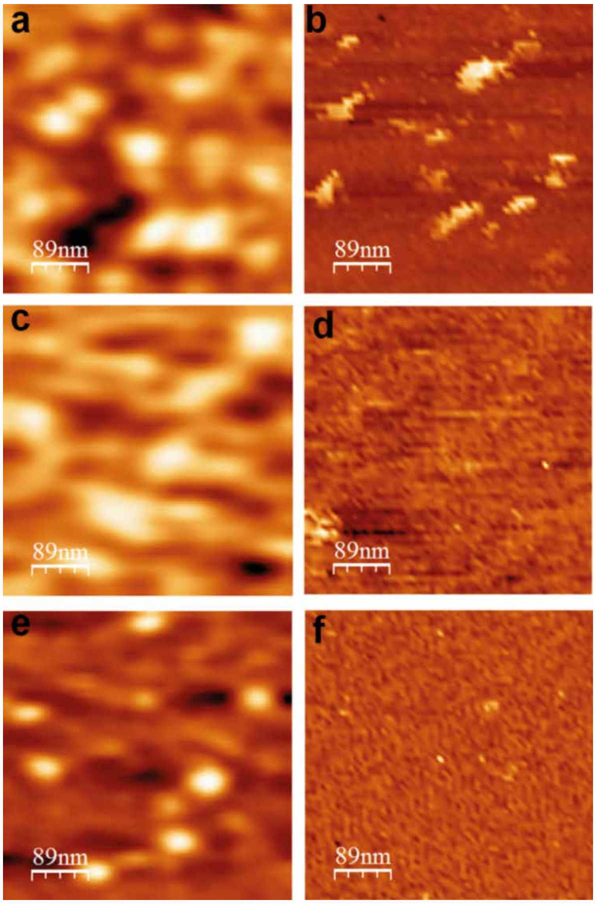

Figure Caption: Simultaneous a) topography and b) adhesion maps of a FNRc (oriented immobilized) sample. Single FNR molecules are resolved in the topography map. The high adhesion peaks in the adhesion map are due to molecular recognition events. Blocking effect after addition of free Fld into the imaging liquid cell is shown simultaneously in c) topography and d) adhesion maps. Recognition is blocked as deduced from the lack of adhesion peaks in the adhesion map. Simultaneous e) topography and f) adhesion image of a FNRr (randomly immobilized) sample. The z-axis height varies from 0 nm (black) to 8 nm (white) in the topography images. The adhesion force scale varies from 0 pN (black) to 74 pN (white) in the adhesion images. The measurements were taken in PBS using JM with functionalized Fd-tips at a scanning rate of 190 pixel s-1.

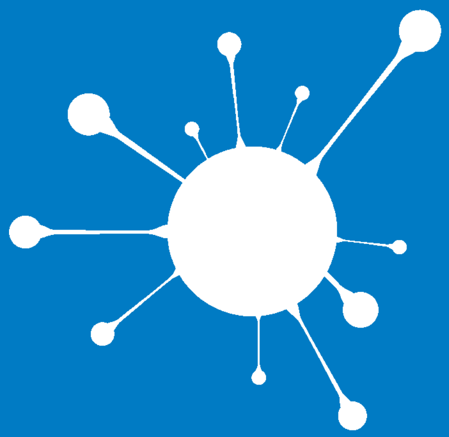

Scientific publications

1. **Self-assembled quantum dots in a nanowire system for quantum photonics.**
Heiss, M; Fontana, Y; Gustafsson, A; Wust, G; Magen, C; O'Regan, D D; Luo, J W; Ketterer, B; Conesa-Boj, S; Kuhlmann, A V; Houel, J; Russo-Averchi, E; Morante, J R; Cantoni, M; Marzari, N; Arbiol, J; Zunger, A; Warburton, R J; Fontcuberta I Morral, A
Nature Materials, 12, 5, 439-444, (2013) **IF: 35.749**

2. **Nanoscale strain-induced pair suppression as a vortex-pinning mechanism in high-temperature superconductors**
Llordes, A ; Palau, A; Gazquez, J ; Coll, M ; Vlad, R ; Pomar, A ; Arbiol, J; Guzman, R ; Ye, S ; Rouco, V ; Sandiumenge, F ; Ricart, S ; Puig, T; Varela, M ; Chateigner, D ; Vanacken, J ; Gutierrez, J ; Moshchalkov, V ; Deutscher, G ; Magen, C ; Obradors, X
Nature Materials, 11, 329-336, (2012) **IF: 32.841**

3. **Control of single-spin magnetic anisotropy by exchange coupling**
Oberg, J C; Calvo M R; Delgado, F; Moro, M; Serrate, D; Jacob, D; Fernandez-Rossier, J; Hirjibeheding, C.
Nature Nanotechnology, DOI: 10.1038/nnano.2013.264, (2013) **IF: 31.170**

4. **Surface-Confined Molecular Coolers for Cryogenics**
Lorusso, G ; Jenkins, M ; Gonzalez-Monje, P ; Arauzo, A ; Sese, J ; Ruiz-Molina, D ; Roubeau, O ; Evangelisti, M
Advanced Materials, 25, 21, 2984-2988, (2013) **IF: 14.829**

5. **Tuning Complex Shapes in Platinum Nanoparticles: From Cubic Dendrites to Fivefold Stars**
Lacroix, LM ; Gatel, C ; Arenal, R ; Garcia, C ; Lachaize, S ; Blon, T ; Warot-Fonrose, B ; Snoeck, E ; Chaudret, B ; Viau, G
Angewandte Chemie-International Edition, 51, 4690-4694, (2012) **IF: 13.455**

6. **Self-Assembled GaN Nanowires on Diamond**
Schuster, F ; Furtmayr, F ; Zamani, R ; Magen, C ; Morante, JR ; Arbiol, J ; Garrido, JA ; Stutzmann, M
Nano Letters, 12, 2199-2204, (2012) **IF: 13.198**

7. **Polarity Assignment in ZnTe, GaAs, ZnO, and GaN-AlN Nanowires from Direct Dumbbell Analysis**
de la Mata, M ; Magen, C ; Gazquez, J ; Utama, MIB ; Heiss, M ; Lopatin, S ; Furtmayr, F ; Fernandez-Rojas, CJ ; Peng, B ; Morante, JR ; Rurali, R ; Eickhoff, M ; Morral, AFI ; Xiong, QH; Arbiol, J
Nano Letters, 12, 2579-2586, (2012) **IF: 13.198**

8. **Incommensurate van der Waals Epitaxy of Nanowire Arrays: A Case Study with ZnO on Muscovite Mica Substrates**
Utama, MIB ; Belarre, FJ ; Magen, C ; Peng, B ; Arbiol, J; Xiong, QH
Nano Letters, 12, 2146-2152, (2012) **IF: 13.198**

9. **Yield and Shape Selection of Graphene Nanoislands Grown on Ni(111)**
Olle, M ; Ceballos, G ; Serrate, D ; Gambardella, P
Nano Letters, 12, 4431-4436, (2012) **IF:13.198**

10. **Spatially-Resolved EELS Analysis of Antibody Distribution on Biofunctionalized Magnetic Nanoparticles**
Arenal, R ; De Matteis, L ; Custardoy, L ; Mayoral, A ; Tence, M ; Grazu, V ; De La Fuente, JM ; Marquina, C ; Ibarra, MR
ACS Nano, 7, 5, 4006-4013, (2013) **IF: 12.062**

11. **Atomistic Description of Electron Beam Damage in Nitrogen-Doped Graphene and Single-Walled Carbon Nanotubes**
T.Susi, J. Kotakoski, R. Arenal, S. Kurasch, H. Jiang, V. Skakalova, O. Stephan, A.V. Krasheninnikov, E.I Kauppinen, U. Kaiser, J.C. Meyer
ACS Nano, 7, 7436, (2013) **IF: 12.062**

12. **Monosaccharides versus PEG-Functionalized NPs: Influence in the Cellular Uptake**
Moros, M ; Hernaez, B ; Garet, E ; Dias, JT ; Saez, B ; Grazu, V ; Gonzalez-Fernandez, A ; Alonso, C ; de la Fuente, JM
ACS Nano, 6, 1565-1577, (2012) **IF: 11.421**

13. **Atomistic Description of Electron Beam Damage in Nitrogen-Doped Graphene and Single-Walled Carbon Nanotubes**
Susi, T ; Kotakoski, J ; Arenal, R ; Kurasch, S ; Jiang, H ; Skakalova, V ; Stephan, O ; Krasheninnikov, AV ; Kauppinen, EI ; Kaiser, U ; Meyer, JC
ACS Nano, 6, 8837-8846, (2012) **IF: 11.421**

14. Design of Multifunctional Gold Nanoparticles for In Vitro and In Vivo Gene Silencing
Conde, J; Ambrosone, A ; Sanz, V ; Hernandez, Y ; Marchesano, V ; Tian, FR ; Child, H ; Berry, CC ; Ibarra, MR ; Baptista, PV ; Tortiglione, C ; de la Fuente, JM
ACS Nano, 6, 8316-8624, (2012) **IF: 11.421**

15. High Flux Thin Film Nanocomposite Membranes Based on Metal-Organic Frameworks for Organic Solvent Nanofiltration
Sorribas, S ; Gorgojo, P ; Tellez, C ; Coronas, J ; Livingston, AG
Journal of the American Chemistry Society, 135, 40, 15201-15208, (2013) **IF: 10.677**

16. Magnetic field-induced dissipation-free state in superconducting nanostructures
Cordoba, R; Baturina, T I; Sese, J; Yu Mironov, A; De Teresa, J M; Ibarra, M R; Nasimov, D A; Gutakovskii, A K; Latyshev, A V; Guillamon, I; Suderow, H; Vieira, S; Baklanov, M R; Palacios, J J; Vinokur, V M
Nature Communications, 4, 1437, (2013) **IF: 10.015**

17. 3D Analysis of the Morphology and Spatial Distribution of Nitrogen in Nitrogen-Doped Carbon Nanotubes by Energy-Filtered Transmission Electron Microscopy Tomography
Florea, I ; Ersen, O ; Arenal, R ; Ihiawakrim, D ; Messaoudi, C ; Chizari, K ; Janowska, I ; Pham-Huu, C
Journal of the American Chemical Society, 134, 9672-9680, (2012) **IF: 9.907**

18. Spin-to-charge conversion using Rashba coupling at the interface between non-magnetic materials, Rojas-Sanchez, JC; Vila, L; Desfonds, G; Gambarelli, S; Attané, JP; De Teresa, JM; Magen, C; Fert, A.
Nature Communications, 4, 2944, (2013) **IF: 10.015**

19. Twinning-, Polytypism-, and Polarity-Induced Morphological Modulation in Nonplanar Nanostructures with van der Waals Epitaxy
Utama, MIB ; de la Mata, M ; Magen, C ; Arbiol, J; Xiong, QH
Advanced Functional Materials, 23, 13, 1636-1646, (2013) **IF: 9.765**

20. Conical Spin-Spiral State in an Ultrathin Film Driven by Higher-Order Spin Interactions
Yoshida, Y ; Schroder, S ; Ferriani, P ; Serrate, D ; Kubetzka, A ; von Bergmann, K ; Heinze, S ; Wiesendanger, R
Physical Review Letters, 108, 8, 087205, (2012) **IF: 7.370**

21. Ultrathin MgO Coating of Superparamagnetic Magnetite Nanoparticles by Combined Coprecipitation and Sol-Gel Synthesis
De Matteis, L Custardoy, L Fernandez-Pacheco, R ; Magen, C ; de la Fuente, JM ; Marquina, C ; Ibarra, MR
Chemistry of Materials, 24, 451-456, (2012) **IF: 7.286**

22. Enhancing of plasmonic photothermal therapy through heat-inducible transgene activity
Cebrian, V ; Martin-Saavedra, F ; Gomez, L ; Arruebo, M ; Santamaria, J ; Vilaboa, N
Nanomedicine-Nanotechnology Biology and Medicine, 9, 5, 646-656, (2013) **IF: 6.930**

23. Laser-driven heterogeneous catalysis: efficient amide formation catalysed by Au/SiO2 systems
Pineda, A ; Gomez, L ; Balu, AM ; Sebastian, V ; Ojeda, M ; Arruebo, M ; Romero, AA ; Santamaria, J ; Luque, R
Green Chemistry, 15, 8, 2043-2049, (2013) **IF: 6.828**

24. Magnetically-driven selective synthesis of Au clusters on Fe_3O_4 nanoparticles
Sebastian, V ; Calatayud, MP ; Goya, GF ; Santamaria, J
Chemical Communications, 49, 7, 716-718, (2013) **IF: 6.378**

25. Insights into the microwave-assisted preparation of supported iron oxide nanoparticles on silica-type mesoporous materials
Balu, AM; Dallinger, D ; Obermayer, D ; Campelo, JM ; Romero, AA ; Carmona, D ; Balas, F ; Yohida, K ; Gai, PL ; Vargas, C ; Kappe, CO; Luque, R
Green Chemistry, 14, 393-402, (2012) **IF: 6.320**

26. Controlled 3D-coating of the pores of highly ordered mesoporous antiferromagnetic Co_3O_4 replicas with ferrimagnetic $Fe_xCo_{3-x}O_4$ nanolayers
Pellicer, E ; Cabo, M ; Lopez-Ortega, A ; Estrader, M ; Yedra, L ; Estrade, S ; Peiro, F ; Saghi, Z ; Midgley, P ; Rossinyol, E ; Golosovsky, IV (; Mayoral, A ; Prades, JD ; Surinach, S ; Baro, MD ; Sort, J ; Nogues, J
Nanoscale, 5, 12, 5561-5567, (2013) **IF: 6.233**

27. Structural and compositional properties of Er-doped silicon nanoclusters/oxides for multilayered photonic devices studied by STEM-EELS
Eljarrat, A ; Lopez-Conesa, L ; Rebled, JM ; Berencen, Y ; Ramirez, JM ; Garrido, B ; Magen, C ; Estrade, S ; Peiro, F
Nanoscale, 5, 9963-9970, (2013) **IF: 6.233**

28. Solution phase van der Waals epitaxy of ZnO wire arrays
Zhu, Y; Zhou, Y; Utama, MIB ; de la Mata, M ; Zhao, YY ; Zhang, Q; Peng, B (Peng, Bo) ; Magen, C ; Arbiol, J; Xiong, QH
Nanoscale, 5, 7242-7249, (2013) **IF: 6.233**

29. Reduced graphene oxide: firm support for catalytically active palladium nanoparticles and game changer in selective hydrogenation reactions
Cano, M ; Benito, AM; Urriolabeitia, EP ; Arenal, R ; Maser, WK
Nanoscale, 5, 10189-10193, (2013) **IF: 6.233**

30. Mn12 single molecule magnets coupled on micro-SQUID sensors: the role of interphases and structural modifications
E. Bellido, P. González-Monje, A. Repollés, M. Jenkins, J. Sesé, D. Drung, Th. Schurig, K. Awaga, F. Luis, D. Ruiz-Molina
Nanoscale, 5, 12565-12573, (2013) **IF: 6.233**

31. Chemical synthesis of oriented ferromagnetic LaSr-2 x 4 manganese oxide molecular sieve nanowires
Carretero-Genevrier, A ; Gazquez, J ; Magen, C ; Varela, M ; Ferain, E ; Puig, T ; Mestres, N ; Obradors, X
Chemical Communications, 48, 6223-6225, (2012) **IF: 6.169**

32. Ordered mesoporous silica-(ZIF-8) core-shell spheres
Sorribas, Sara; Zornoza, Beatriz; Tellez, Carlos; Coronas, Joaquin
Chemical Communications, 48, 8388-8390, (2012) **IF: 6.169**

33. Nanoscale mapping of plasmon resonances of functional multibranched gold nanoparticles
Mayoral, A ; Magen, C ; Jose-Yacaman, M
Chemical Communications, 48, 8667-8669, (2012) **IF: 6.169**

34. Neuronal cells loaded with PEI-coated Fe_3O_4 nanoparticles for magnetically guided nerve regeneration
Calatayud, MP ; Riggio, C ; Raffa, V ; Sanz, B ; Torres, TE ; Ibarra, MR ; Hoskins, C ; Cuschieri, A ; Wang, L ; Pinkernelle, J ; Keilhofff, G ; Goya, GF
Journal of Materials Chemistry B 1, 29, 3607-3616, (2013) **IF: 6.108**

35. Induced cell toxicity originates dendritic cell death following magnetic hyperthermia treatment
Asin, L; Goya, G F; Tres, A; Ibarra, M R
Cell Death & Disease, 4, E596, (2013) **IF: 6.044**

36. Facile synthesis of SiO_2-Au nanoshells in a three-stage microfluidic system
Gomez, L ; Arruebo, M ; Sebastian, V ; Gutierrez, L ; Santamaria, J
Journal of Materials Chemistry, 22, 21420-21425, (2012) **IF: 5.968**

37. The synergistic behavior of polyoxometalates and metal nanoparticles: from synthetic approaches to functional nanohybrid materials
S. G. Mitchell, J. M. de la Fuente
Journal of Materials Chemistry, 22, 18091-18100, (2012) **IF: 5.968**

38. Development and evaluation of 90Y-labeled albumin microspheres loaded with magnetite nanoparticles for possible applications in cancer therapy
Radovic, M, Vranjes S, Nikoli N, Jankovi D, Goya GF, Torres, TE, Calatayud MP, Bruvera IJ, Ibarra MR, Spasojevic V, Jancar B, Antic B.
Journal of Materials Chemistry, 22, 24017-24025, (2012) **IF: 5.968**

39. Suppression of three dimensional twinning for a 100% yield of vertical GaAs nanowires on silicon
Russo-Averchi, E ; Heiss, M ; Michelet, L ; Krogstrup, P ; Nygard, J ; Magen, C ; Morante, JR ; Uccelli, E ; Arbiol, J; Morral, AFI
Nanoscale, 4, 1486-1490, (2012) **IF: 5.914**

40. A ceramic microreactor for the synthesis of water soluble CdS and CdS/ZnS nanocrystals with on-line optical characterization
Gomez-de Pedro, S ; Puyol, M ; Izquierdo, D ; Salinas, I ; de la Fuente, JM ; Alonso-Chamarro, J
Nanoscale, 4, 1328-1335, (2012) **IF: 5.914**

41. Self-organized growth of GaN quantum wires on GaN-AlN nanowire templates
J. Arbiol, C. Magen, A. Chernikov, F. Furtmayr, J. Teubert, S. Chatterjee, J. R. Morante, M. Eickhoff
Nanoscale, 4, 7517-7524, (2012) **IF: 5.914**

42. In situ transmission electron microscopy observation of keV-ion irradiation of single-walled carbon and boron nitride nanotubes
Liu, ACY ; Arenal, R ; Montagnac, G
Carbon, 62, 248-255, (2013) **IF: 5.868**

43. Controlling the structural and electrical properties of diacid oligo(phenylene ethynylene) langmuir-blodgett films
Ballesteros, Luz Marina; Martin, Santiago; Cortes, Javier; Marques-Gonzalez, Santiago; Higgins, Simon J; Nichols, Richard J; Low, Paul J; Cea, Pilar
Chemistry-A European Journal, 19, 17, 5352-5363, (2013) **IF: 5.831 2013**

44. **Gold-nanobeacons for real-time monitoring of RNA synthesis**
Rosa, J ; Conde, J ; de la Fuente, JM ; Lima, JC; Baptista, PV
Biosensors & Bioelectronics, 36, 161-167, (2012) **IF: 5.602**

45. **Incorporation of boron and nitrogen in carbon nanomaterials and its influence on their structure and opto-electronical properties**
Arutyunyan, NR ; Arenal, R ; Obraztsova, ED ; Stephan, O ; Loiseau, A ; Pozharov, AS ; Grebenyukov, VV
Carbon, 50, 791-799, (2012) **IF: 5.378**

46. **Influence of the growth conditions on the defect density of single-walled carbon nanotubes**
Picher, M ; Navas, H ; Arenal, R ; Quesnel, E ; Anglaret, E ; Jourdain, V
Carbon, 50, 2407-2416, (2012) **IF: 5.378**

47. **Atomic Resolution Analysis of Microporous Titanosilicate ETS-10 through Aberration Corrected STEM Imaging**
Mayoral, A; Coronas, J; Casado, C; Tellez, C; Diaz, I
ChemCatChem, 5, 4, 2595-2598, (2013) **IF: 5.181**

48. **Accelerating the controlled synthesis of metal-organic frameworks by a microfluidic approach: A nanoliter continuous reactor**
Paseta, L ; Seoane, B ; Julve, D ; Sebastian, V ; Tellez, C ; Coronas, J
ACS Applied Materials & Interfaces, 5, 19, 9405-9410, (2013) **IF: 5.008**

49. **On the inoroporation of protic ionic liquids imbibed in large pore zeolites to polybenzimidazole membranes for high temperature proton exchange membrane fuel cells**
Eguizabal A, Lemus J, Pina MP.
Journal of Power Sources, 222, 483-492, (2012) **IF: 4.951**

50. **Thermal Diffusion at Nanoscale: From CoAu Alloy Nanoparticles to Co@Au Core/Shell Structures**
Perez, DL ; Espinosa, A ; Martinez, L ; Roman, E ; Ballesteros, C ; Mayoral, A ; Garcia-Hernandez, M ; Huttel, Y
Journal of Physical Chemistry C, 117, 6, 3101-3108, (2013) **IF: 4.814**

51. **Acetylene Used as a New Linker for Molecular Junctions in Phenylene-Ethynylene Oligomer Langmuir-Blodgett Films**
Ballesteros, LM ; Martin, S ; Momblona, C ; Marques-Gonzalez, S ; Lopez, MC ; Nichols, RJ ; Low, PJ ; Cea, P
Journal of Physical Chemistry C, 116, 9142-9150, (2012) **IF: 4.805**

52. Direct Evidence of Atomic Structure Conservation Along Ultra-Long Carbon Nanotubes
Arenal, R ; Lothman, P ; Picher, M ; Than, T ; Paillet, M ; Jourdain, V
Journal of Physical Chemistry C, 116, 14103-14107, (2012) **IF: 4.805**

53. The Growth of Ultralong ZnTe Micro/Nanostructures: The Influence of Polarity and Twin Direction on the Morphogenesis of Nanobelts and Nanosheets
Utama, MIB ; de la Mata, M ; Zhang, Q ; Magen, C ; Arbiol, J ; Xiong, QH
Crystal Growth & Design, 13, 6, 2590-2596, (2013) **IF: 4.689**

54. CAF@ZIF-8: One-step encapsulation of caffeine in MOF
Liédana, N., Galve, A., Rubio, C., Téllez, C., Coronas, J
Applied Materials and Interfaces, 4, 5016-5021, (2012) **IF: 4.525**

55. Self-assembly and luminescence of pyrazole supergelators
Moyano, S ; Serrano, JL ; Elduque, A ; Gimenez, R
Soft Matter, 8, 2799-2806, (2012) **IF: 4.390**

56. Probing the Relationship between Silicalite-1 Defects and Polyol Adsorption Properties
Mallon, EE ; Jeon, MY ; Navarro, M ; Bhan, A ; Tsapatsis, M
Langmuir, 29, 22, 6546-6555, (2013) **IF: 4.187**

57. L- and D-Proline Adsorption by Chiral Ordered Mesoporous Silica
Casado, C ; Castan, J ; Gracia, I ; Yus, M ; Mayoral, A ; Sebastian, V ; Lopez-Ram-de-Viu, P ; Uriel, S ; Coronas, J
Langmuir, 28, 6638-6644, (2012) **IF: 4.186**

58. Tailoring the Synthesis and Heating Ability of Gold Nanoprisms for Bioapplications
Pelaz, B ; Grazu, V ; Ibarra, A ; Magen, C ; del Pino, P ; de la Fuente, JM
Langmuir, 28, 8965-8970, (2012) **IF: 4.186**

59. Nanostructured electrolyte membranes based on zeotypes, protic ionic liquids and porous PBI membranes: Preparation, characterization and MEA testing
Eguizabal, A ; Lemus, J ; Roda, V ; Urbiztondo, M ; Barreras, F ; Pina, MP
International Journal of Hydrogen Energy, 37, 7221-7234, (2012) **IF: 4.054**

60. Surface functionalization for tailoring the aggregation and magnetic behaviour of silica-coated iron oxide nanostructures.
Roca, A G; Carmona, D; Miguel-Sancho, N; Bomati-Miguel, O; Balas, F; Piquer, C; Santamaria, J
Nanotechnology, 23, 155603, (2012) **IF: 3.979**

61. Synthesis and characterization of ultra-small magnetic FeNi/G and NiCo/G nanoparticles
Castrillon, M; Mayoral, A; Magen, C; Meier, J G; Marquina, C; Irusta, S; Santamaria, J
Nanotechnology, 23, (2012) **IF: 3.979**

62. Correlation between the magnetic imaging of cobalt nanoconstrictions and their magnetoresistance response
Fernandez-Pacheco, A ; Serrano-Ramon, LE ; Tyliszczak, T ; Chou, KW ; Cordoba, R ; Szkudlarek, A ; Brien, LO ; Kapusta, C ; Ibarra, MR ; De Teresa, JM
Nanotechology, 23, 105703, (2012) **IF: 3.979**

63. Transient magnetic birefringence for determining magnetic nanoparticle diameters in dense, highly light scattering media
Kober, M ; Moros, M ; Grazu, V ; de la Fuente, JM ; Luna, M ; Briones, F
Nanotechnology, 23, 155501, (2012) **IF: 3.979**

64. Functionalized Fe3O4@Au superparamagnetic nanoparticles: in vitro bioactivity
Salado, J ; Insausti, M ; Lezama, L ; de Muro, IG ; Moros, M ; Pelaz, B ; Grazu, V ; de la Fuente, JM ; Rojo, T
Nanotechnology, 23, 315102, (2012) **IF: 3.979**

65. Use of a polyol liquid collection medium to obtain ultrasmall magnetic nanoparticles by laser pyrolysis
Martinez, G ; Malumbres, A ; Mallada, R ; Hueso, JL ; Irusta, S ; Bomati-Miguel, O ; Santamaria, J
Nanotechnology, 23, 425605, (2012) **IF: 3.979**

66. Use of a polyol liquid collection medium to obtain ultrasmall magnetic nanoparticles by laser pyrolysis
Martinez, G ; Malumbres, A ; Mallada, R ; Hueso, JL ; Irusta, S ; Bomati-Miguel, O ; Santamaria, J
Nanotechnology, 23, 425605, (2012) **IF: 3.979**

67. Tailoring the physical properties of thin nanohole arrays grown on flat anodic aluminum oxide templates
Leitao, DC ; Ventura, J ; Sousa, CT ; Teixeira, JM ; Sousa, JB ; Jaafar, M ; Asenjo, A ; Vazquez, M ; De Teresa, JM ; Araujo, JP
Nanotechnology, 23, 425701, (2012) **IF: 3.979**

68. Preparation of side-chain liquid crystalline Azopolymers by CuAAC postfunctionalization using bifunctional azides: Induction of chirality using circularly polarized light
Royes, J ; Rebole, J ; Custardoy, L ; Gimeno, N ; Oriol, L ; Tejedor, RM ; Pinol, M
Journal of Polymer Science Part A-Polymer Chemistry, **50**, 1579-1590, (2012) **IF: 3.919**

69. Application of ETS-10 microporous titanosilicate as support of Ru nanoparticles for hydrogen production
Faroldi, BM Lombardo, EA Cornaglia, LM ; Irusta, S
Applied Catalysis A-General, 417, 43-47, (2012) **IF: 3.903**

70. Microwave-assisted mild-temperature preparation of neodymium-doped titania for the improved photodegradation of water contaminants
Gomez, V ; Balu, AM ; Serrano-Ruiz, JC ; Irusta, S ; Dionysiou, DD ; Luque, R ; Santamaria, J
Applied Catalysis A-General, 417, 47-52, (2012) **IF: 3.903**

71. Nanoporous silicalite-only cantilevers as micromechanical sensors: Fabrication, resonance response and VOCs sensing performance
Pellejero, I ; Agusti, J ; Urbiztondo, MA ; Sese, J ; Pina, MP ; Santamaria, J ; Abadal, G
Sensors and Actuators B-Chemical, 168, 74-82, (2012) **IF: 3.898**

72. Detection of organic vapours with Si cantilevers coated with inorganic (zeolites) or organic (polymer) layers
Urbiztondo, MA ; Peralta, A ; Pellejero, I ; Sese, J ; Pina, MP ; Dufour, I; Santamaria, J
Sensors and Actuators B-Chemical, 171, 822-831, (2012) **IF: 3.898**

73. Crystallization in THF: the possibility of one-pot synthesis of mixed matrix membranes containing MOF MIL-68(Al)
Seoane, B ; Sebastian, V Tellez, C Coronas, J
CrystEngComm, 15, 45, 9483-9490, (2013) **IF: 3.879**

74. Low frequency noise in $La_{0.7}Sr_{0.3}MnO_3$ based magnetic tunnel junctions
Guerrero, R ; Solignac, A ; Fermon, C ; Pannetier-Lecoeur, M ; Lecoeur, P ; Fernandez-Pacheco, R
Applied Physics Letters, 100, 142402, (2012) **IF: 3.844**

75. Sonocrystallization of zeolitic imidazolate frameworks (ZIF-7, ZIF-8, ZIF-11 and ZIF-20)
Seoane, B ; Zamaro, JM ; Tellez, C ; Coronas, J
Crystengcomm, 14, 3103-3107, (2012) **IF: 3.842**

76. Insight into the synthesis and characterization of zeolite millimeter-sized crystals Navarro, M.;
Mateo, E.; Diosdado, B.; Coronas, J
Crystengcomm, 14, 6016-6022, (2012) **IF: 3.842**

77. Preparation and characterization of chitosan-silver nanocomposite films and their antibacterial activity against Staphylococcus aureus
Regiel, A ; Irusta, S ; Kyziol, A ; Arruebo, M ; Santamaria, J
Nanotechnology, 24, 1, 015101, (2013) **IF: 3.842**

78. Continuous production of iron-based nanocrystals by laser pyrolysis. Effect of operating variables on size, composition and magnetic response
Malumbres, A; Martinez, G; Mallada, R; Hueso, J L; Bomati-Miguel, O; Santamaria, J
Nanotechnology, 24, 32, 325603, (2013) **IF: 3.842**

79. Improvement of domain wall conduit properties in cobalt nanowires by global gallium irradiation.
Serrano-Ramon, L; Fernandez-Pacheco, A; Cordoba, R; Magen, C; Rodriguez, L A; Petit, D; Cowburn, R P; Ibarra, M R; De Teresa, J M
Nanotechnology, 24, 34, 345703, (2013) **IF: 3.842**

80. Facile preparation of transparent and conductive polymer films based on silver nanowire/polycarbonate nanocomposites
Moreno, I ; Navascues, N ; Arruebo, M ; Irusta, S ; Santamaria, J
Nanotechnology, 24, 27, 275603, (2013) IF: 3.842

81. Atomic resolution structural insights into PdPt nanoparticle-carbon interactions for the design of highly active and stable electrocatalysts
Slanac, DA ; Li, L ; Mayoral, A ; Yacaman, MJ ; Manthiram, A ; Stevenson, KJ ; Johnston, KP
Electrochimica Acta, 64, 35-45, (2012) **IF: 3.832**

82. Conductance steps in electromigrated Bi nanoconstrictions
Sangiao, S ; Michalik, JM ; Casado, L ; Martinez-Velarte, MC ; Morellon, L ; Ibarra, MR ; De Teresa, JM
Physical Chemistry Chemical Physics, 15, 14, 5132-5139, (2013) **IF: 3.829**

83. Simplifying the conductance profiles of molecular junctions: the use of the trimethylsilylethynyl moiety as a molecule-gold contact
Marques-Gonzalez, S ; Yufit, DS; Howard, JAK; Martin, S ; Osorio, HM ; Garcia-Suarez, VM; Nichols, RJ; Higgins, SJ; Cea, P; Low, PJ
Dalton Transactions, 42, 2, 338-341, (2013) **IF: 3.806**

84. On the influence of diphosphine ligands on the chemical order in small RuPt nanoparticles: combined structural and surface reactivity studies
Lara, P ; Ayvali, T ; Casanove, MJ ; Lecante, P ; Mayoral, A ; Fazzini, PF; Philippot, K ; Chaudret, B
Dalton Transactions, 42, 2, 372-382, (2013) **IF: 3.806**

85. Optimized cobalt nanowires for domain wall manipulation imaged by in situ Lorentz microscopy
Rodriguez, LA ; Magen, C; Snoeck, E ; Serrano-Ramon, L ; Gatel, C ; Cordoba, R ; Martinez-Vecino, E ; Torres, L ; De Teresa, JM; Ibarra, MR
Applied Physics Letters, 102, 2, 022418, (2013) **IF: 3.794**

86. Strain-driven broken twin boundary coherence in YBa2Cu3O7-delta nanocomposite thin films
Guzman, R ; Gazquez, J; Rouco, V ; Palau, A; Magen, C ; Varela, M; Arbiol, J ; Obradors, X ; Puig, T
Applied Physics Letters, 102, 8, 081906, (2013) **IF: 3.794**

87. Thickness scaling of ferroelastic domains in PbTiO3 films on DyScO3
Nesterov, O ; Matzen, S ; Magen, C ; Vlooswijk, AHG ; Catalan, G ; Noheda, B
Applied Physics Letters, 103, 142901, (2013) **IF: 3.794**

88. Nanomechanics of ferredoxin-NADP(+) reductase complexes analyzed by AFM single-molecule force spectroscopy
Marcuello, C ; de Miguel, R ; Medina, M ; Martinez-Julvez, M ; Gomez-Moreno, C ; Lostao, A
FEBS Journal, 279, 513, (2012) **IF: 3.790**

89. Atomic force microscopy reveals a dimer of trimers organization in Corynebacterium ammoniagenes FAD synthetase
Marcuello, C ; Arilla-Luna, S ; Medina, M ; Lostao, A
FEBS Journal, 279, 513-514, (2012) **IF: 3.790**

90. Strain induced spin reorientation in epitaxial Cu/Ni/Cu rings
Corredor, EC ; Coffey, D ; Ciria, M ; Arnaudas, JI ; Aisa, J ; Ross, CA
Physical Review B, 88, 054418, (2013) **IF: 3.767**

91. Detection of a quaternary organization into dimer of trimers of Corynebacterium ammoniagenes FAD synthetase at the single-molecule level and at the in cell level
Marcuello, C ; Arilla-Luna, S ; Medina, M ; Lostao, A
Biochimica et Biophysica Acta-Proteins and Proteomics, 1834, 3, 665-676, (2013) **IF: 3.733**

92. X-ray photoemission electron microscopy studies of local magnetization in Py antidot array thin films
Merazzo, KJ ; Castan-Guerrero, C ; Herrero-Albillos, J ; Kronast, F ; Bartolome, F ; Bartolome, J ; Sese, J ; del Real, RP ; Garcia, LM ; Vazquez, M
Physical Review B, 85, 035113, (2012) **IF: 3.691**

93. Co/Ni(111) superlattices studied by microscopy, x-ray absorption, and ab initio calculations
Gottwald, M ; Andrieu, S ; Gimbert, F ; Shipton, E ; Calmels, L ; Magen, C ; Snoeck, E ; Liberati, M ; Hauet, T ; Arenholz, E ; Mangin, S ; Fullerton, EE
Physical Review B, 86, 014425, (2012) **IF: 3.691**

94. Photocrosslinking, micropatterning and cell adhesion studies of sodium hyaluronate with a trisdiazonium salt
Lomba, M ; Oriol, L ; Sanchez, C ; Grazu, V ; Gutierrez, BS ; Serrano, JL ; De la Fuente, JM
Carbohydrate Polymers, 90, 419-430, (2012) **IF: 3.628**

95. Investigation of diesel ash particulate matter: a scanning electron microscope and transmission electron microscope study
Liati A, Dimopoulos P, Muller E, Schreiber D, Aguirre M.
Atmospheric Environment, 49, 391-402, (2012) **IF: 3.465**

96. HKUST-1 MOF: A matrix to synthesize CuO and CuO-CeO_2 nanoparticle catalysts for CO oxidation
Zamaro, JM ; Perez, NC ; Miro, EE ; Casado, C ; Seoane, B ; Tellez, C ; Coronas, J
Chemical Engieering Journal, 195, 180-187, (2012) **IF: 3.461**

97. Porous orthopedic steel implant as an antibiotic eluting device: Prevention of post-surgical infection on an ovine model
Gimeno, M ; Pinczowski, P ; Vazquez, FJ ; Perez, M ; Santamaria, J ; Arruebo, M ; Lujan, L
International Journal of Pharmaceutics, 452, 1-2, 166-172, (2013) **IF: 3.458**

98. Laser Control of Zeolite Nucleation
Navarro, M ; Mayoral, A ; Mateo, E; Lahoz, R ; de la Fuente, GF; Coronas, J
ChemPhysChem, 13, 736-740, (2012) **IF: 3.412**

99. Atomic resolution analysis of porous solids: A detailed study of silver ion-exchanged zeolite A
Mayoral, A ; Carey, T ; Anderson, PA ; Diaz, I
Microporous and Mesoporous Materials, 166, 117-122, (2013) **IF: 3.365**

100. Effect of PEG biofunctional spacers and TAT peptide on dsRNA loading on gold nanoparticles
Sanz, V ; Conde, J ; Hernandez, Y ; Baptista, PV ; Ibarra, MR ; de la Fuente, JM
Journal of Nanoparticles Research, 14, 917, (2012) **IF: 3.287**

101. Self organization in oleic acid-coated $CoFe_2O_4$ colloids: a SAXS study
van Raap, MBF ; Zelis, PM ; Coral, DF ; Torres, TE ; Marquina, C ; Goya, GF; Sanchez, FH
Journal of Nanoparticles Research, 14, 1072, (2012) **IF: 3.287**

102. Strong bactericidal synergy between peracetic acid and silver-exchanged zeolites
Lalueza, P ; Carmona, D ; Monzon, M ; Arruebo, M ; Santamaria, J
Microporous and Mesoporous Materials, 156, 171-175, (2012) **IF: 3.285**

103. Mesoporous silica loaded with peracetic acid and silver nanoparticles as a dual-effect, highly efficient bactericidal agent
Carmona, D ; Lalueza, P ; Balas, F ; Arruebo, M ; Santamaria, J
Microporous and Mesoporous Materials, **161**, 84-90, (2012) **IF: 3.285**

104. Atomic resolution analysis of porous solids:A detailed study of silver ion-exchanged zeolite A
Mayoral; T. Carey; P. A. Anderson; I. Diaz
Microporous and Mesoporous Materials, 166, 117-122, (2012) **IF: 3.285**

105. Poly-l-lysine-coated magnetic nanoparticles as intracellular actuators for neural guidance
Riggio, C ; Calatayud, MP ; Hoskins, C ; Pinkernelle, J ; Sanz, B ; Torres, TE ; Ibarra, MR ; Wang, LJ ; Keilhoff, G ; Goya, GF ; Raffa, V ; Cuschieri, A
International Journal of Nanomedicine, 7, 3155-3166, (2012) **IF: 3.130**

106. Simultaneous Synthesis of Polyoxometalates and Metal Nanoparticles from Molecular Precursors
Mitchell S, De la Fuente, JM
European Journal of Inorganic Chemistry, 32, 5504, (2013) **IF: 3.120**

107. Green Synthesis of Chitosan-Stabilized Copper Nanoparticles
Tokarek, K ; Hueso, JL ; Kustrowski, P ; Stochel, G ; Kyziol, A
European Journal of Inorganic Chemistry, 28, 4940-4947, (2013) **IF: 3.120**

108. Magnetic nanoparticles in primary neural cell cultures are mainly taken up by microglia
Pinkernelle, J ; Calatayud, P ; Goya, GF ; Fansa, H ; Keilhoff, G
BMC Neuroscience, 13, 32, (2012) **IF: 3.042**

109. In-situ TEM observation of keV-ion irradiation of single-walled carbon nanotubes and single-walled boron nitride nanotubes
R. Arenal, A.C.Y. Liu
Microscopy and Microanalysis, 18, 1544, (2012) **IF: 3.007**

110. First in-situ TEM Studies of Young Modulus and Elastic Properties of individual and bundled Single-Walled BN nanotubes
R. Arenal, M.S. Wang, Z. Xu, D.Golberg
Microscopy and Microanalysis, 18, 750-751, (2012) **IF: 3.007**

111. Atomic Structure of Ultra-Long Carbon Nanotubes
R. Arenal, P. Löthman, M. Picher, V. Jourdain
Microscopy and Microanalysis, 18, 1518, (2012) **IF: 3.007**

112. Optoelectronic Properties of InAlN/GaN Distributed Bragg Reflector Heterostructure Examined by Valence Electron Energy Loss Spectroscopy
Eljarrat, S. Estradé, Ž. Gačević, S. Fernández-Garrido, E. Calleja, C. Magén, and F. Peiró
Microscopy and Microanalysis, 18, 1143-1154, (2012) **IF: 3.007**

113. Efficient method for enzyme immobilization demonstrated by atomic force microscopy
C. Marcuello, R. de Miguel, M. Martínez-Júlvez C. Gómez-Moreno, A. Lostao
Protein Engieering, Desing & Selection, 25, 715-723, (2012) **IF: 2.937**

114. Three dimensional magnetic nanowires grown by focused electron-beam induced deposition
Fernandez-Pacheco, A ; Serrano-Ramon, L ; Michalik, JM; Ibarra, MR ; De Teresa, JM ; O'Brien, L; Petit, D; Lee, J ; Cowburn, RP
Scientific Reports, 3, 1492, (2013) **IF: 2.927**

115. VOCs abatement using thick eggshell Pt/SBA-15 pellets with hierarchical porosity
Usón, L., Colmenares, M. G., Hueso, J. L., Sebastián, V., Balas, F., Arruebo, M., Santamaría, J
Catalysis Today, doi: 10.1016/j.cattod.2013.08.014, (2013) **IF: 2.908**

116. NH2-MIL-53(Al) and NH2-MIL-101(Al) in sulfur-containing copolyimide mixed matrix membranes for gas separation
Seoane, B ; Tellez, C ; Coronas, J ; Staudt, C
Separation and Purification Technology, 111, 72-81, (2013) **IF: 2.894**

117. Location of enzyme in lipase-SBA-12 hybrid biocatalyst
Mayoral, A ; Blanco, RM ; Diaz, I
Journal of Molecular Catalysis B-Enzymatic, 90, 23-25, (2013) **IF: 2.823**

118. Fluidized Bed Generation of Stable Silica Nanoparticle Aerosols
Clemente, A ; Balas, F ; Lobera, MP ; Irusta, S ; Santamaria, J
Aerosol Science and Technology, 47, 8, 867-874, (2013) **IF: 2.780**

119. Photoluminescence Enhancement of InAs(Bi) Quantum Dots by Bi Clustering
Reyes, DF ; Gonzalez, D ; Bastiman, F ; Dominguez, L ; Hunter, CJ ; Guerrero, E ; Roldan, MA ; Mayoral, A ; David, JPR ; Sales, DL
Applied Physics Express, 6, 4, 042103, (2013) **IF: 2.731**

120. Thermal stability of Mo/Au bilayers for TES applications
Parra-Borderias, M ; Fernandez-Martinez, I ; Fabrega, L ; Camon, A ; Gil, O ;Gonzalez-Arrabal, R ; Sese, J ; Costa-Kramer, JL ; Warot-Fonrose, B ; Serin, V ; Briones, F
Superconductor Science & Technology, **25**, 095001, (2012) **IF: 2.662**

121. Adsorption of Adenine and Thymine on Zeolites: FT-IR and EPR Spectroscopy and X-Ray Diffractometry and SEM Studies
Bau, JPT ; Carneiro, CEA ; de Souza, IG ; de Souza, CMD ; da Costa, ACS ; di Mauro, E ; Zaia, CTBV ; Coronas, J ; Casado, C ; de Santana, H ; Zaia, DAM
Origins of Life and Evolution of Biospheres, 42, 19-29, (2012) **IF: 2.660**

122. Platinum Electrodeposition on Unsupported SingleWall Carbon Nanotubes and Its Application as Methane Sensing Material
E. Contes-de Jesus, D. Santiago, G. Casillas, A. Mayoral, C. Magen, M. José-Yacaman, J. Li, and C. R. Cabrera
Journal of the Electrochemical Society, 160, H1-H7, (2012) **IF: 2.590**

123. Platinum Electrodeposition on Unsupported Single Wall Carbon Nanotubes and Its Application as Methane Sensing Material
Contes-de Jesus, E ; Santiago, D ; Casillas, G ; Mayoral, A ; Magen, C; Jose-Yacaman, M ; Li, J ; Cabrera, CR
Journal of the Electrochemical Society, 160, 2, H98-H104, (2013) **IF: 2.588**

124. **Beyond gold: rediscovering tetrakis-(hydroxymethyl)-phosphonium chloride (THPC) as an effective agent for the synthesis of ultra-small noble metal nanoparticles and Pt-containing nanoalloys**
Hueso, JL ; Sebastian, V ; Mayoral, A ; Uson, L ; Arruebo, M ; Santamaria, J
RSC Advances, 3, 26, 10427-10433, (2013) **IF: 2.562**

125. **Giant anomalous Hall effect in Fe-based microwires grown by focused-electron-beam-induced deposition**
Cordoba, R ; Lavrijsen, R ; Fernandez-Pacheco, A ; Ibarra, MR ; Schoenaker, F ; Ellis, T ; Barcones-Campo, B ; Kohlhepp, JT ; Swagten, HJM Koopmans, B; Mulders, JJL ; De Teresa, JM
Journal of Physics D – Applied Physics, 45, 035001, (2012) **IF: 2.544**

126. **Conversion of glucose to lactic acid derivatives with mesoporous Sn-MCM-41 and microporous titanosilicates**
Murillo B, Sanchez A, Sebasian V, Casado C, De la Iglesia O, Lopez Ram de Viu P, Tellez C, Coronas J.
Journal of Chemical Technology & Biotechnology, DOI: 10.1002/jctb.4210

127. **Insight into the Compositional and Structural Nano Features of AlN/GaN DBRs by EELS-HAADF**
Eljarrat, A ; Lopez-Conesa, L ; Magen, C; Gacevic, Z ; Fernandez-Garrido, S ; Calleja, E ; Estrade, S ; Peiro, F
Microscopy and Microanalysis, 19, 3, 698-705, (2013) **IF: 2.495**

128. **Spectroscopic Studies on Nitrogen-doped Multi-Walled Carbon Nanotubes Using Monochromated STEM-EELS at Low-Voltage**
R. Arenal
Microscopy and Microanalysis, 19, S2, 1230-1231, (2013) **IF: 2.495**

129. **Antibody Distribution on Bio-Functionalized Magnetic Nanoparticles Analyzed by Spatial-Resolved EELS**
R. Arenal, L. De Matteis, L. Custardoy, A. Mayoral, M. Tence, V. Grazu, J.M. de la Fuente, C. Marquina, M.R. Ibarra
Microscopy and Microanalysis, 19, S2, 1628, (2013) **IF: 2.495**

130. **Solution-processable exfoliated zeolite nanosheets purified by density gradient centrifugation**
Agrawal, KV ; Topuz, B ; Jiang, ZY ; Nguenkam, K ; Elyassi, B ; Francis, LF ; Tsapatsis, M ; Navarro, M
AICHE Journal, 59, 9, 3458-3467, (2013) **IF: 2.493**

131. Layered titanosilicates JDF-L1 and AM-4 for biocide applications
Perez-Carvajal, J ; Lalueza, P Casado, C Tellez, C Coronas, J
Applied Clay Science, 56, 30-35, (2012) **IF: 2.474**

132. EEL spectroscopic tomography: Towards a new dimension in nanomaterials analysis
Ll. Yedra, A. Eljarrat, R. Arenal, E. Pellicer, M. Cabo, A. Lopez-Ortega, M. Estrader, J. Sort, M.D. Baro, S. Estrade, F. Peiro
Ultramicroscopy, 122, 12-18, (2012) **IF: 2.471**

133. A new linear transfer theory and characterization method for image detectors. Part II: Experiment
Lubk, A ; Roder, F ; Niermann, T ; Gatel, C ; Joulie, S ; Houdellier, F ; Magen, C ; Hytch, MJ
Ultramicroscopy, 122, 78-87, (2012) **IF: 2.471**

134. Quantitative in situ magnetization reversa lstudies in Lorentz microscopy and electronholography
Rodriguez, LA ; Magen, C ; Snoeck, E ; Gatel, C ; Marin, L ; Serrano-Ramon, L ; Prieto, JL Munoz, M ; Algarabel, PA ; Morellon, L ; De Teresa, JM ; Ibarra, MR
Ultramicroscopy, 134, 144-154, (2013) **IF: 2.470**

135. Generation of Magnetized Olfactory Ensheathing Cells for Regenerative Studies in the Central and Peripheral Nervous Tissue
Riggio, C ; Nocentini, S ; Catalayud, MP ; Goya, GF ; Cuschieri, A ; Raffa, V ; del Rio, JA
International Journal of Molecular Science, 14, 6, 10852-10868, (2013) **IF: 2.464**

136. NS3 protease from hepatitis C virus: biophysical studies on an intrinsically disordered protein domain
Vega, S; Neira, J; Marcuello, C; Lostao, A; Abian, O; Velazquez-Campoy, A
International Journal of Molecular Sciences, 14, 7, 13282-13306, (2013) **IF: 2.464**

137. Preparation and characterization of ITQ-29/polysulfone mixed-matrix membranes for gas separation: Effect of zeolite composition and crystal size
Casado-Coterillo, C ; Soto, J ; Jimare, MT ; Valencia, S ; Corma, A ; Tellez, C ; Coronas, J
Chemical Engineering Science, 73, 116-122, (2012) **IF: 2.431**

138. Superplastic deformation of directionally solidified nanofibrillar Al_2O_3-$Y_3Al_5O_{12}$-ZrO_2 eutectics
Pastor, JY ; Martin, A ; Molina-Aldareguia, JM ; LLorca, J ; Oliete, PB ; Larrea, A Pena, JI ; Orera, VM ; Arenal, R
Journal of the European Ceramic Society, 33, 13-14, 2579-2586, (2013) **IF: 2.360**

139. Correlations among magnetic, electrical and magneto-transport properties of NiFe nanohole arrays
Leitao, DC; Ventura, J; Teixeira, JM; Sousa, CT ; Pinto, S ; Sousa, JB; Michalik, JM ; De Teresa, JM; Vazquez, M; Araujo, JP
Journal of Physics Condensed Matter, 25, 6, 066007, (2013) **IF: 2.355**

140. Discrimination of protein receptors through quantitative adhesion force maps
Marcuello, C; De Miguel, R; Gómez-Moreno, C; Lostao A.
European Biophysics Journal, 42, S1, 201, (2013) **IF: 2.274**

141. Fluorescent Magnetic Bioprobes by Surface Modification of Magnetite Nanoparticles
Pinheiro, PC; Daniel-da-Silva, AL; Tavares, DS; Calatayud MP; Goya, GF; Trinidade, T
Materials, 6, 3213-3225, (2013) **IF: 2.247**

142. Synthesis of Magnetic Nanocrystals by Thermal Decomposition in Glycol Media: Effect of Process Variables and Mechanistic Study
Miguel-Sancho, N ; Bomati-Miguel, O Roca, AG Martinez, G ; Arruebo, M Santamaria, J
Industrial & Engineering Chemistry Research, 51, 8348-8357, (2012) **IF: 2.237**

143. Electrical, rheological and mechanical characterization of multiscale composite materials based on poly(etherimide)/short glass fibers/multiwalled carbon nanotubes
Salinier, A ; Dagreou, S ; Leonardi, F ; Derail, C ; Navascues, N
Composite Structures, 102, 81-89, (2013) **IF: 2.231**

144. Critical magnetic behavior of magnetocaloric materials with the Gd5Si4-type structure
Belo, JH ; Pereira, AM ; Magen, C ; Morellon, L ; Ibarra, MR ; Algarabel, PA ; Araujo, JP
Journal of Applied Physics, 113, 13, 133909, (2013) **IF: 2.210**

145. Size dependence of the magnetic relaxation and specific power absorption in iron oxide nanoparticles
Lima, E ; Torres, TE ; Rossi, LM; Rechenberg, HR ; Berquo, TS ; Ibarra, A ; Marquina, C ; Ibarra, MR ; Goya, GF
Journal of Nanoparticle Research, 15, 5, 1654, 2.175

146. Encapsulation of titanium dioxide nanoparticles in PLA microspheres using supercritical emulsion extraction to produce bactericidal nanocomposites
Campardelli, R ; Della Porta, G ; Gomez, V ; Irusta, S ; Reverchon, E ; Santamaria, J
Journal of Nanoparticle Research, 15, 10, UNSP 1987, (2013) **IF: 2.175**

147. Magnetization enhancement and cation valences in nonstoichiometric (Mn,Fe)(3-delta)O-4 nanoparticles
Antic, B ; Kremenovic, A ; Jovic, N ; Pavlovic, MB ; Jovalekic, C ; Nikolic, AS ; Goya, GF ; Weidenthaler, C
Journal of Applied Physics, 111, 074309, (2012) **IF: 2.168**

148. High temperature finite-size effects in the magnetic properties of Ni nanowires
R. López-Ruiz, C. Magén, F. Luis, and J. Bartolomé
Journal of Applied Physics, 111, 073906, (2012) **IF: 2.168**

149. Autocatalytic growth of Co on pure Co surfaces using Co2(CO)8 precursor
R. Córdoba, J. Sesé, M. R. Ibarra and J. M. De Teresa
Applied Surface Science, 263, 242-246, (2012) **IF: 2.103**

150. Stability and biocompatibility of photothermal gold nanorods after lyophilization and sterilization
Gomez, L ; Cebrian, V ; Martin-Saavedra, F ; Arruebo, M ; Vilaboa, N ; Santamaria, J
Materials Research Bulletin, 48, 10, 4051-4057, (2013) **IF: 1.913**

151. Identification of the atomic scale structure of the $La_{0.65}Nd_{0.15}Mg_{0.20}Ni_{3.5}$ synthesized by spark plasma sintering alloy
Serin, V ; Zhang, JX ; Magen, C; Serra, R ; Hytch, MJ ; Lemort, L ; Latroche, M; Ibarra, MR ; Knosp, B; Bernard, P
Intermetallics, 32, 103-108, (2013) **IF: 1.857**

152. Magnetic properties of lithium ferrite nanoparticles with a core/shell structure
Jovic N, Antic B, Goya GF, Spasojevic V
Current Nanoscience, 8, 651-658, (2012) **IF: 1.776**

153. Effect of Magnet Implant on Iron Biodistribution of Fe@C Nanoparticles in the Mouse
Escribano, E ; Fernandez-Pacheco, R ; Valdivia, JG ; Ibarra, MR ; Marquina, C ; Queralt, J
Archives of Pharmacal Research, 35, 93-100, (2012) **IF: 1.592**

154. Magnetic Properties of Epitaxial Discontinuous Fe/MgO Multilayers
Garcia-Garcia, A ; Pardo, JA ; Strichovanec, P ; Magen, C ; Vovk, A ; De Teresa, JM ; Kakazei, GN ; Pogorelov, YG ; Golub, V ; Salyuk, O ; Morellon, L ; Algarabel, PA ; Ibarra, MR
Journal of Nanoscience and Nanotechnolgy, 12, 7505-7509, (2012) **IF: 1.563**

155. Fabrication and Magnetic Characterization of Cobalt Antidot Arrays: Effect of the Surrounding Continuous Film
Castan-Guerrero, C ; Sese, J ; Bartolome, J ; Bartolome, F ; Herrero-Albillos, J; Kronast, F ; Strichovanec, P ; Merazzo, KJ ; Vazquez, M ; Vavassori, P ; Garcia, LM
Journal of Nanoscience and Nanotechnolgy, 12, 7437-7441, (2012) **IF: 1.563**

156. On the structure of bimetallic noble metal nanoparticles as revealed by aberration corrected scanning transmission electron microscopy (STEM)
Mayoral, A ; Deepak, FL ; Esparza, R ; Casillas, G ; Magen, C ; Perez-Tijerina, E ; Jose-Yacaman, M
Micron, 43, 557-564, (2012) **IF: 1.527**

157. Modification of domain-wall propagation in Co nanowires via Ga^{+} irradiation
Serrano-Ramon, L ; Fernandez-Pacheco, A ; Ibarra, MR ; Petit, D ; Cowburn, RP] ; Tyliszczak, T ; De Teresa, JM
European Physical Journal B, 86, 3, 97, (2013) **IF: 1.282**

158. Transverse magnetization in Cu/Ni/Cu epitaxial nanorings
Corredor, EC ; Coffey, D ; Arnaudas, JI ; Ibarra, A ; Ross, CA ; Ciria, M
European Physical Journal B, 86, 4, 134, (2013) IF: 1.282

159. Nanoparticles of Ni in ZnO single crystal matrix
Borges, RP ; Ribeiro, B ; Cruz, MM ; Godinho, M ; Wahl, U ; da Silva, RC ; Goncalves, AP ; Magen, C
European Physical Journal B, 86, 6, 254, (2013) **IF: 1.282**

160. Coercivity dependence on periodicity of Co and Py antidot arrays
Castan-Guerrero, C ; Bartolome, J ; Bartolome, F ; Garcia, LM ; Sese, J ; Strichovanec, P ; Herrero-Albillos, J ; Merazzo, KJ ; Vazquez, M ; Vavassori, P
Journal of the Korean Physical Society, 62, 10, 1521-1524, (2013) **IF: 0.506**

161. Comparative Raman Study of Individual Double-Walled Carbon Nanotubes and Single-Walled Carbon Nanotubes
Levshov, D ; Michel, T ; Than, T ; Paillet, M; Arenal, R ; Jourdain, V; Yuzyuk, YI; Sauvajol, JL
Journal of Nanoelectronics and Optoelectronics, 8, 1, 9-15, (2013) **IF: 0.479**

162. New Insigths on Photo-Active Molecules Within Host Carbon Nanotubes
Alvarez, L ; Almadori, Y ; Mariot, S ; Aznar, R ; Arenal, R ; Michel, T ; Le Parc, R ; Dieudonne, P ; Jousselme, B ; Campidelli, S ; Bantignies, JL
Journal of Nanoelectronics and Optoelectronics, 8, 1, 28-35, (2013) **IF: 0.479**

Organization of scientific events

LMA Colloquia

A series of topical Colloquia on the three scientific áreas (TEM, Dual & SPM), devoted to informing local researchers about the capabilities of our infrastructures and to promote interdisciplinar work.

> Colloquium on nanofabrication installations: February 2, 2012

> Colloquium on local probe microscopy: February 12, 2012

> Colloquium on transmission electron microscopy: May 17, 2012

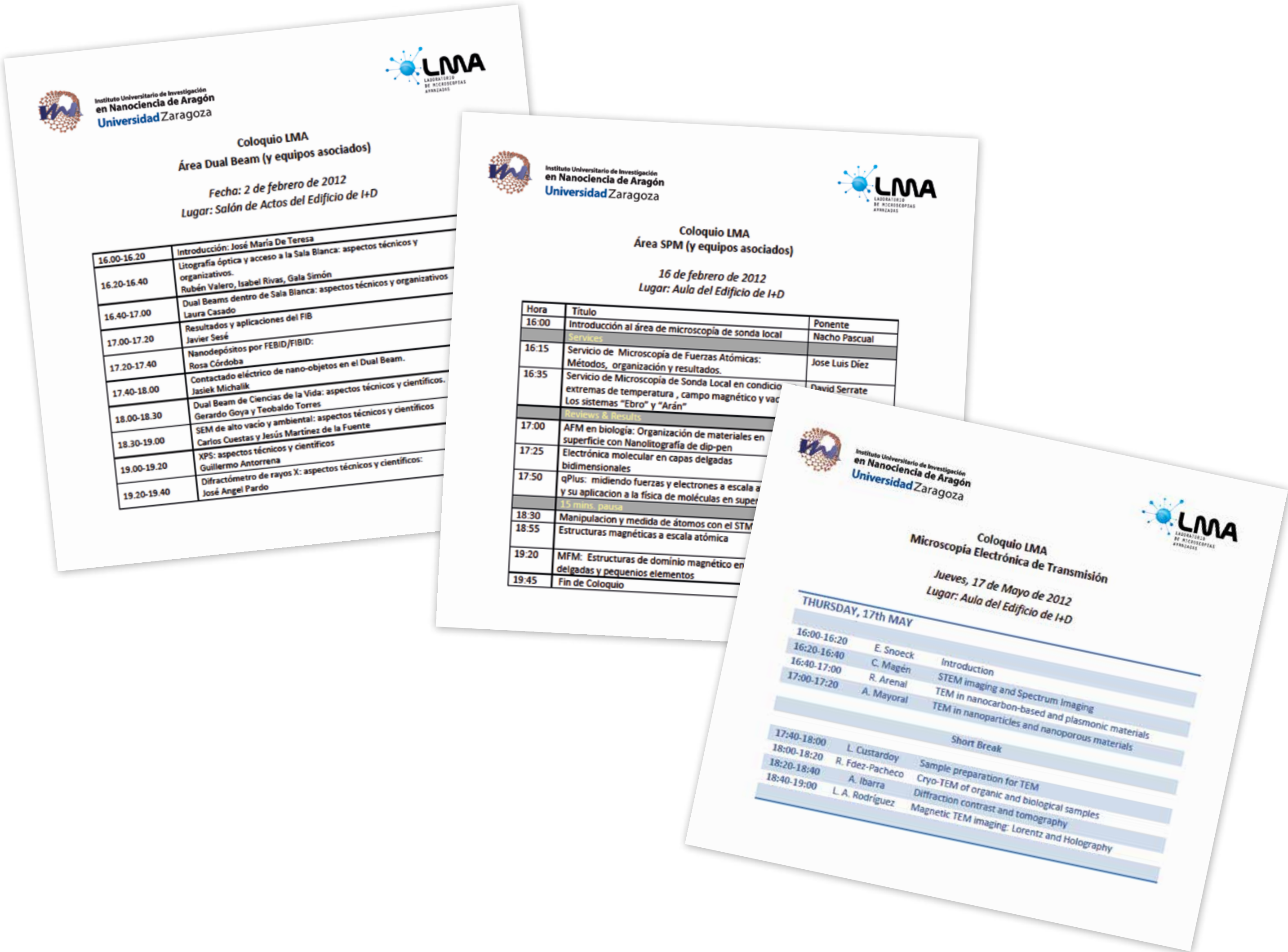

Instituto Universitario de Investigación en Nanociencia de Aragón
Universidad Zaragoza
LMA

Coloquio LMA
Área Dual Beam (y equipos asociados)

Fecha: 2 de febrero de 2012
Lugar: Salón de Actos del Edificio de I+D

16.00-16.20	Introducción: José María De Teresa
16.20-16.40	Litografía óptica y acceso a la Sala Blanca: aspectos técnicos y organizativos. Rubén Valero, Isabel Rivas, Gala Simón
16.40-17.00	Dual Beams dentro de Sala Blanca: aspectos técnicos y organizativos Laura Casado
17.00-17.20	Resultados y aplicaciones del FIB Javier Sesé
17.20-17.40	Nanodepósitos por FEBID/FIBID: Rosa Córdoba
17.40-18.00	Contactado eléctrico de nano-objetos en el Dual Beam. Jasiek Michalik
18.00-18.30	Dual Beam de Ciencias de la Vida: aspectos técnicos y científicos. Gerardo Goya y Teobaldo Torres
18.30-19.00	SEM de alto vacío y ambiental: aspectos técnicos y científicos Carlos Cuestas y Jesús Martínez de la Fuente
19.00-19.20	XPS: aspectos técnicos y científicos Guillermo Antorrena
19.20-19.40	Difractómetro de rayos X: aspectos técnicos y científicos: José Angel Pardo

Instituto Universitario de Investigación en Nanociencia de Aragón
Universidad Zaragoza
LMA

Coloquio LMA
Área SPM (y equipos asociados)

16 de febrero de 2012
Lugar: Aula del Edificio de I+D

Hora	Título	Ponente
16:00	Introducción al área de microscopía de sonda local	Nacho Pascual
	Services	
16:15	Servicio de Microscopía de Fuerzas Atómicas: Métodos, organización y resultados.	Jose Luis Díez
16:35	Servicio de Microscopía de Sonda Local en condicio[...] extremas de temperatura, campo magnético y vac[...] Los sistemas "Ebro" y "Arán"	David Serrate
	Reviews & Results	
17:00	AFM en biología: Organización de materiales en superficie con Nanolitografía de dip-pen	
17:25	Electrónica molecular en capas delgadas bidimensionales	
17:50	qPlus: midiendo fuerzas y electrones a escala a[...] y su aplicacion a la física de moléculas en super[...]	
	15 mins. pausa	
18:30	Manipulacion y medida de átomos con el STM	
18:55	Estructuras magnéticas a escala atómica	
19:20	MFM: Estructuras de dominio magnético en delgadas y pequeños elementos	
19:45	Fin de Coloquio	

Instituto Universitario de Investigación en Nanociencia de Aragón
Universidad Zaragoza
LMA

Coloquio LMA
Microscopía Electrónica de Transmisión

Jueves, 17 de Mayo de 2012
Lugar: Aula del Edificio de I+D

THURSDAY, 17th MAY

16:00-16:20	E. Snoeck	Introduction
16:20-16:40	C. Magén	STEM imaging and Spectrum Imaging
16:40-17:00	R. Arenal	TEM in nanocarbon-based and plasmonic materials
17:00-17:20	A. Mayoral	TEM in nanoparticles and nanoporous materials
		Short Break
17:40-18:00	L. Custardoy	Sample preparation for TEM
18:00-18:20	R. Fdez-Pacheco	Cryo-TEM of organic and biological samples
18:20-18:40	A. Ibarra	Diffraction contrast and tomography
18:40-19:00	L. A. Rodríguez	Magnetic TEM imaging: Lorentz and Holography

LMA-Solid State Chemistry Open Day.

The aim of this Open day is to establish new links between the Spanish communities involved in Solid-state chemistry and in Electron Microscopy and to promote the use of advanced (S) TEM techniques for solving materials science and inorganic chemistry issues. May 3, 2012

Instituto Universitario de Investigación en Nanociencia de Aragón
Universidad Zaragoza

LMA
Laboratorio de Microscopías Avanzadas

LMA- Chemistry Open Day

The 2012 Open day LMA- Chemistry will be held on Thursday the 3rd of May at the Institute of Nanoscience of Aragón (INA), Zaragoza.

Solid-state chemistry is an active interdisciplinary field, attracting investigators from chemistry, condensed-matter physics, materials science engineering, ceramics, chemical engineering, and mineralogy/geology, to name but a few. The scope and importance of solid-state chemistry has been growing intensively these last years with the discovery of innovative materials for new applications but also through the progress of advanced techniques for preparing and studying them. Our knowledge of the diverse properties of solids continues to expand and the understanding the synthesis-structure-property relationships and the precise control of microstructure are of fundamental importance for novel functional materials and their technological applications. Aberration corrected (S)TEM and related spectroscopic techniques using monochromated electron beams play an important role in the fine characterization and quantification of these properties.

The aim of this Open day is to establish new links between the Spanish communities involved in **Solid-state chemistry** and in **Electron Microscopy** and to promote the use of advanced (S)TEM techniques for solving materials science and inorganic chemistry issues.

This Open-day symposium therefore invites researchers from inorganic chemistry and solid state chemistry communities to describe in short their research problems where the advanced microscopy can give the answer. The including topics are but not limited to:

- Crystal structures of inorganic solids
- Structure-property relationships
- Microstructure of inorganic solids,
- Inorganic solids with useful properties (*including superconductors, solid-state ionic conductors, magnetic materials, ferroelectric and piezoelectric materials, complex oxides, nonlinear optical materials, multiferroics, and framework materials)*
- Colloids, and materials for catalysis
- Carbon based materials
- …

An introducing conference will be given by **Prof. G. Van Tendeloo** (EMAT Antwerpen) on the contribution of Electron Microscopy in solving Solid-state chemistry questions. A description of new and developing capabilities of Electron Microscopy in the Laboratory of Advanced Microscopy at INA will be provided with the aim to bring together our scientific community and promote fruitful collaboration projects. Abstract and registration can be submitted to LMA@unizar.es.

Myriam H. Aguirre & Etienne Snoeck

1st International Workshop on Recent Advances in Scanning Probe Microscopies

With this initiative, LMA aimed at introducing Scanning Probe Microscopies to the local scientific community, with the goal of supporting new collaborations and expanding their use of SPM methods. It was open to any student or researcher interested in obtaining an updated view of the modern scientific research employing SPM and it gathered a group of renown scientists in the field. Date: April 10, 2012

4th Workshop on Focused Electron Beam Induced Processing, FEBIP 2012

This Workshop was the fourth of a series of international meetings on focused electron beam induced processing which gathered 80 specialists in the field from more than 10 countries and 5 exhibiting companies to share the latest scientific and technological advances in the use of focused electron beams to fabricate nanometric devices. The event provided an excellent opportunity to show participants LMA most advanced facilities and a detailed account of the services offered by LMA to industry and research centers. June 20 and 21, 2012

FEBIP 2012
Zaragoza, Spain.
June 20-21, 2012

PROGRAM

Day 0	TUESDAY, JUNE 19th
18:00-21:00	**Welcome reception** **Visit to the INA-LMA installations** **Demonstration by FEI.** **Buffet dinner supported by FEI.**

Day 1	WEDNESDAY, JUNE 20th
9:00-9:15	**Official Inauguration**
	Chairman: C.W. Hagen
9:15-09:45 (invited)	**Philip D. Rack** *(University of Tennessee, Knoxville, USA)* Modeling of Focused Electron Beam Induced Deposition (FEBID) and Etching (FEBIE)
09:45-10:45 (oral contr.)	**A.G. Fedorov** (O-1) Using energetic inert gas jets to enable new modes of Focused Electron Beam Induced Deposition (FEBID) **J. Bishop** (O-4) Effects of Temperature on Electron Beam Induced Growth Kinetics **H. Fairbrother** (O-6) Rationalizing the Influence of Substrate Temperature and Electron Fluence on the Composition of Electron Beam Deposited Structures **M. Toth** (O-13) Kinetics of Gas-Mediated Electron Beam Induced Etching
10:45-11:15	Coffee break
	Chairman: M. Toth
11:15-11:45 (invited)	**Andrew Bass** *(Université de Sherbrooke, Canada)* Experimental investigations of the interactions of Low Energy Electrons with condensed Atoms and Molecules
11:45-13:00 (oral contr.)	**H.D. Wanzenboeck** (O-2) Electrical Nano-Tailoring of Silicon Nanowires by Cl-FEBIE **S. Rosenberg** (O-12) Influence of Organometallic Ligand Architecture on the Mechanisms of Electron Beam Induced Deposition **S.J. Randolph** (O-16) Rapid Localized Deposition of High Purity Platinum by Spontaneous Reaction of $Pt(PF_3)_4$ with XeF_2 in a Scanning Electron Microscope **F. Vollnhals** (O-27) Electron Beam Induced Surface Activation on Oxides: An Overview **M.R. Phillips** (O-9) Effects of Reactive and Inert Background Gases on Electron Beam Induced Deposition
13:00-14:30	*LUNCH AT HOTEL ZARAGOZA ROYAL*

FEBIP 2012
Zaragoza, Spain.
June 20-21, 2012

DAY 1 AFTERNOON SESSION	
14:30-16:00	Poster Session and Company Exhibition
	Chairman: M.R. Ibarra
16:00-16:30 (invited)	**Hans Mulders** *(FEI, The Netherlands)* Precursor aspects related to Beam Chemistry results and instrument components
16:30-17:00 (oral contr.)	**F. Porrati** (O-10) Room temperature $L1_0$ phase transformation in binary CoPt nanostructures **H. Plank** (O-18) Minimization of unwanted proximity deposition during electron beam induced Pt deposition
17:00-17:30	Coffee break
	Chairman: H. Wanzenboeck
17:30-18:00 (invited)	**Stefano Cabrini** *(Lawrence Berkeley National Laboratory, USA)* Nano-manipulating Light by Plasmonic Antennas
18:00-19:00 (oral contr.)	**A.V. Riazanova** (O-11) Purity and Shape Control of Au EBID Patterns **H. Marbach** (O-26) FEBIP-based concepts to locally anchor and/or functionalize molecules on surfaces, or: how to mount a molecular switch? **W.F. Van Dorp** (O-15) Molecule-by-molecule focused electron beam induced deposition **C.J. Lobo** (O-23) High resolution electron beam nanofabrication using NH_3 as both imaging and etch medium
20:00	*VISIT TO TEATRO ROMANO AND DINNER AT LA BASTILLA RESTAURANT*

FEBIP 2012
Zaragoza, Spain.
June 20-21, 2012

Day 2	THURSDAY, JUNE 21st
	Chairman: G. Gazzadi
9:00-09:30 (invited)	**Masayuki Shimojo** *(Shibaura Institute of Technology, Japan)* Deposition of Magnetic and Photoconductive Nanostructures
09:30-10:45 (oral contr.)	**A. Fernández-Pacheco** (O-3) Cobalt nanoconstrictions grown by FEBID: magnetoresistance and magnetic imaging **B. Barcones** (O-24) Iron EBID: magnetic and electric properties **E. Nikulina** (O-8): Optimization of deposition conditions of cobalt EBID **L. Serrano-Ramón** (O-29): Domain wall conduit enhancement and localized pinning induced by Ga irradiation in Co nanowires grown by Focused Electron Beam Induced Deposition **M. Winhold** (O-28): Preparation and analysis of as-grown and post-treated binary Pt-Si nanostructures prepared by focused electron-beam-induced deposition
10:45-11:15	Coffee break
	Chairman: I. Utke
11:15-11:45 (invited)	**Michael Huth** *(University of Frankfurt, Germany)* New Concepts in Sensing based on FEBID
11:45-13:00 (oral contr.)	**A. Romano-Rodriguez** (O-25) FEBID-aided Integration of Nanowires onto Microhotplates for the Fabrication of Low Power Consumption and Fast Operated Gas Nanosensors **O. Idigoras** (O-7) Magneto-Optical Magnetometry of individual 30 nm cobalt nanowires grown by electron beam induced deposition **J. Michalik** (O-22) Combined Focused Electron Beam Deposition and Electron Beam Litography Processing of Graphene Based Devices for Spin Transport Measurements **M. Gavagnin** (O-17) Electron Beam Induced Deposition of Iron as a novel nanofabrication approach for Magnetic Sensors and Logic operations **M. Gabureac** (O-19) Detection of individual Superparamagnetic beads by nanocomposite Co-C Hall nanosensors produced by FEBID and FIB milling
13:00-14:30	*LUNCH AT HOTEL ZARAGOZA ROYAL*

FEBIP 2012
Zaragoza, Spain.
June 20-21, 2012

DAY 2 AFTERNOON SESSION	
14:30-16:00	Poster Session and Company Exhibition
	Chairman: P. D. Rack
16:00-16:30 (invited)	**W.M.M. Kessels** *(Eindhoven University of Technology, The Netherlands)* Nanopatterning by combining FEBID with atomic layer deposition (ALD)
16:30-17:00 (oral contr.)	**A. Botman** (O-5) Liquid Precursors for in-situ Beam-Induced Electrochemistry **J.T. Hastings** (O-21) Electron Beam Induced Deposition from Liquid Phase Precursors – New Directions and Current Challenges
17:00-17:30	Coffee break
	Chairman: K. Edinger
17:30-18:15 (oral contr.)	**H. Koops** (O-20) The Need for FEBIP Processing to Develop Advanced Electronic and Optical Products **I. Utke** (O-14) FEBID for Photonic and Plasmonic Applications: Sub-wavelength Gratings for Telecom Lasers and Templating of Individual Nanowires for Tip Enhanced Raman Spectroscopy **A. Beyer** (O-30) Fabrication of Carbon Nanomembranes (CNMs) using FEBIP
18:15-18:45 (invited)	**John Melngailis** (O31, invited oral talk) *(University of Maryland, USA)* Review of non-gallium FIB nanofabrication - new possibilities
18:45-19:15	**Concluding Remarks**
21:00	*WORKSHOP DINNER AT HOTEL ALFONSO*

1st LMA Users Meeting

This was the first of a series of periodical meetings which gathered LMA's users, technicians and scientists to share and discuss experiences, expertise and experimental programs carried out at the Laboratory's infrastructures. The meeting featured selected invited talks and oral contributions, and finished with a visit to all laboratories and equipment.

June 11 & 12, 2013

Scanning Probe Laboratory Inauguration

On June 13, 2013, the Sanning Probe Microscopies Laboratory was inaugurated within the LMA by the President of the Government of Aragon, Mrs. Luisa Fernanda Rudi, together with the President of the University of Zaragoza, Mr. Manuel López, and the Director of INA & LMA, Mr. M. Ricardo Ibarra.

With this laboratory, LMA completes its research capacity as it allows to scan the materials surface to be surveyed by using a probe whose tips is only a few atoms thick. This probe can study and transfor materials atom by atom.

LMA and the industry

LMA and the industry

In 2012 and 2013, the Advanced Microscopy Laboratory has offered the experience of their researchers and technical staff to provide service to several private companies in order to help them to solve production problems and advance in their R&D programs. They have been able to benefit from the transfer of our technical knowledge and experience in highly advanced characterization and fabrication techniques. These companies belong to branches of industry as diverse as electronics and microelectronics, biotechnology, white goods industry, telecommunications, chemistry, logistics or automotive industry. A list of several private companies both from Spain and abroad which have benefited from these services is provided below. A short descripton of their industrial activity and the type of study carried out at LMA is also mentioned.

Valeo Térmico, S.A.

Veeo Group is fully focused on the design, production and sale of components, integrated systems and modules for the automotive industry.

Study of soldering proceses by X-Ray photelectron spectroscopy (XPS) and analysis of production samples.

Nurel (Samca Group)

A Chemical company belonging to SAMCA industrial group which supplies polyamide 6 for the engineering thermoplastic market.

Analysis of size, morphology and distribution of organic particles dispersed in polymeric materials by ESEM. Analysis of both production and R+D samples by SEM, EDX and XPS.

Baolab Microsystems, S.L.

Design and commercialization of products based on Nano Embedded Mechanical Systems technology (NanoEMSTM).

CMOS devices fabricated by optical lithography techniques were teseted by X-ray photoelectron spectroscopy.

Abalonyx AS

Norwegian Cleantech SME with focus on nanostructured, biomimetic materials based on nano-composites, nano-laminates and coatings.

Structural and christaline characterization of graphene-based samples by Ultra-High Resolution Transmission Electron Microscopy (UHRTEM).

Laboratorios Argenol, S.L.

Manufacture and Sale of silver-based products, with its main activity focused on the fabrication of chemical products for the pharmaceutical industry.

Microstructural characterization of Ag-based and other metalorganic composites nanoparticles by High Resolution Transmission Electron Microscopy (HRTEM). Analysis of size, morphology and chemical composition of silver-based nanoparticles by STEM-HAADF imaging and EDS spectroscopy.

Tecnalia

Tecnalia is the leading private Technology Centre in Spain and one of the main organisations devoted to applied research in Europe, whose mission is to transform knowledge into GDP into GDP improving people´s quality of life by generating business opportunities for companies.

Characterization of organic nanostructured samples by Transmission Electronic Microscopy. Analysis of size, morphology, crystalline structure and chemical composition of metallic nanoparticles dispersed on inorganic and carbonous matrixes by SEM and by HRTEM and STEM-HAADF imaging and EELS and EDS spectroscopies.

NanoInmunotec

It is the first European Company in the sector of Nanobiotechnology, devoted to the biological and physico-chemical characterization and to the conjugation of nanoparticles and products containing them.

Microstructural characterization of magnetic nanoparticles by Transmission Electron Microscopy (TEM), Scanning Electron Microscopy (SEM) and energy-dispersive X-ray spectroscopy (EDX). Detection of metallic nanoparticles in processed cross-sections of a given material.

DropSens, S.L.

DropSens is an Innovative Technology-Based Firm specialised in the design and manufacture of instruments for Electrochemistry Research.

Nanofabrication in Dual-Beam by using ion beam.

Abengoa

An international company which applies innovative technology solutions for sustainability in the energy and environment sectors, generating electricity from renewable resources, converting biomass into biofuels and producing drinking water from sea water.

Lamellae fabrication in Dual Beam for Transmission Electron Microscopy.

AlphaSIP

The company's main goal is to design, develop and produce molecular diagnostic chips that allow immediate and effective illness detection.

Analyses by Scanning Electron Microscopy (SEM) and by Energy-Dispersive X-ray spectroscopy (EDX).

Industrias químicas del Ebro, S.A. (IQE)

A Company specialized in the field of basic inorganic chemistry, it produces soluble sillicates and derivatives.

Sample characterization by Scanning Electron Microscopy (SEM) and by Energy-dispersive X-ray Spectroscopy (EDX).

Eficiencia Energética Aplicada, S.L.

A company based on clean energies and the care of the environment offering services of energy certification, led lighting.

Analysis of size, morphology and chemical composition of graphene and materials composed of graphene particles by SEM…

EDITA
Laboratorio
de Microscopías Avanzadas
C/ Mariano Esquillor, s/n.
50018 Zaragoz (Spain)
Tel. +34 976 762 980
Fax +34 976 762 777
Email: lma@unizar.es
http://ina.unizar.es/lma

DISEÑO GRÁFICO
José Luis Lizano

LMA

LABORATORIO
DE MICROSCOPIAS
AVANZADAS

LMA
LABORATORIO
DE MICROSCOPIAS
AVANZADAS

GOBIERNO DE ESPAÑA MINISTERIO DE ECONOMÍA Y COMPETITIVIDAD

Universidad Zaragoza 1542

GOBIERNO DE ARAGON